Online ISSN : 2186-490X
Print ISSN : 1346-4272

# 地質調査研究報告

## BULLETIN OF THE GEOLOGICAL SURVEY OF JAPAN

Vol. 73 No. 3 2022

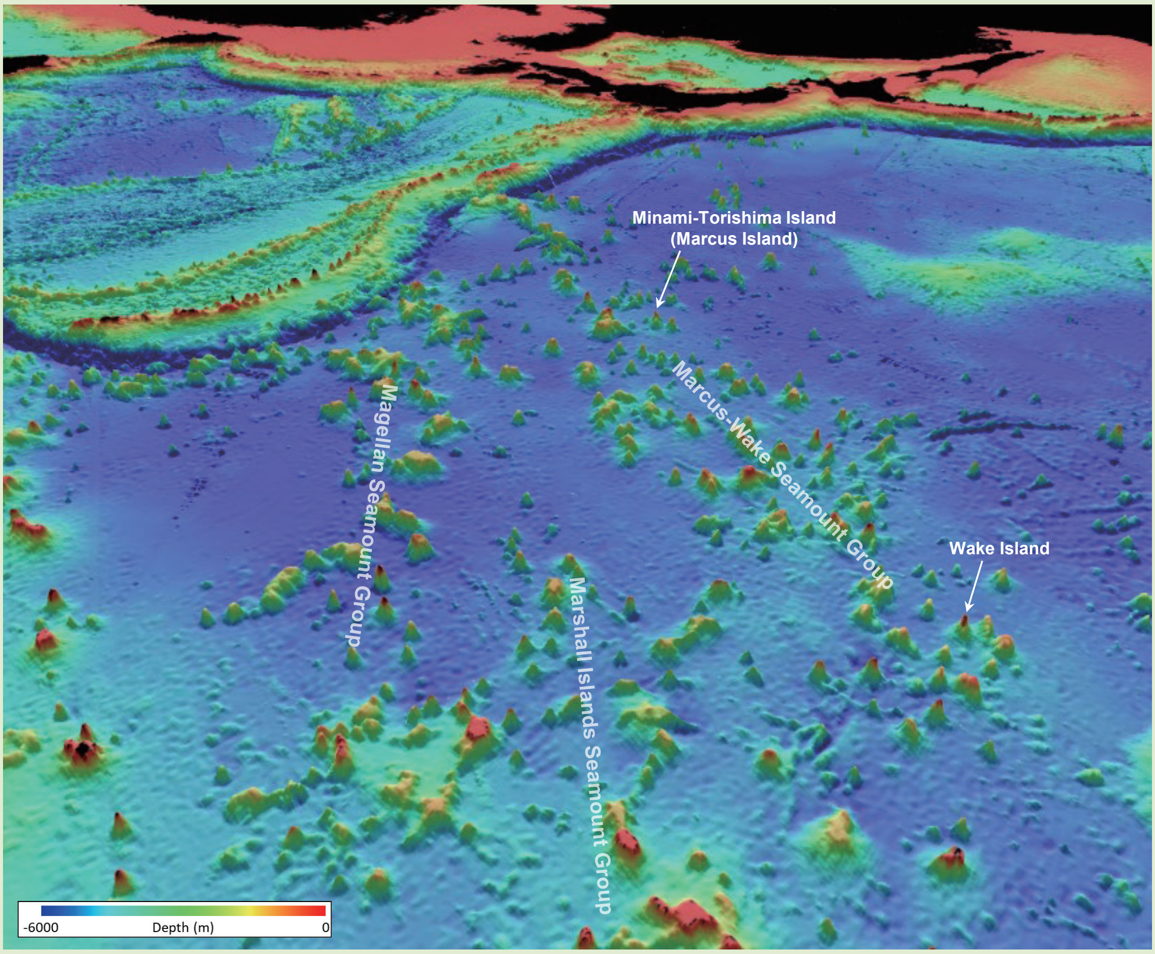


産総研 地質調査総合センター
令和4年

地質調査研究報告

**BULLETIN OF THE GEOLOGICAL SURVEY OF JAPAN**

**Vol. 73 No. 3 2022**

**概報**



## 表紙の図

3D 海底地形図で見る北西太平洋の海山群

アメリカ海洋大気庁国立環境情報センター（NOAA NCEI）が公開している海底地形図（ETOPO1）を用い，北西向き，高さ 10 倍強調で作成した．図の右側から，マーカス・ウェーク海山群，マーシャル諸島海山群，マゼラン海山群が連なる．これらの海山の多くは，白亜紀のホットスポット火山活動で噴出した玄武岩を基盤とする巨大な平頂海山（ギヨー）である．露岩域には最大で 10 cm を超える厚いマンガン酸化物が分布し，コバルトリッチクラストの有望海域とされている．現在この海域には，日本，中国，韓国，ロシアが鉱区を保有し，国際海底機構の下で，開発に向けた資源量調査や環境影響評価が進められている．

（図：日野ひかり（独立行政法人石油天然ガス・金属鉱物資源機構），文：山岡香子）

## Cover Figure

3D topographic map of seamounts in Northwest Pacific

A 3D topographic map was created using ETOPO1 published by the NOAA National Centers for Environmental Information (NCEI), oriented northwest with a height enhancement of 10 times. From right to left: the Marcus-Wake Seamount Group, the Marshall Islands Seamount Group, and the Magellan Seamount Group. Most of these seamounts are flat-topped seamounts (Guyots), whose basement consists of basalt that erupted during Cretaceous hotspot volcanism. This area is of interest for the mining of cobalt-rich crusts, since manganese oxides with a thickness of up to 10 cm or more are distributed over exposed rocks. Currently, Japan, China, Republic of Korea, and Russia hold exploration areas here, and resource surveys and environmental assessments are ongoing under the auspices of the International Seabed Authority (ISA).

(Figure: HINO Hikari (Japan Oil, Gas and Metals National Corporation), Caption: YAMAOKA Kyoko)

Bulletin of the Geological Survey of Japan, vol. 73 (3), p. 93–101, 2022

Report

# Late Triassic radiolarians and conodonts from a chert pebble within the Lower Pleistocene Higashihigasa Formation of the Kazusa Group, Boso Peninsula, Japan

ITO Tsuyoshi[1,*], MUTO Shun[1] and UTSUNOMIYA Masayuki[1]

ITO Tsuyoshi, MUTO Shun and UTSUNOMIYA Masayuki (2022) Late Triassic radiolarians and conodonts from a chert pebble within the Lower Pleistocene Higashihigasa Formation of the Kazusa Group, Boso Peninsula, Japan. *Bulletin of the Geological Survey of Japan*, vol. 73(3), p. 93–101, 6 figs and 1 table.

**Abstract:** Radiolarians and conodonts were obtained from a chert pebble within the conglomerate of the Higashihigasa Formation, Kazusa Group, Boso Peninsula, Japan. Based on the occurrence of radiolarians (*Praemesosaturnalis* sp. cf. *P. heilongjiangensis*) and conodonts (*Mockina* sp.), the chert pebble is considered to be Late Triassic (middle to late Norian) in age. This chert pebble is presumably derived from a Jurassic accretionary complex distributed in its provenance.

**Keywords**: radiolarian, conodont, Triassic, Pleistocene, Kazusa Group, conglomerate, provenance, Jurassic accretionary complex, Boso Peninsula, Chiba Prefecture

## 1. Introduction

Clasts within sediments, such as conglomerate, are supplied from the surrounding geologic units and record information of the provenance. Microfossils including radiolarians and conodonts can assign the age of the clasts, even if they are small clasts.

Radiolarian-bearing clasts have been reported from the Paleozoic to Cenozoic (Table 1) and compiled (e.g. Ishida *et al.*, 2003; Ito *et al.*, 2017a, e), but radiolarian-bearing clasts within the Quaternary are poorly investigated: only by Ito *et al.* (2020) as far as we know. Ito *et al.* (2020) indicated the presence of a water system different from the present one in the Nishi-Mikawa region, central Japan, based on microfossil-bearing clasts. Accumulation of the data of microfossil-bearing clasts within the Quaternary in several areas and horizons will contribute to reconstruction of changes of provenances and water systems.

The Pleistocene Kazusa Group is distributed in the Boso Peninsula (Fig. 1). Some formations of the group include conglomerate layers. We investigated the conglomerate for the accumulation of data of microfossil-bearing clasts within the Quaternary. We consequently discovered radiolarians and conodonts from a chert pebble within the conglomerate of the Higashihigasa Formation of the Pleistocene Kazusa Group, Boso Peninsula (Fig. 1). In this article, we note the microfossils as the first report of microfossil-bearing clasts within the Quaternary in the Boso Peninsula.

## 2. Geologic setting

The Kazusa Group is mainly composed of shallow- to deep-marine successions (>3,000 m in total thickness). The group generally comprises the Kurotaki, Katsuura, Namihana, Ohara, Tomiya, Kiwada, Otadai, Umegase, Higashihigasa, Kokumoto, Kakinokidai, Ichijiku, Chonan, Mandano, Kasamori and Kongochi formations (Tokuhashi and Endo, 1984; Nakajima and Watanabe, 2005; Utsunomiya and Ooi, 2019) (Fig. 2).

The microfossil-bearing pebble dealt with in this study was collected from the conglomerate of the Higashihigasa Formation. The Higashihigasa Formation is considered as a canyon-fill deposit which interfingers with the submarine-fan deposits defined as the Otadai and Umegase formations (Yamauchi *et al.*, 1990). Chronostratigraphy based on magneto-, tephro- and bio-stratigraphy suggests the Otadai and Umegase formations were deposited during the Early Pleistocene (Calabrian) (Kazaoka *et al.*, 2015). The clast-bearing conglomerate is intercalated above the U10 tephra bed, which is near the Marine Isotope Stage 24 (Pickering *et al.*, 1999), at about 0.9 Ma.

The sample locality is along a tributary of the Obitsu River, north of Mt. Otsuka (Fig. 3). It is located in Otomi, Kimitsu City, Chiba Prefecture in administrative division. The chert clasts occur at the basal part of a conglomerate (2 m in thickness), associated with bioclasts (e.g. mollusks) and other kinds of gravels such as sedimentary rocks and volcanic rocks (Fig. 4A).

[1] AIST, Geological Survey of Japan, Research Institute of Geology and Geoinformation

[*] Corresponding author: ITO, T., Central 7, 1-1-1 Higashi, Tsukuba, Ibaraki 305-8567, Japan. Email: ito-t@aist.go.jp

Table 1 Major previous studies of radiolarian-bearing clasts.

| Erathem | System | Series | Reference |
|---|---|---|---|
| Cenozoic | Quaternary | Pleistocene | Ito *et al.* (2020) |
| | | | Ito *et al.* (2022) [this study] |
| | Neogene | Pliocene? | Matsuoka (1998) |
| | | | Yamamoto *et al.* (2012) |
| | | Pliocene | Kawajiri and Kashiwagi (2012) |
| | | | Kashiwagi *et al.* (2013) |
| | | | Utagawa *et al.* (2017) |
| | | Miocene | Umeda *et al.* (1992) |
| | | | Kashiwagi (2012) |
| | | | Ito and Nakamura (2021) |
| | | | Yabuta *et al.* (2021) |
| | Paleogene | Oligocene | Umeda (1997) |
| | | Eocene? | Kamemura and Okamura (1994) |
| | | Paleocene? | Kishu Shimanto Research Group (2017) |
| Mesozoic | Cretaceous | Upper | Suzuki *et al.* (1996) |
| | | | Inose *et al.* (2018) |
| | | Lower | Kojima (1986) |
| | | | Takeuchi *et al.* (1991) |
| | | | Umeda *et al.* (1995) |
| | | | Ishida and Hashimoto (1997) |
| | | | Ishida (1999) |
| | | | Umeda and Sugiyama (1998) |
| | | | Matsukawa and Takahashi (1999) |
| | | | Nikaido and Matsuoka (2004) |
| | | | Tomita *et al.* (2007) |
| | | | Ito *et al.* (2012) |
| | | | Ito *et al.* (2014) |
| | | | Ito *et al.* (2015) |
| | | | Kashiwagi and Isaji (2015) |
| | | | Takeuchi *et al.* (2015) |
| | | | Ozeki *et al.* (2021) |
| | Jurassic | Upper | Saida (1987) |
| | | Middle? | Ito *et al.* (2016) |
| | | | Ito *et al.* (2017b) |
| | | Lower | Kumazaki and Kojima (1996) |
| | | | Ito *et al.* (in press) |
| | Triassic | Upper | Kametaka (1997) |
| | Triassic? | | Saito and Tsukamoto (1993) |
| | | | Kamata (1997) |
| Paleozoic | Permian | Gudalupian–Lopingian | Matsuoka and Kuwahara (2021) |
| | | | Takemura *et al.* (1996) |
| | Carboniferous | Mississippian | Uchino and Kurihara (2019) |
| Paleozoic? | | | Ito *et al.* (2017c) |
| | | | Ito *et al.* (2017d) |

## 3. Method

Four pebbles collected from the conglomerate were processed with the following method to extract microfossils. They were crushed into some fragments to create more surface area. The crushed pebbles were soaked in 5 % hydrofluoric acid at room temperature, about 20–25 °C, for 24 h. The residues were collected by a sieve with a mesh opening of 0.054 mm. This process was repeated four times. Fossil specimens in the residues were picked up and mounted on stabs. The specimens on the stabs were photographed by scanning electron microscopy. Part of the residues was enclosed within a slide prepared with a photocrosslinkable mounting medium (GJ-4006, Gluelabo Ltd.). The slides were photographed using a transmitted light microscope.

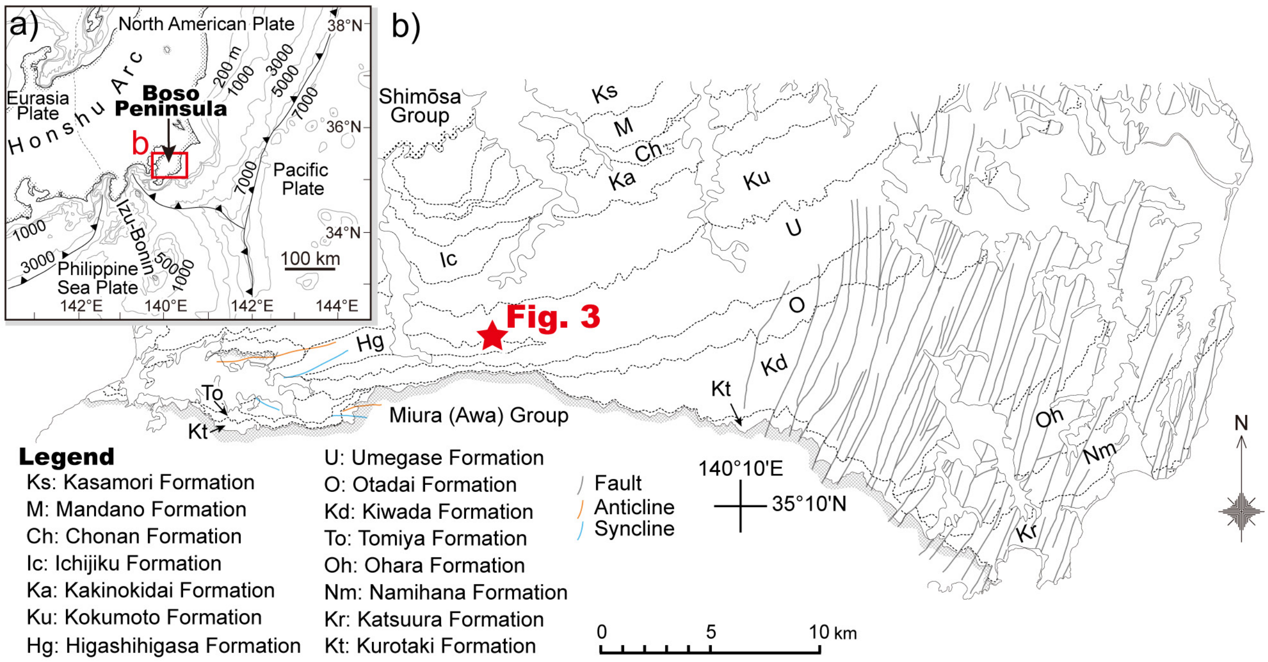


Fig. 1 Index and simplified geologic maps of Boso Peninsula (modified after from Utsunomiya *et al.*, 2019).

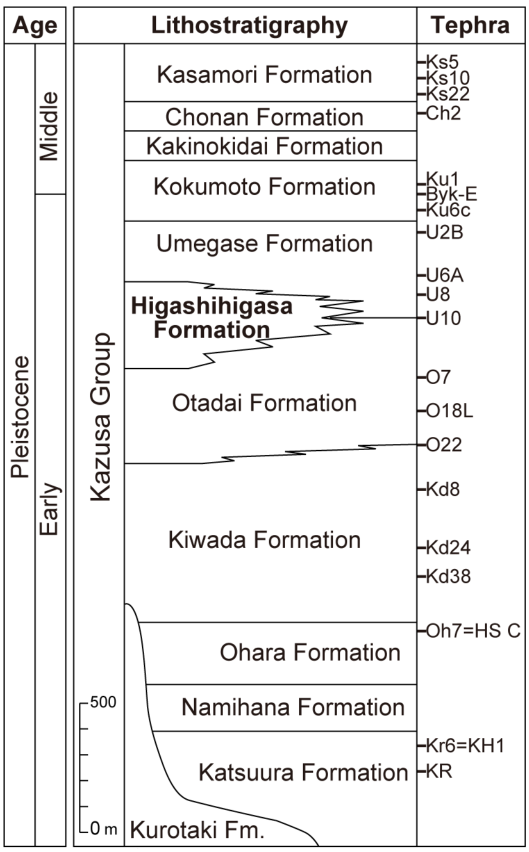


Fig. 2 Stratigraphy of the Kazusa Group in the Boso Peninsula (modified after from Utsunomiya *et al.*, 2019).

## 4. Microfossil occurrences

Among the four pebbles, only one pebble (sample 21112309a) yielded radiolarians and conodonts. The pebble is a rounded reddish chert, and its diameter is about 3 cm (Fig. 4B). The radiolarian and conodont specimens are shown in Fig. 5.

Some radiolarians, *Praemesosaturnalis* sp. cf. *P. heilongjiangensis* Yang and Mizutani, *Praemesosaturnalis*? sp., *Paroertlispongus*? sp., Poulpidae? gen. et sp. indet. and Spumellaria gen. et sp. indet. were extracted. The specimens identified as *Praemesosaturnalis* sp. cf. *P. heilongjiangensis* (Figs. 5.1–5.5) seem to have spines with an elevated margin and bifurcated end. Such a spine is known in a broken specimen of *Praemesosaturnalis heilongjiangensis* (Yang and Mizutani, 1991).

Two specimens of conodonts were extracted. One specimen (Fig. 5.33) can be identified as *Mockina* sp. due to the following characters: a carina extending to the posterior end, a platform with only one sharp denticle on the lateral margin and an anteriorly shifted basal pit, at which the basal margin is upturned.

## 5. Age assignment

*Praemesosaturnalis heilongjiangensis* was originally described in the Norian (Upper Triassic) in the Nadanhada Terrane, Northeast China (Yang and Mizutani, 1991). The species has also been reported from the Norian in other areas (e.g. Yao, 1982; Yoshida, 1986; Tekin, 2002). According to Sugiyama (1997), *Praemesosaturnalis*

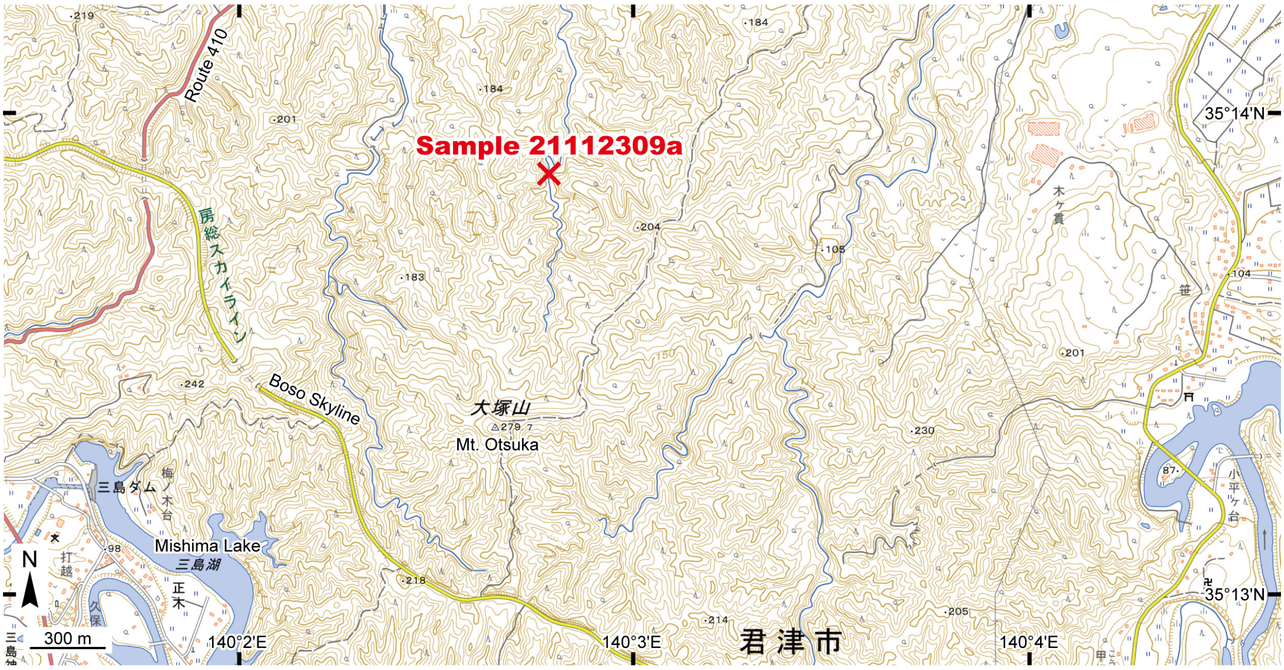


Fig. 3 Locality map. The map is modified from the topographic map published by Geospatial Information Authority of Japan (https://maps.gsi.go.jp/).

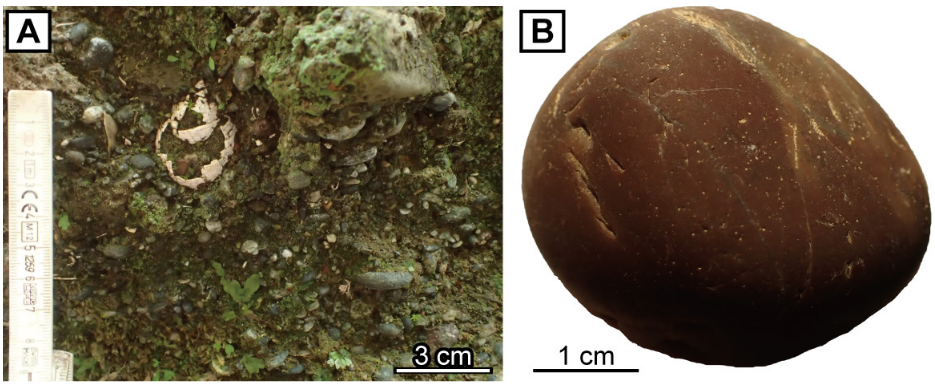


Fig. 4 Photographs of conglomerate and pebble. (A) Conglomerate of the Higashihigasa Formation of the Kazusa Group, Boso Peninsula. (B) Microfossil-bearing red chert pebble (sample 21112309a).

*heilongjiangensis* group mainly occurs in TR8A to TR8C, Norian, Upper Triassic.

The genus *Mockina* occurs in the middle to upper Norian (upper Alaunian to lower Sevatian) (Mazza *et al.*, 2012; Rigo *et al.*, 2018). The updated integrated biostratigraphy of radiolarians and conodonts by Yamashita *et al.* (2018) showed the co-occurrence of *Praemesosaturnalis heilongjiangensis* group and species of *Mockina* in the middle to upper Norian.

Based on the above-mentioned radiolarian and conodont occurrences, the sample is middle to late Norian in age.

## 6. Implication

In Southwest Japan, Triassic chert is a component rock of Jurassic accretionary complexes of the Tamba–Mino–Ashio and Chichibu belts (e.g. Nakae, 2000; Matsuoka *et al.*, 1998; Kojima *et al.*, 2016). Consequently, the chert pebble dealt with in this study must be derived from one of these Jurassic accretionary complexes. Meanwhile, the Jurassic accretionary complex is not exposed near the Boso Peninsula (Fig. 6). The nearest-exposed Jurassic accretionary complexes are those in the Yamizo Mountains (Ashio Belt), Ashio Mountains (Ashio Belt) and Kanto

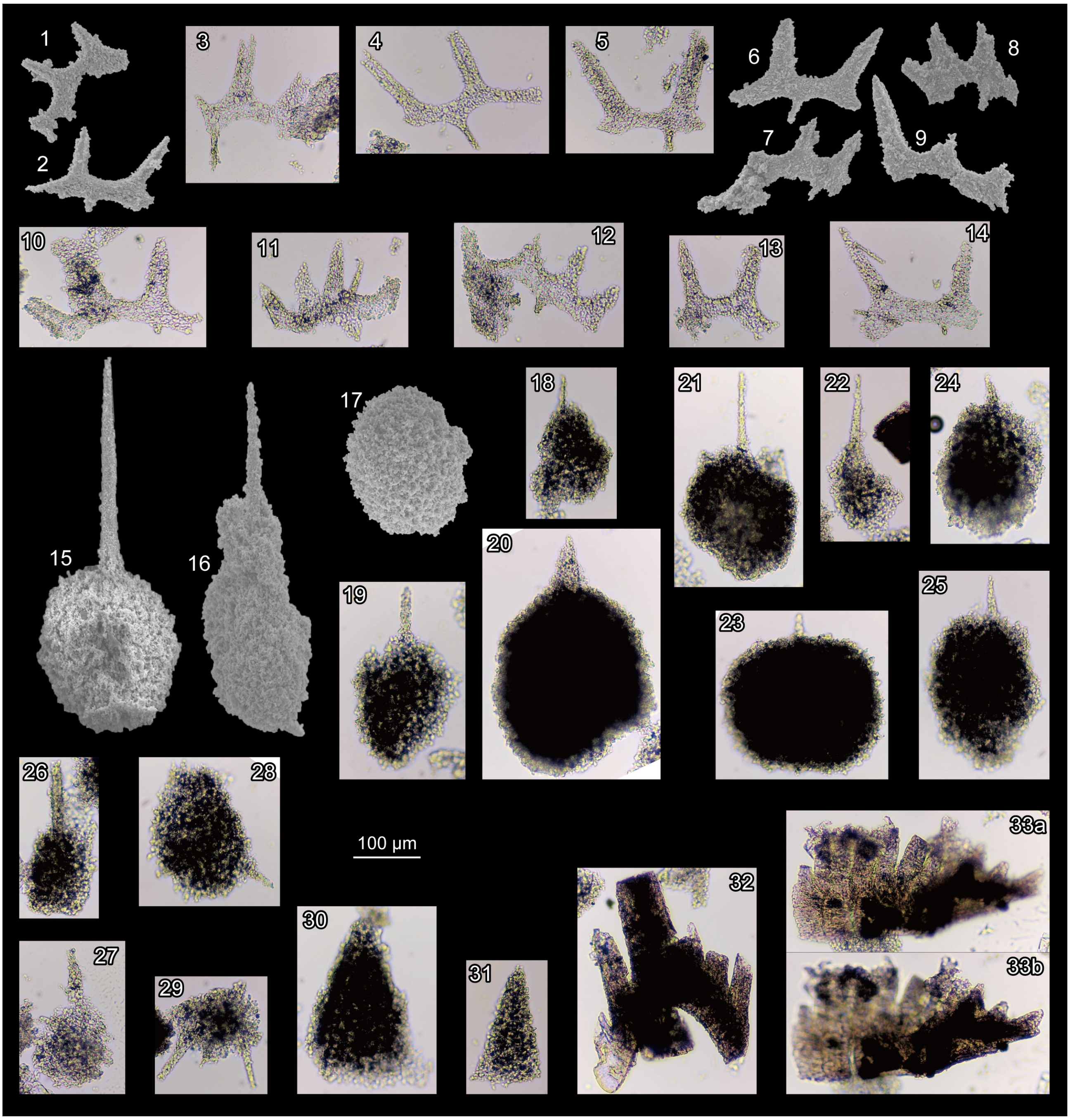


Fig. 5 Late Triassic radiolarians (1–31) and conodonts (32, 33) from the chert pebble (sample 21112309a). (1–5) *Praemesosaturnalis* sp. cf. *P. heilongjiangensis* Yang and Mizutani. (6–14) *Praemesosaturnalis*? sp. (15) *Paroertlispongus*? sp. (16–28) Spumellaria gen. et sp. indet. (29) Poulpidae? gen. et sp. indet. (30, 31) Nassellaria gen. et sp. indet. (32) Breviform digyrate conodont element (M element?). (33) *Mockina* sp.

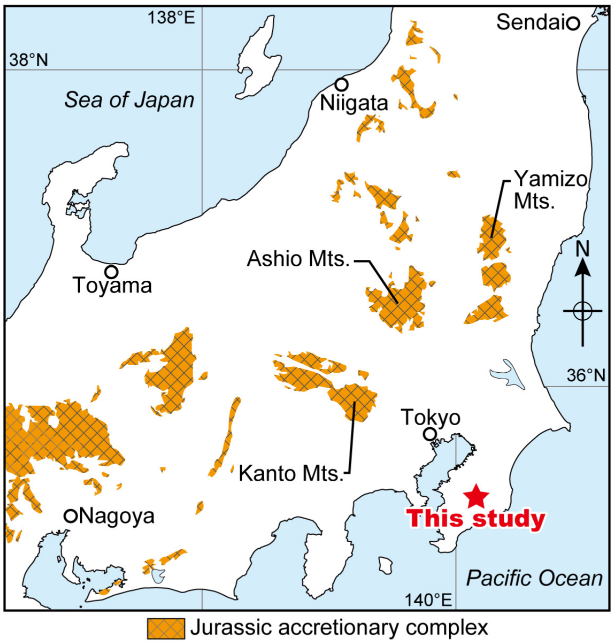


Fig. 6 Distribution of Jurassic accretionary complexes in central Japan. The distribution is based on Geological Survey of Japan, AIST (2020).

Mountains (Chichibu Belt). The Jurassic accretionary complex in one of these mountains is the presumable origin of the chert pebble. Triassic chert pebbles have also been reported from the Neogene in the Boso Peninsula (Yamamoto *et al.*, 2012), so the chert pebble might be secondarily derived from such strata.

In the current knowledge, the origin of the pebble is not conclusive. Triassic chert is found throughout most of the Jurassic accretionary complex, whereas some lithologies (e.g. limestone, Permian chert, Upper Jurassic mudstone) are unevenly distributed in the complex. If clasts of these lithologies can be found, their origin can be determined in more detail. Further accumulation of the data of the Quaternary in and near the Boso Peninsula will clarify its origin more accurately.

**Acknowledgments:** We thank Dr. NAYA Tomonori (editor) and Dr. UCHINO Takayuki (reviewer) for constructive comments that improved this manuscript.

## References

Geological Survey of Japan, AIST (2020) Seamless digital geological map of Japan 1: 200,000. Geological Survey of Japan, AIST. https://gbank.gsj.jp/seamless/v2.html [Accessed: Aug. 8th, 2021].

Inose, H., Furuuchi, K., Ito, T., Sashida, K. and Agematsu, S. (2018) Radiolarian fossils from conglomerate layers of the Upper Cretaceous Nakaminato Group exposed along the Pacific coast of Ibaraki Prefecture, central Japan: Staged denudation of the mid-Mesozoic accretionary complexes in the Kanto District. *Paleontological Research*, **22**, 307–325.

Ishida, K. (1999) Radiolarians as tracers for provenance of gravels in Lower Cretaceous molasse (Outer Zone of SW Japan). *Geodiversitas*, **21**, 637–656.

Ishida, K. and Hashimoto, H. (1997) Mesozoic and Paleozoic radiolarians from the chert pebbles and fine clastics of the Ryoseki and Monobegawa groups in East Shikoku. *News of Osaka Micropalaeotologist (NOM), Special Volume*, no. 10, 217–235 (in Japanese with English Abstract).

Ishida, K., Kozai, T., Park, S. O. and Mitsugi, T. (2003) Gravel bearing radiolarian as tracers for erosional events: a review of the status of recent research in SW Japan and Korea. *Journal of Asian Earth Sciences*, **21**, 909–920.

Ito, T. and Nakamura, Y. (2021) Radiolarians from Jurassic accretionary complex of the Chichibu belt in the western Akaishi Mountains and chert pebbles of the Miocene Wada Formation in Minami-Shinano, central Japan. *Fossils (Kaseki)*, no. 110, 3–16. (in Japanese with English abstract)

Ito, T., Sakai, Y., Ibaraki, Y., Yoshino, K., Ishida, N., Umetsu, T., Nakada, K., Matsumoto, A., Hinohara, T., Matsumoto, K. and Matsuoka, A. (2012) Radiolarian fossils from siliceous rock pebbles within conglomerates in the Mizukamidani Formation of the Tetori Group in the Itoigawa area, Niigata Prefecture, central Japan. *Bulletin of Itoigawa City Museums*, no. 3, 13–25. (in Japanese with English abstract)

Ito, T., Sakai, Y., Ibaraki, Y. and Matsuoka, A. (2014) Middle Jurassic radiolarians from a siliceous mudstone clast within conglomerate of the Tetori Group in the Itoigawa area, Niigata Prefecture, central Japan. *Science Reports of Niigata University (Geology)*, no. 29, 1–11.

Ito, T., Sakai, Y., Feng, Q. L. and Matsuoka, A. (2015) Middle Jurassic radiolarians from chert clasts in conglomerates of the Tetori Group in the Taniyamadani valley, Fukui Prefecture, central Japan. *Science Reports of Niigata University (Geology)*, no. 30, 1–13.

Ito, T., Kitagawa, Y. and Matsuoka, A. (2016) Middle and Late Permian radiolarians from chert blocks within conglomerates of the Kamiaso Unit of the Mino terrane in Gifu Prefecture, central Japan. *The Journal of the Geological Society of Japan*, **122**, 249–259. (in Japanese with English abstract)

Ito, T., Ibaraki, Y. and Matsuoka, A. (2017a) Outline and history of the Itoigawa UNESCO Global Geopark in Niigata Prefecture in central Japan, with radiolarian occurrences in Itoigawa. *Science Reports of Niigata University (Geology)*, no. 32 (supplement), 71–90.

Ito, T., Kitagawa, Y. and Matsuoka, A. (2017b) An aberrant bi-apical Follicucullus (Albaillellaria) from the late Guadalupian (Middle Permian), with the possible oldest evidence on double malformation in radiolarians. *Journal of Micropalaeontology*, **36**, 222–223.

Ito, T., Kurihara, T., Hakoiwa, H., Ibaraki, Y. and Matsuoka, A. (2017c) Late Silurian radiolarians from a radiolarite pebble within a conglomerate, Kotaki, Itoigawa, Niigata Prefecture, central Japan. *Science Reports of Niigata University (Geology)*, no. 32, 1–14.

Ito, T., Kurihara, T., Hakoiwa, H., Ibaraki, Y. and Matsuoka, A. (2017d) Discovery of the oldest fossil in Niigata Prefecture of central Japan from the Kotaki area, Itoigawa: A report on collaboration research of Itoigawa City, Niigata University, and Geological Survey of Japan, AIST. *Bulletin of Itoigawa City Museums*, no. 4, 23–31. (in Japanese with English abstract)

Ito, T., Sakai, Y., Feng, Q. L. and Matsuoka, A. (2017e) Review of microfossil-bearing clasts within Late Mesozoic strata in East Asia: staged denudation of mid-Mesozoic accretionary complexes. *Ofioliti*, **42**, 39–54.

Ito, T., Abe, T. and Miyakawa, A. (2020) Paleozoic and Mesozoic radiolarian fossils from siliceous rock pebbles of the Pleistocene in sediment core from Nishimikawa Plain, central Japan: Estimation of a source of the pebbles. *The Quaternary Research (Daiyonki-Kenkyu)*, **59**, 105–116. (in Japanese with English abstract)

Ito, T., Kawajiri, T. and Matsuoka, A. (in press) Permian radiolarians and spicules from conglomerate of the Lower Jurassic Kuruma Group in Itoigawa, Niigata Prefecture, central Japan. *Paleontological Research*.

Kamata, Y. (1997) Late Permian to Late Triassic radiolarians obtained from a float of the sandstone and chert breccia on the Ashio Mountains (preliminary report). *News of Osaka Micropalaeotologist (NOM), Special Volume*, no. 10, 97–107. (in Japanese with English abstract)

Kamemura, T. and Oakmura, M. (1994) Geologic age and it's source of radiolarites from the Paleogene formations, eastern Hokkaido. *Abstracts of the 101st Annual Meeting of the Geological Society of Japan*, 142. (in Japanese)

Kametaka, M. (1997) Radiolarian fossils from conglomerate of the Upper Triassic Nariwa Group, and their geological significance. *News of Osaka Micropalaeotologist (NOM), Special Volume*, no. 10, 127–131. (in Japanese with English abstract)

Kashiwagi, K. (2012) Sedimentary environment of the Nirehara Formation (Lower Miocene) in the Yatsuo area, Toyama Prefecture of central Japan and Paleozoic and Mesozoic radiolarian fossils from chert pebbles and cobbles. *Memoir of the Fukui Prefectural Dinosaur Museum*, **11**, 27–47. (in Japanese with English abstract)

Kashiwagi, K. and Isaji, S. (2015) Paleozoic and Mesozoic radiolarians from chert pebbles and cobbles of the Lower Cretaceous Choshi Group, Japan. *Natural History Research (Natural History Museum and Institute, Chiba)*, **14**, 35–46.

Kashiwagi, K., Isaji, S. and Asai, H. (2013) Latest Late Jurassic to early Late Cretaceous radiolarians extracted from a gravel of the calcareous nodule originated from the basal conglomerate of the Pliocene Naarai Formation, Choshi area of Kanto Region, central Japan. *The Journal of the Geological Society of Japan*, **119**, 647–652. (in Japanese with English abstract)

Kawajiri, K. and Kashiwagi, K. (2012) Triassic and Jurassic radiolarians from the chert pebbles of the Plio–Pleistocene Nakatsu Group in the central part of Kanagaw Prefecture, central Japan. *Bulletin of the Sagamihara City Museum*, no. 20, 65–74. (in Japanese)

Kazaoka, O., Suganuma, Y., Okada, M., Kameo, K., Head, M.J., Yoshida, T., Sugaya, M., Kameyama, S., Ogitsu, I., Nirei, H., Aida, N. and Kumai, H. (2015) Stratigraphy of the Kazusa Group, Boso Peninsula and highly-resolved marine sedimentary record from the Lower and Middle Pleistocene of central Japan. *Quaternary International*, **383**, 116–135.

Kishu Shimanto Research Group (2017) Discovery of the Paleocene radiolarian fossils from mudstone gravels in the Nyunokawa Formation of the Shimanto Superbelt in the Kii Peninsula—The Study of the Shimanto Terrain in the Kii Peninsula, Southwest Japan (Part 16)—. *Earth Science (Chikyu Kagaku)*, **71**, 167–184. (in Japanese with English abstract)

Kojima, S. (1986) Occurrence of Permian radiolarians from chert pebbles in conglomerate at Yokoo, Nyukawa Village, Gifu prefecture, central Japan. *News of Osaka Micropalaeotologist (NOM), Special Volume*, no. 7, 175–179. (in Japanese with English abstract)

Kojima, S., Hayasaka, Y., Hiroi, Y., Matsuoka, A., Sano, H., Sugamori, Y., Suzuki, N., Takemura, S., Tsujimori, T. and Uchino, T. (2016) Pre-Cretaceous accretionary complexes. *In* Moreno, T., Wallis, S. and Gibbons, W., eds., *The Geology of Japan, Geological Society of London*, London, 61–100.

Kumazaki, N. and Kojima, S. (1996) Depositional history and structural development of the Kuruma Group (Lower Jurassic) on the basis of clastic rock composition. *The Journal of the Geological Society of Japan*, **102**, 285–302. (in Japanese with English abstract)

Matsukawa, M. and Takahashi, O. (1999) Radiolarian fossils occurred from the Itoshiro Subgroup of the Tetori Group and its geological significance. *Abstracts of the 106th Annual Meeting of the Geological Society of Japan*, 165. (in Japanese)

Matsuoka, A., Yamakita, S., Sakakibara, M. and Hisada, K. (1998) Unit division for the Chichibu Composite Belt from a view point of accretionary tectonics and geology of western Shikoku Japan. *The Journal of* *the Geological Society of Japan*, **104**, 634–653. (in Japanese with English abstract)

Matsuoka, K. (1998) Cretaceous radiolarian red shale pebbles from the Hannou Gravel in the eastern margin of Kanto Mountains, Japan. *Earth Science (Chikyu Kagaku)*, **52**, 324–328. (in Japanese with English abstract)

Matsuoka, K. and Kuwahara, K. (2021) Discovery of Capitanian (Permian) radiolarians and occurrence of conglomerate in volcaniclastic rocks in the Sumaizuku Unit of the Northern Chichibu Belt in the Kanto Mountains, Central Japan. *Earth Science (Chikyu Kagaku)*, **75**, 119–124. (in Japanese with English abstract)

Mazza, M., Rigo, M. and Gullo, M. (2012) Taxonomy and biostratigraphic record of the Upper Triassic conodonts of the Pizzo Mondello section (western Sicily, Italy), GSSP candidate for the base of the Norian. *Rivista Italiana di Paleontologia e Stratigrafia*, **118**, 85–130.

Nakae, S. (2000) Regional correlation of the Jurassic accretionary complex in the Inner Zone of Southwest Japan. *The Memoirs of the Geological Society of Japan*, no. 55, 73–98. (in Japanese with English abstract)

Nakajima, T. and Watanabe, M. (2005) *Geology of the Futtsu District.* Quadrangle Series, 1:50,000, Geological Survey of Japan, AIST, 102p. (in Japanese with English abstract)

Nikaido, T. and Matsuoka, A. (2004) Middle Jurassic radiolarian fossils from clasts of the Raga Formation and provenance of Raga Formation, Miyako Group in Iwate Prefecture. *Abstracts of the 111st Annual Meeting of the Geological Society of Japan*, 34. (in Japanese)

Ozeki, M., Shimizu, N., Agematsu, S. and Sashida, K. (2021) Microfossils from siliceous rock pebbles contained in the Lower Cretaceous Ishido Formation of the Sanchu Group, central Japan. *Journal of Geography (Chigaku Zasshi)*, **130**, 311–329. (in Japanese with English abstract)

Pickering, K. T., Souter, C., Oba, T., Taira, A., Schaaf, M. and Platzman, E. (1999) Glacio-eustatic control on deep-marine clastic forearc sedimentation, Pliocene–mid-Pleistocene (c. 1180–600 ka) Kazusa Group, SE Japan. *Journal of the Geological Society*, London, **256**, 125–136.

Rigo, M., Mazza, M., Karádi, V. and Nicora, A. (2018) New Upper Triassic conodont biozonation of the Tethyan realm. *In* Tanner, L., ed., *The Late Triassic World*. *Topics in Geobiology*, **46**. 189–235.

Saida, T. (1987) Triassic and Jurassic radiolarians in chert clasts of the Tetori Group in Tamodani area of Izumi Village, Fukui Prefecture, central Japan. *The Journal of the Geological Society of Japan*, **93**, 57–59. (in Japanese)

Saito, M. and Tsukamoto, H. (1993) Chert breccia, its occurrence and radiolarian fossils in the Hichiso-Mugi area, central Mino Terrane, central Japan. *The Journal of the Geological Society of Japan*, **99**, 117–133. (in Japanese with English abstract)

Sugiyama, K. (1997) Triassic and Lower Jurassic radiolarian biostratigraphy in the siliceous claystone and bedded chert units of the southeastern Mino terrane, central Japan. *Bulletin of the Mizunami Fossil Museum*, no. 24, 79–193.

Suzuki, N., Takashima, R., Nishi, H. and Saito, T. (1996) Triassic and Jurassic Polycystine (Radiolaria) from the siliceous shale pebbles of the Lowest Middle Ezo Group, Soushunai Area, Hokkaido. *Abstracts of the 103rd Annual Meeting of the Geological Society of Japan*, 140. (in Japanese)

Takemura, S., Umeda, M., Yao, A. and Suzuki, S. (1996) Middle and Late Permian radiolarian fossils yielding from siliceous rock pebbles in the Middle and Upper Permian Maizuru Group, Southwest Japan. *The Journal of the Geological Society of Japan*, **102**, 820–823. (in Japanese with English abstract)

Takeuchi, M., Saito, M. and Takizawa F. (1991) Radiolarian fossils obtained from conglomerate of the Tetori Group in the upper reaches of the Kurobegawa River, and its geologic significance. *The Journal of the Geological Society of Japan*, **97**, 345–359. (in Japanese with English abstract)

Takeuchi, M., Takenouchi, K. and Tokiwa, T. (2015) Range Metamorphic Rocks and the Mesozoic terrigenous strata. *The Journal of the Geological Society of Japan*, **121**, 193–216. (in Japanese with English abstract)

Tekin, U. K. (2002) Late Triassic (Late Norian–Rhaetian) radiolarians from the Antalya Nappes, Central Taurides, Southern Turkey. *Rivista Italiana di Paleontologia e Stratigrafia*, **108**, 415–440.

Tokuhashi, S. and Endo, H. (1984) *Geology of the Anesaki District*. Quadrangle Series, scale 1:50,000, Geological Survey of Japan, 136 p. (in Japanese with English abstract)

Tomita, S., Takeuchi, M. and Kametaka, M. (2007) Radiolarian fossils obtained from conglomerate of the Tetori Group in the northeastern part of Toyama Prefecture and its geological significance. *Abstracts of the 114th Annual Meeting of the Geological Society of Japan*, 243. (in Japanese)

Uchino, T. and Kurihara, T. (2019) Middle Devonian–early Carboniferous radiolarian fossils extracted from the conglomerate in the Nedamo Complex, Nedamo Terrane, Northeast Japan. *Bulletin of the Geological Survey of Japan*, **70**, 109–115. (in Japanese with English abstract)

Umeda, M. (1997) Petrography of orthoquartzite clasts and radiolarian fossils in chert clasts in the Late Oligocene conglomerate on the Mesozoic complex of the Nanjo Massif in the Mino Terrane, Central Japan. *Earth Science (Chikyu Kagaku)*, **51**, 199–211. (in Japanese with English abstract)

Umeda, M. and Sugiyama, K. (1998) Paleozoic and

Mesozoic radiolarians from pebbles of siliceous rocks of the Upper Jurassic Shiranezaki Formation in the Toba area, Mie Prefecture, Southwest Japan. *The Journal of the Geological Society of Japan*, **104**, 454–461. (in Japanese with English abstract)

Umeda, M., Kugimiya, Y. and Ishiga, H. (1992) Late Triassic–Early Jurassic Radiolarians from chert pebbles of the Middle Miocene in northern part of Ooda City, Shimane Prefecture, Japan. *Geological Reports of Shimane University*, **11**, 71–76. (in Japanese with English abstract)

Umeda, M., Takemura, S. and Yao, A. (1995) Mesozoic and Paleozoic radiolarians from the chert pebbles of the Lower Cretaceous Sasayama Group in the eastern part of Hyogo Prefecture, Southwest Japan. *The Journal of the Geological Society of Japan*, **101**, 937–939. (in Japanese with English abstract)

Utagawa, F., Sashida, K., Agematsu, S. and Kozu, S. (2017) Triassic and Jurassic radiolarian fossils from siliceous rock pebbles contained in the Nojimazaki Conglomerate Member of the upper Pliocene Shirahama Formation, Chikura Group, Central Japan. *The Journal of the Geological Society of Japan*, **123**, 969–976. (in Japanese with English abstract)

Utsunomiya, M. and Ooi, S. (2019) Geology of the Kazusa-Ohara District. Quadrangle Series, 1:50,000, Geological Survey of Japan, AIST, 127p. (in Japanese with English abstract)

Utsunomiya, M., Mizuno, K. and Tamura, I. (2019) Stratigraphic positions and characteristics of tephra beds in the lower to middle Kiwada Formation (lower Pleistocene), Kazusa Group. *Bulletin of the Geological Survey of Japan*, **70**, 373–441. (in Japanese with English abstract)

Yabuta, S., Takeuchi, M. and Saito, M. (2021) Conglomerate in the Kuroze Formation of the Miocene Shidara Group, eastern Aichi Prefecture, central Japan: Change in the provenance during the deposition of the Hokusetsu Subgroup. *The Journal of the Geological Society of Japan*, **127**, 689–700. (in Japanese with English abstract)

Yamamoto, Y., Chiyonobu, S., Kurihara, T., Yamaguchi, A., Hina, S., Hamahashi, M., Raimbourg, H., Augier, R. and Gadenne, L. (2012) Unconformity between a Late Miocene–Pliocene accretionary prism (Nishizaki Formation) and Pliocene trench-slope sediments (Kagamigaura Formation), central Japan. *Island Arc*, **21**, 231–234.

Yamauchi, S., Mitsunashi, T. and Okubo, S. (1990) Growth pattern of the Early Pleistocene Higashihigasa Submarine Channel, Boso Peninsula, central Japan. *The Journal of the Geological Society of Japan*, **96**, 523–536.

Yamashita, D., Kato, H., Onoue, T. and Suzuki, N. (2018) Integrated Upper Triassic conodont and radiolarian biostratigraphies of the Panthalassa Ocean. *Paleontological Research*, **22**, 167–197.

Yang, Q. and Mizutani, S. (1991) Radiolaria from the Nadanhada Terrane, Northeast China. *The Journal of Earth Sciences, Nagoya University*, **38**, 49–78.

Yao, A. (1982) Middle Triassic to Early Jurassic Radiolarians from the Inuyama Area, Central Japan. *Journal of Geosciences, Osaka City University*, **25**, 53–70.

Yoshida, H. (1986) Upper Triassic to Lower Jurassic radiolarian biostratigraphy in Kagamigahara City, Gifu Prefecture, central Japan. *The Journal of Earth Sciences, Nagoya University*, **34**, 1–21.

*Translated by the authors.

Recieved January 21, 2022
Accepted June 16, 2022
Published on-line July 20, 2022

## 房総半島，上総層群の下部更新統東日笠層のチャート礫から産出した後期三畳紀放散虫及びコノドント

伊藤　剛・武藤　俊・宇都宮正志

### 要　旨

房総半島の上総層群の下部更新統東日笠層に挟在する礫岩中のチャート礫から，放散虫及びコノドントが産出した．放散虫（*Praemesosaturnalis* sp. cf. *P. heilongjiangensis*）とコノドント（*Mockina* sp.）の同定に基づくと，このチャート礫は後期三畳紀（中期～後期ノーリアン期）の年代を示す．本チャート礫は当時後背地に分布していたジュラ紀付加体に由来すると考えられる．

Bulletin of the Geological Survey of Japan, vol. 73 (3), p. 103–135, 2022

Report

# Chemical compositions and ages of basalts from seamounts in the Northwest Pacific

YAMAOKA Kyoko[1,*], ISHIZUKA Osamu[2], MOROZUMI Haruhisa[3] and HINO Hikari[3]

YAMAOKA Kyoko, ISHIZUKA Osamu, MOROZUMI Haruhisa and HINO Hikari (2022) Chemical compositions and ages of basalts from seamounts in the Northwest Pacific. *Bulletin of the Geological Survey of Japan*, vol. 73(3), p. 103–135, 16 figs and 4 tables.

**Abstract:** As part of the exploration for cobalt-rich ferromanganese crusts in the Northwest Pacific, seamount basalts were collected for chemical composition analysis and K–Ar/Ar–Ar dating. Although the primary chemical compositions of the seamount basalts were not well preserved due to alteration and phosphatization, all 20 seamounts sampled showed typical characteristics of ocean island alkaline basalts. K–Ar dating did not provide reliable ages due to alteration, but Ar–Ar dating provided reliable plateau ages for several seamounts. Formation ages of 67–116 Ma were obtained from the Marcus-Wake Seamount Group, 87 Ma and 105 Ma from the Magellan Seamount Group, and 90 Ma from the Marshall Islands Seamount Group, which were generally consistent with those reported in previous studies.

**Keywords**: Northwest Pacific, hot spot volcanism, K–Ar/Ar–Ar dating, geochemistry

## 1. Introduction

The Japan Oil, Gas and Metals National Corporation (JOGMEC, formerly the Metal Mining Agency of Japan) has been conducting exploration for cobalt-rich ferromanganese crusts (referred to as cobalt-rich crusts) in the Northwest Pacific (JA area, Fig. 1) since 1987 commissioned by the Ministry of Economy, Trade and Industry (METI, formerly the Ministry of International Trade and Industry). Promising seamounts were selected based on the evaluation of the mineral resources in each seamount, and a 15-year exploration contract was signed with the International Seabed Authority (ISA) in January 2014 for a total of 3,000 km$^2$ of the flat tops of six seamounts (JA02, JA03, JA04, JA06, JA12, JA17) off the southeast of Minami-Torishima Island. The exploration contract requires that an environmental baseline survey be conducted in order to assess the environmental impact of future mining activities in addition to the resource estimation survey.

In this paper, we report on the chemical composition and age of the seamount basement rocks obtained in previous surveys. The formation history of the seamounts inferred from these data provides basic geological information and is useful for understanding the formation mechanism of cobalt-rich crusts. It is also important to understand the characteristics of the particles derived from the basement rock for the suspended plume generated during the mining activity.

## 2. Study area

The JA area is in the southwest of the North Pacific, extending from around Minami-Torishima Island (Marcus Island) in the north to the Caroline Islands in the south, and from Wake Island in the east to the Mariana Trench in the west. In the northern part of the JA area, the Marcus-Wake Seamounts (JA01-JA06, JA11, JA12, JA17, JA18, MT473) are linked in an east-west direction, and their eastern extension is continuous with the Central Pacific Seamounts. The Magellan Seamounts (JA09, JA13-JA15, JA19, JA22) are arranged in the NW-SE direction from the central to the southern part of the JA area. To the southeast of the JA area, the Marshall Islands Seamounts are aligned in the NNW-SSE direction, and some of the seamounts at their northwestern end are distributed in the southeast of this area (JA10, JA16) (Fig. 1).

Most JA seamounts are flat-topped (Guyots), and their tops are generally shallower than 1,400 m in depth. The basement rocks of the seamounts are mainly basalt, hyaloclastite, and conglomerate, which are covered by shallow-water limestones and pelagic sediments.

[1] AIST, Geological Survey of Japan, Research Institute of Geology and Geoinformation
[2] AIST, Geological Survey of Japan, Research Institute of Earthquake and Volcano Geology
[3] Japan Oil, Gas and Metals National Corporation (JOGMEC)
[*] Corresponding author: YAMAOKA, K., Central 7, 1-1-1 Higashi, Tsukuba, Ibaraki 305-8567, Japan. Email: k.yamaoka@aist.go.jp

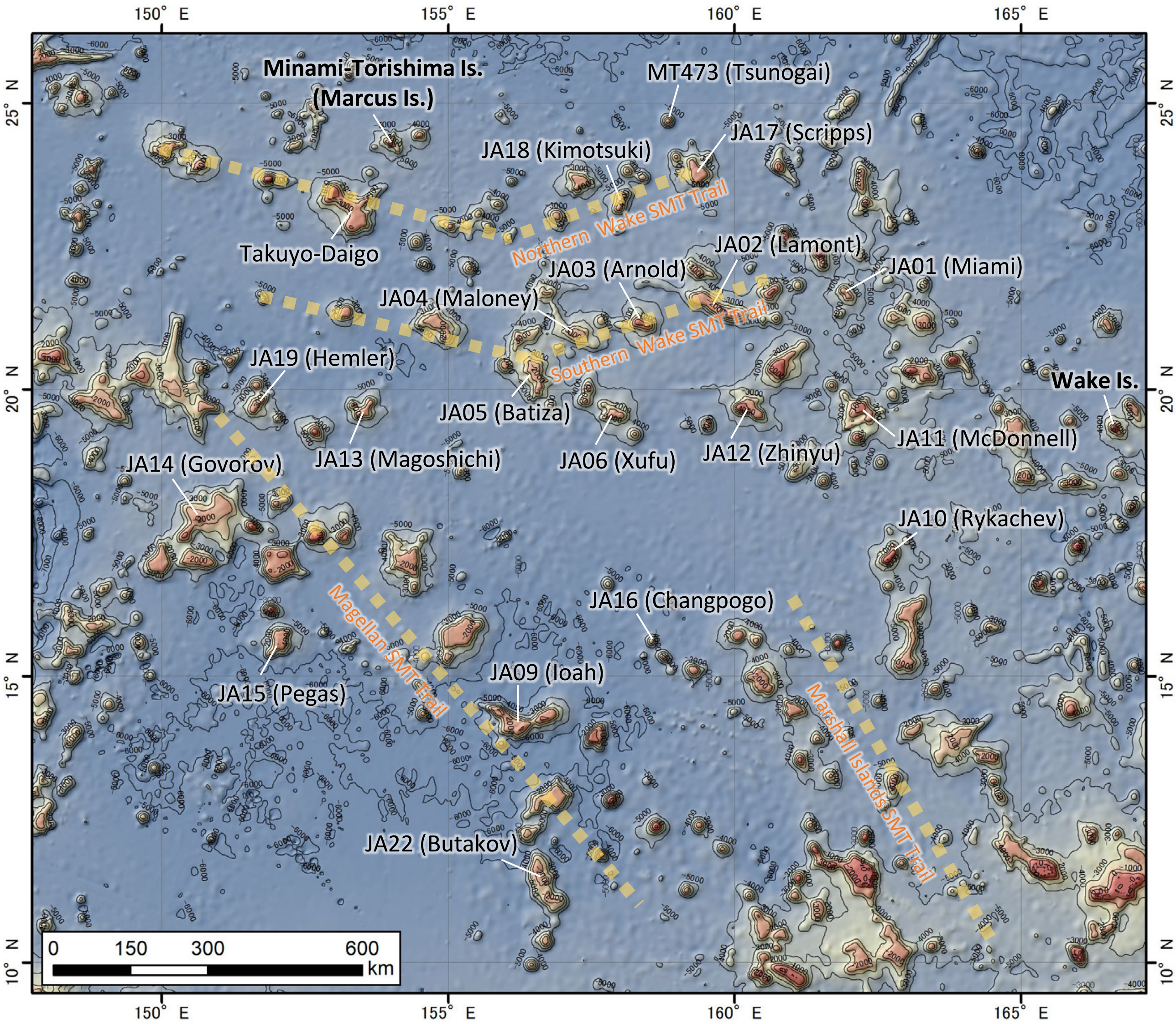


Fig. 1 JJA area in the Northwest Pacific with seamount names. The map was created using ArcGIS ver10.8.1 (ESRI Japan). The used topographic data is ETOPO1 published by NOAA National Centers for Environmental Information (NCEI). The coordinate system is the World Geodetic System (WGS 84).

The limestones contain fossils of corals and thick-toothed bivalves, suggesting that the volcanic islands or atolls gradually subsided and reached the present depth. Limestones are sometimes phosphatized to form phosphate rocks. The exposed basement rocks are covered with ferromanganese crusts of several to ten centimeters thick, and foraminiferal sand is deposited on the flat tops (Watkins *et al.*, 1995, Usui and Someya, 1997).

The depth of the basin is 5,500–6,000 m, and it is known to belong to the oldest zone in terms of geological age of anywhere on Earth, which corresponds to the Cretaceous-Jurassic period according to paleomagnetism (e.g., Larson *et al.*, 1985, Abrams *et al.*, 1993). Based on the $^{40}Ar/^{39}Ar$ age of basalts, it is considered that the Marcus-Wake Seamount Group was formed 100–120 Ma (Early Cretaceous), while the Magellan Seamount Group and the Marshall Islands Seamount Group were formed 70–100 Ma (Late Cretaceous) (Smith *et al.*, 1989, Staudigel *et al,* 1991, Koppers *et al.* 2003).

The chemical composition of these basalts is similar to that of basalts from hotspot volcanoes in French Polynesia in the South Pacific, suggesting that these seamounts were formed by volcanic activity in the French Polynesian region, and have been subducting since the Cretaceous, moving with plate movements to their present positions (Smith *et al.*, 1989, Staudigel *et al.*, 1991). Volcanic activity in French Polynesia is often characterized by unique isotopic features such as HIMU mantle endmember (Zindler and Hart, 1986), and is referred to as the South Pacific Isotope and Thermal Anomaly (SOPITA) (e.g., Staudigel *et al.*, 1991). However, Koppers *et al.* (2003) proposed that the seamount chain was formed by intermittent short-term hotspot activity with diverse isotopic compositions, rather than continuous hotspot activity over a long period of time, based on the diversity of isotopic ratios and the contrast between the two regions.

## 3. Materials and methods

In each seamount, rock samples were collected mainly by arm type dredge (AD) or chain-bag dredge (CB), and core samples were collected by deep-sea drill machine (BMS: Benthic Multi-Coring System) from 2001. The year and project name for which samples were collected and/or analyzed are shown in Table 1 and 2.

### 3. 1 Chemical analyses

Analytical methods for bulk chemical composition vary with each analysis year.

**FY1989–1990:** Detailed analysis methods are unknown.

**FY1997:** Major elements were measured by Inductively Coupled Plasma Atomic Emission Spectrometry (ICP-AES), FeO by titration, $CO_2$ by high-frequency combustion infrared absorption method, $H_2O$ and loss on ignition (LOI) by gravimetric method, and rare earth elements by instrumental neutron activation analysis.

**FY1998–2002:** Major elements were measured by ICP-AES, FeO by titration, $CO_2$ and $H_2O^+$ by high-frequency combustion infrared absorption method, $H_2O^-$ and LOI by gravimetric method, and trace elements by Inductively Coupled Plasma Mass Spectrometry (ICP-MS).

**FY2005:** Major elements were measured by X-ray Fluorescence Spectroscopy (XRF), FeO by titration, C by electrometric analysis, $H_2O^+$ by high-frequency combustion infrared absorption method, $H_2O^-$ and LOI by gravimetric method, and trace elements by ICP-MS.

**FY2018–2019:** Analysis was performed at ALS Canada Ltd., Canada, including pretreatment. Major elements were measured by XRF or ICP-AES after mixed lithium tetraborate and lithium metaborate melt treatment. Trace elements were measured by ICP-AES or ICP-MS after mixed acid treatment or lithium metaborate melting treatment; $H_2O^+$ was measured by high-frequency combustion infrared absorption method; $H_2O^-$ and LOI were measured by gravimetric method.

**FY2020:** Analysis was performed at GSJ/AIST. Rock samples were dissolved using mixed acid ($HNO_3$+HF), and then trace elements were measured by ICP-MS (Agilent 7700x) combined with the indium internal standard technique.

### 3. 2 K–Ar/Ar–Ar dating

Based on the observation under microscope, samples with minimal alteration were selected for dating. The K–Ar dating was conducted through 1998, and the Ar–Ar dating was conducted starting 1999.

In the K–Ar dating, potassium was determined using a flame photometer and argon isotope ratios were determined using a noble gas mass spectrometer. The decay constants used are based on Steiger and Jaeger (1977).

$\lambda e = 0.581 \times 10^{-10}$ /year

$\lambda\beta = 4.962 \times 10^{-10}$ /year

The ratio of $^{40}K$ in K was determined to be $^{40}K/K$ = 0.01167 atom%.

For the Ar–Ar dating, the analysis was carried out by the step heating method. When a constant Ar–Ar age is obtained from contiguous heating steps comprising >50 % of total $^{39}Ar$, the age is called a plateau age. Plateau ages are considered to indicate the age of formation of the sample without secondary Ar loss. The isochron age can also be determined from the Ar isotope ratios obtained from each step.

For the measurements, the samples were crushed, dried at 105 °C for 3 h, and then finely ground to 180–250 µm. The sample (2 g) was washed twice with 20 % nitric acid and once with 5 % hydrofluoric acid to prevent the formation of gases from carbonate minerals and other secondary minerals that could interfere with Ar analysis. The acid-washed sample was washed thoroughly with pure water, methanol and acetone. A portion of this sample was packed in aluminum foil and set in the reactor. Detailed procedures were described in Ishizuka *et al.* (2006).

Neutron irradiation was carried out at McMaster University in Canada in FY1999, 2000, and 2001. The samples and the standard samples for J-value measurement were irradiated for 45 hours. The standard samples used were LP-6 (biotite, 127.8 Ma) and Fish Canyon sanidine (27.95 Ma). The samples were heated in 8 to 11 steps in the range of 800 to 1800 K. In 2002, neutron irradiation was performed at the research reactor of Oregon State University. The samples and the standard samples for J-value measurement were irradiated for 16 hours. The standard sample used was Taylor Creek Rhyolite Sanidine (27.92 Ma). The sample was heated in 11 to 15 steps for the range of 460–1100 K.

Ar isotope corrections for K, Ca, and Cl originating from atmospheric and neutron irradiation were performed to determine the $^{40}Ar/^{39}Ar$ ratio. The $^{40}Ar/^{39}Ar$ ratio of the measured sample was then calculated from the J-value of the standard sample. The criteria for determining the age of the plateau were: 1) three or more consecutive heating age values in the medium to high temperature range must agree with each other with 95 % confidence limits, 2) the plateau must contain more than 50 % of the total $^{39}Ar$. The weighted average of all the age values comprising the plateau was used as the plateau age (Dalrymple *et al.*, 1980).

## 4. Chemical composition

The chemical compositions of the basement rocks from each seamount are summarized in Table 1 and 2, and the plots of $H_2O_{total}$ ($H_2O^+ + H_2O^-$) and $CO_2$ against LOI are shown in Fig. 2. The ratios of major elements to $SiO_2$ are shown in Fig. 3. LOI is >5 % in most of the samples, suggesting that they have suffered strong alteration.

Table 1 Major elemental compositions of basement rocks from seamounts in the JA area

| Year | Seamount | Sample ID | Rock type | (wt%) $SiO_2$ | $TiO_2$ | $Al_2O_3$ | $Fe_2O_3t$ | $Fe_2O_3$ | FeO | MnO | MgO | CaO | $Na_2O$ | $K_2O$ | $P_2O_5$ | $H_2O^+$ | $H_2O^-$ | $H_2O_{total}$ | $CO_2$ | LOI | Total | FeO* | Mg# | FeO*/MgO | Project name |
|---|---|---|---|---|---|---|---|---|---|---|---|---|---|---|---|---|---|---|---|---|---|---|---|---|---|
| 1999 | JA01 | 99JA01AD12 | Clinopyroxene olivine alkali basalt | 39.8 | 3.4 | 12.2 | | 8.9 | 2.3 | 0.3 | 7.1 | 11.8 | 2.0 | 1.4 | 1.8 | 4.0 | 4.2 | 8.1 | 0.3 | 8.8 | 99.9 | 10.3 | 0.41 | 1.45 | DMRS 1999 |
| 1999 | JA01 | 99JA01AD13 | Olivine clinopyroxene basalt | 42.8 | 3.2 | 15.2 | | 8.7 | 3.9 | 0.2 | 5.1 | 10.2 | 2.1 | 1.2 | 0.5 | 3.0 | 3.7 | 6.7 | 0.1 | 7.5 | 100.5 | 11.7 | 0.30 | 2.31 | DMRS 1999 |
| 1999 | JA01 | 99JA01AD18 | Clinopyroxene olivine alkali basalt | 40.3 | 3.7 | 14.3 | | 9.5 | 2.8 | 0.2 | 7.3 | 12.0 | 1.6 | 1.0 | 1.2 | 2.4 | 3.3 | 5.6 | 0.1 | 6.0 | 99.9 | 11.3 | 0.39 | 1.56 | DMRS 1999 |
| 1999 | JA01 | 99JA01AD23 | Clinopyroxene olivine alkali basalt | 48.6 | 2.4 | 18.4 | | 6.1 | 2.5 | 0.2 | 3.8 | 7.0 | 5.0 | 3.1 | 0.4 | 1.5 | 1.5 | 3.0 | >0.05 | 2.8 | 100.3 | 8.0 | 0.32 | 2.12 | DMRS 1999 |
| 2001 | JA02 | 01JA02BM02C | Olivine clinopyroxene basalt | 40.1 | 3.3 | 12.5 | | 8.3 | 4.7 | 0.2 | 8.0 | 13.0 | 2.8 | 1.2 | 1.2 | 2.7 | 1.2 | 3.9 | 0.2 | 4.7 | 99.9 | 12.1 | 0.40 | 1.51 | DMRS 2001 |
| 2001 | JA02 | 01JA02BM03A | Clinopyroxene olivine basalt | 39.3 | 3.0 | 11.5 | | 9.3 | 3.3 | 0.2 | 10.1 | 12.4 | 1.5 | 0.6 | 1.1 | 4.0 | 2.9 | 6.9 | 0.0 | 7.5 | 99.8 | 11.7 | 0.46 | 1.16 | DMRS 2001 |
| 2001 | JA02 | 01JA02BM05A | Olivine basalt | 36.9 | 3.2 | 11.8 | | 12.1 | 3.2 | 0.1 | 7.6 | 12.9 | 1.9 | 0.9 | 1.1 | 3.6 | 2.3 | 5.9 | 0.0 | 7.4 | 99.0 | 14.1 | 0.35 | 1.86 | DMRS 2001 |
| 2002 | JA02 | 02JA02BMS06B | | 39.4 | 2.4 | 13.1 | | 5.3 | 6.3 | 0.2 | 9.7 | 12.4 | 1.6 | 0.5 | 0.6 | 3.5 | 2.2 | 5.7 | 1.8 | 7.8 | 99.2 | 11.1 | 0.47 | 1.14 | DMRS 2002 |
| 2005 | JA02 | 01JA02BMS05B | | | | | | | | | | | | | | | | | | | | | | | SOPET 2005 |
| 2005 | JA02 | 01JA02BMS02B | | | | | | | | | | | | | | | | | | | | | | | SOPET 2005 |
| 2005 | JA02 | 02JA02BMS06B | | | | | | | | | | | | | | | | | | | | | | | SOPET 2005 |
| 2005 | JA02 | 02JA02BMS07A | | | | | | | | | | | | | | | | | | | | | | | SOPET 2005 |
| 2018 | JA02 | 18JA02#016BMS01A | Basalt | 45.8 | 1.8 | 14.4 | 12.1 | | | 0.2 | 7.5 | 9.3 | 2.9 | 1.0 | 0.7 | 3.2 | 4.1 | 7.3 | | 6.2 | 101.8 | 10.9 | 0.41 | 1.46 | SRAPT 2018 |
| 2018 | JA02 | 18JA02#016BMS01C | Basalt | 43.0 | 1.9 | 14.6 | 12.5 | | | 0.2 | 5.0 | 11.1 | 2.9 | 1.3 | 0.8 | 2.7 | 2.8 | 5.5 | | 6.9 | 100.1 | 11.2 | 0.31 | 2.23 | SRAPT 2018 |
| 2018 | JA02 | 18JA02#018BMS01A | Basalt | 39.0 | 2.7 | 14.4 | 12.4 | | | 1.2 | 6.3 | 6.6 | 1.8 | 2.2 | 1.8 | 5.1 | 6.6 | 11.8 | | 10.3 | 98.6 | 11.2 | 0.36 | 1.79 | SRAPT 2018 |
| 2018 | JA02 | 18JA02#018BMS01C | Basalt | 40.5 | 2.8 | 13.5 | 13.9 | | | 0.9 | 5.8 | 11.6 | 2.2 | 1.4 | 1.5 | 2.9 | 3.5 | 6.4 | | 5.9 | 100.0 | 12.5 | 0.32 | 2.13 | SRAPT 2018 |
| 2018 | JA02 | 18JA02#019BMS01A | Basalt | 42.4 | 1.3 | 13.8 | 12.3 | | | 0.2 | 8.9 | 8.9 | 2.4 | 1.4 | 0.5 | 3.7 | 5.0 | 8.7 | | 9.7 | 101.6 | 11.0 | 0.45 | 1.24 | SRAPT 2018 |
| 2018 | JA02 | 18JA02#020BMS01A | Basalt | 40.8 | 2.1 | 12.9 | 13.0 | | | 0.4 | 10.2 | 8.7 | 1.8 | 1.2 | 1.1 | 3.5 | 6.8 | 10.4 | | 8.3 | 100.4 | 11.7 | 0.47 | 1.15 | SRAPT 2018 |
| 2018 | JA02 | 18JA02#020BMS01B | Basalt | 41.0 | 2.4 | 14.4 | 14.9 | | | 1.2 | 5.9 | 4.3 | 2.4 | 1.8 | 0.8 | 6.2 | 8.7 | 14.8 | | 11.3 | 100.2 | 13.4 | 0.31 | 2.28 | SRAPT 2018 |
| 2018 | JA02 | 18JA02#020BMS01C | Basalt | 43.0 | 2.2 | 13.6 | 11.1 | | | 1.3 | 9.2 | 7.0 | 2.1 | 1.4 | 0.7 | 5.2 | 5.8 | 11.0 | | 9.8 | 101.3 | 9.9 | 0.48 | 1.08 | SRAPT 2018 |
| 2018 | JA02 | 18JA02#021BMS01B | Basalt | 39.8 | 2.8 | 12.5 | 12.0 | | | 0.2 | 9.5 | 12.1 | 1.7 | 0.8 | 1.1 | 2.8 | 4.1 | 6.9 | | 6.3 | 98.6 | 10.8 | 0.47 | 1.14 | SRAPT 2018 |
| 2018 | JA02 | 18JA02#021BMS01C | Basalt | 37.2 | 2.0 | 13.3 | 16.0 | | | 1.4 | 4.1 | 12.2 | 3.0 | 1.3 | 3.1 | 2.1 | 3.9 | 6.0 | | 5.9 | 99.4 | 14.4 | 0.22 | 3.48 | SRAPT 2018 |
| 2018 | JA02 | 18JA02#033BMS01A | Basalt | 38.1 | 1.8 | 14.9 | 12.7 | | | 1.7 | 2.2 | 10.6 | 2.8 | 1.7 | 4.5 | 4.8 | 4.9 | 9.7 | | 9.4 | 100.2 | 11.4 | 0.16 | 5.20 | SRAPT 2018 |
| 2018 | JA02 | 18JA02#033BMS01B | Basalt | 42.5 | 1.9 | 15.8 | 11.7 | | | 2.3 | 2.4 | 8.6 | 3.0 | 1.8 | 2.5 | 5.0 | 4.1 | 9.2 | | 8.7 | 101.2 | 10.5 | 0.19 | 4.33 | SRAPT 2018 |
| 2018 | JA02 | 18JA02#034BMS01A | Basalt gravel | 33.4 | 1.4 | 11.4 | 10.2 | | | 0.2 | 5.6 | 14.6 | 2.5 | 1.7 | 7.4 | 5.2 | 6.8 | 12.0 | | 10.8 | 99.1 | 9.2 | 0.38 | 1.64 | SRAPT 2018 |
| 2018 | JA02 | 18JA02#034BMS01B | Basalt | 31.4 | 1.5 | 11.9 | 8.8 | | | 0.3 | 4.7 | 18.1 | 2.4 | 1.0 | 1.3 | 4.0 | 3.7 | 7.7 | | 17.1 | 98.5 | 7.9 | 0.37 | 1.70 | SRAPT 2018 |
| 2018 | JA02 | 18JA02#034BMS01C | Basalt gravel | 38.0 | 1.8 | 14.2 | 10.7 | | | 0.3 | 3.9 | 12.4 | 2.9 | 1.6 | 5.8 | 4.3 | 5.2 | 9.4 | | 8.5 | 100.1 | 9.6 | 0.29 | 2.45 | SRAPT 2018 |
| 2018 | JA02 | 18JA02#038BMS01A | Basalt | 37.0 | 2.7 | 10.7 | 12.1 | | | 0.8 | 11.5 | 12.6 | 1.1 | 0.5 | 0.6 | 4.4 | 6.3 | 10.7 | | 9.2 | 98.7 | 10.9 | 0.51 | 0.95 | SRAPT 2018 |
| 1997 | JA03 | 97JA03AD19 | | 39.9 | 3.4 | 13.7 | | 7.3 | 6.0 | 0.2 | 7.7 | 12.7 | 1.5 | 0.8 | 0.5 | | 3.3 | 3.3 | 0.2 | 5.9 | 99.6 | 12.5 | 0.38 | 1.62 | DMRS 1997 |
| 2002 | JA03 | 02JA03BMS04B-1 | | 54.5 | 0.6 | 20.2 | | 3.6 | 0.8 | 0.1 | 1.6 | 2.3 | 4.7 | 4.9 | 0.1 | 2.9 | 2.0 | 4.8 | <0.05 | 5.5 | 99.0 | 4.1 | 0.28 | 2.56 | DMRS 2002 |
| 2005 | JA03 | 02JA03BMS04B-2 | | | | | | | | | | | | | | | | | | | | | | | SOPET 2005 |
| 2019 | JA03 | 19JA03#052BMS01C | Fresh basalt | 43.1 | 2.5 | 14.1 | 13.1 | | | 1.5 | 8.6 | 10.9 | 3.6 | 1.4 | 1.0 | | | | | 1.8 | 101.5 | 11.7 | 0.42 | 1.37 | SRAPT 2019 |
| 2019 | JA03 | 19JA03#054BMS01C | Basalt gravel | 41.8 | 3.7 | 14.3 | 11.4 | | | 1.6 | 5.8 | 12.8 | 2.7 | 0.9 | 2.3 | | | | | 4.2 | 101.6 | 10.3 | 0.36 | 1.76 | SRAPT 2019 |
| 2019 | JA03 | 19JA03#062BMS01A | Basalt | 45.9 | 3.5 | 18.7 | 11.1 | | | 0.4 | 3.3 | 6.4 | 2.9 | 2.1 | 0.9 | | | | | 4.9 | 99.9 | 10.0 | 0.25 | 3.06 | SRAPT 2019 |
| 2019 | JA03 | 19JA03#064BMS01A | Basalt | 38.9 | 3.3 | 12.1 | 13.3 | | | 1.1 | 7.1 | 13.2 | 1.6 | 0.7 | 3.2 | | | | | 5.1 | 99.6 | 12.0 | 0.37 | 1.68 | SRAPT 2019 |
| 2019 | JA03 | 19JA03#064BMS01C | Basalt | 39.5 | 3.3 | 13.0 | 13.9 | | | 0.3 | 7.9 | 14.9 | 2.0 | 0.8 | 2.1 | | | | | 3.9 | 101.5 | 12.5 | 0.39 | 1.58 | SRAPT 2019 |
| 2019 | JA03 | 19JA03#072BMS01B | Basalt | 46.1 | 2.5 | 16.4 | 11.7 | | | 0.7 | 4.7 | 10.5 | 2.8 | 1.8 | 1.5 | | | | | 2.5 | 101.1 | 10.5 | 0.31 | 2.22 | SRAPT 2019 |
| 2019 | JA03 | 19JA03#072BMS01D | Weathered basalt | 39.6 | 3.1 | 15.4 | 12.8 | | | 2.1 | 4.0 | 9.6 | 2.0 | 2.4 | 4.1 | | | | | 6.0 | 101.1 | 11.5 | 0.26 | 2.91 | SRAPT 2019 |
| 2002 | JA05 | 02JA05BMS01B | | 42.3 | 3.0 | 15.0 | | 6.8 | 4.3 | 0.3 | 2.8 | 10.2 | 4.1 | 3.4 | 0.9 | 3.8 | 1.2 | 5.0 | <0.05 | 5.5 | 98.6 | 10.4 | 0.21 | 3.70 | DMRS 2002 |
| 1997 | JA06 | 97JA06AD20 | | 39.9 | 3.2 | 16.2 | | 8.1 | 2.4 | 0.4 | 2.9 | 11.6 | 3.1 | 2.1 | 4.3 | | 2.4 | 2.4 | 0.5 | 4.4 | 98.6 | 9.7 | 0.23 | 3.39 | DMRS 1997 |
| 2018 | JA06 | 18JA06#085BMS01B | Basalt gravel | 43.3 | 3.2 | 17.0 | 13.0 | | | 0.6 | 4.6 | 10.9 | 3.1 | 1.3 | 0.7 | 1.7 | 2.2 | 3.9 | | 3.4 | 100.9 | 11.7 | 0.28 | 2.54 | SRAPT 2018 |
| 2018 | JA06 | 18JA06#086BMS02A | Basalt | 44.5 | 2.5 | 14.2 | 12.3 | | | 0.2 | 6.1 | 11.5 | 2.5 | 1.2 | 0.5 | 2.2 | 2.5 | 4.7 | | 4.2 | 99.6 | 11.1 | 0.36 | 1.81 | SRAPT 2018 |
| 2018 | JA06 | 18JA06#086BMS02B | Basalt | 44.5 | 2.5 | 14.4 | 12.5 | | | 0.4 | 6.2 | 12.2 | 2.4 | 1.2 | 0.8 | 2.4 | 2.7 | 5.1 | | 4.6 | 101.4 | 11.2 | 0.36 | 1.82 | SRAPT 2018 |
| 2018 | JA06 | 18JA06#089BMS01C | Basalt | 39.4 | 2.2 | 11.4 | 16.5 | | | 0.8 | 7.3 | 12.9 | 2.2 | 0.7 | 0.7 | 1.8 | 3.0 | 4.7 | | 4.4 | 98.4 | 14.8 | 0.33 | 2.05 | SRAPT 2018 |
| 2018 | JA06 | 18JA06#089BMS01D | Basalt | 39.1 | 2.3 | 11.2 | 10.2 | | | 1.2 | 6.2 | 16.2 | 2.3 | 1.3 | 2.9 | 2.7 | 3.7 | 6.5 | | 6.9 | 99.7 | 9.2 | 0.40 | 1.48 | SRAPT 2018 |
| 2018 | JA06 | 18JA06#093BMS01A | Basalt | 41.3 | 2.9 | 13.6 | 11.8 | | | 0.4 | 6.5 | 13.0 | 2.1 | 1.0 | 1.6 | 2.7 | 3.0 | 5.7 | | 5.1 | 99.1 | 10.6 | 0.38 | 1.63 | SRAPT 2018 |
| 2018 | JA06 | 18JA06#096BMS01A | Basalt | 41.1 | 2.7 | 12.3 | 13.3 | | | 0.5 | 7.2 | 14.1 | 1.9 | 0.9 | 0.9 | 1.9 | 2.3 | 4.2 | | 3.8 | 98.7 | 11.9 | 0.38 | 1.66 | SRAPT 2018 |
| 2018 | JA06 | 18JA06#096BMS01B | Basalt | 36.1 | 2.3 | 12.1 | 13.6 | | | 1.3 | 5.9 | 15.2 | 1.6 | 1.3 | 4.5 | 3.4 | 3.9 | 7.3 | | 7.4 | 101.1 | 12.2 | 0.32 | 2.08 | SRAPT 2018 |
| 2018 | JA06 | 18JA06#096BMS01C | Basalt | 39.2 | 2.6 | 12.3 | 13.1 | | | 1.1 | 7.3 | 14.1 | 1.6 | 0.9 | 1.7 | 2.4 | 3.3 | 5.7 | | 5.2 | 99.0 | 11.8 | 0.38 | 1.61 | SRAPT 2018 |
| 2018 | JA06 | 18JA06#100BMS01A | Basalt | 40.2 | 3.2 | 12.2 | 14.5 | | | 1.0 | 7.8 | 14.6 | 1.4 | 0.7 | 0.8 | 2.6 | 4.0 | 6.6 | | 4.9 | 101.2 | 13.0 | 0.38 | 1.66 | SRAPT 2018 |
| 2018 | JA06 | 18JA06#100BMS01B | Basalt | 43.2 | 2.5 | 13.3 | 13.8 | | | 0.3 | 8.5 | 11.9 | 3.0 | 0.9 | 0.5 | 0.7 | 1.0 | 1.8 | | 1.2 | 98.9 | 12.4 | 0.41 | 1.46 | SRAPT 2018 |
| 2018 | JA06 | 18JA06#100BMS01C | Basalt | 41.9 | 2.4 | 14.2 | 13.3 | | | 1.1 | 7.0 | 10.2 | 3.7 | 1.4 | 0.7 | 1.7 | 2.7 | 4.4 | | 3.4 | 99.1 | 11.9 | 0.37 | 1.70 | SRAPT 2018 |
| 2018 | JA06 | 18JA06#086BMS01A | Basalt | 37.7 | 2.3 | 13.1 | 13.2 | | | 0.8 | 4.8 | 14.0 | 2.2 | 1.1 | 3.5 | 2.8 | 3.8 | 6.6 | | 5.8 | 98.2 | 11.8 | 0.29 | 2.49 | SRAPT 2018 |
| 2018 | JA06 | 18JA06#087BMS01A | Basalt | 39.5 | 3.0 | 14.5 | 14.6 | | | 1.0 | 4.9 | 12.6 | 3.1 | 1.2 | 1.8 | 1.2 | 2.0 | 3.2 | | 3.3 | 99.4 | 13.1 | 0.27 | 2.66 | SRAPT 2018 |
| 2018 | JA06 | 18JA06#087BMS01B | Basalt | 39.9 | 3.0 | 14.5 | 14.2 | | | 1.7 | 5.1 | 11.7 | 2.8 | 1.1 | 1.3 | 1.8 | 2.4 | 4.2 | | 4.0 | 99.0 | 12.7 | 0.28 | 2.52 | SRAPT 2018 |

Table 1 Continued.

| Year | Seamount | Sample ID | Rock type | (wt%) $SiO_2$ | $TiO_2$ | $Al_2O_3$ | $Fe_2O_3t$ | $Fe_2O_3$ | FeO | MnO | MgO | CaO | $Na_2O$ | $K_2O$ | $P_2O_5$ | $H_2O^+$ | $H_2O^-$ | $H_2O_{total}$ | $CO_2$ | LOI | Total | FeO* | Mg# | FeO*/MgO | Project name |
|---|---|---|---|---|---|---|---|---|---|---|---|---|---|---|---|---|---|---|---|---|---|---|---|---|---|
| 2018 | JA06 | 18JA06#087BMS01C | Basalt | 42.8 | 3.1 | 15.3 | 14.1 | | | 0.6 | 5.7 | 11.4 | 3.2 | 1.1 | 0.6 | 1.1 | 1.5 | 2.5 | | 2.1 | 100.0 | 12.7 | 0.31 | 2.23 | SRAPT 2018 |
| 2018 | JA06 | 18JA06#088BMS01C | Basalt | 43.4 | 3.0 | 15.9 | 14.6 | | | 0.5 | 5.7 | 10.5 | 3.4 | 1.1 | 0.6 | 0.8 | 1.8 | 2.5 | | 1.8 | 100.4 | 13.1 | 0.30 | 2.30 | SRAPT 2018 |
| 2018 | JA06 | 18JA06#091BMS01A | Basalt | 43.7 | 2.6 | 13.2 | 13.2 | | | 1.3 | 7.1 | 10.9 | 2.9 | 1.0 | 0.8 | 1.9 | 2.6 | 4.5 | | 3.6 | 100.1 | 11.9 | 0.37 | 1.68 | SRAPT 2018 |
| 2018 | JA06 | 18JA06#091BMS01B | Basalt | 42.9 | 2.7 | 13.7 | 13.4 | | | 0.5 | 7.7 | 11.4 | 3.1 | 1.0 | 0.8 | 1.3 | 1.9 | 3.2 | | 2.8 | 99.9 | 12.1 | 0.39 | 1.57 | SRAPT 2018 |
| 2018 | JA06 | 18JA06#091BMS01C | Basalt | 44.1 | 2.7 | 14.2 | 12.8 | | | 0.4 | 6.0 | 12.5 | 2.8 | 1.2 | 0.7 | 2.0 | 1.9 | 3.8 | | 4.5 | 101.8 | 11.5 | 0.34 | 1.94 | SRAPT 2018 |
| 2018 | JA06 | 18JA06#092BMS01C | Basalt | 41.3 | 2.9 | 16.3 | 11.4 | | | 0.2 | 2.8 | 10.2 | 3.1 | 2.1 | 3.0 | 2.5 | 3.4 | 5.9 | | 6.2 | 99.3 | 10.2 | 0.22 | 3.65 | SRAPT 2018 |
| 1998 | JA09 | 98JA09AD18 | Fine-grained tuff | 19.2 | 1.0 | 5.9 | | 5.6 | <0.01 | 3.1 | 1.6 | 29.5 | 1.3 | 1.5 | 19.5 | 3.3 | 3.4 | 6.7 | 2.4 | 10.8 | 98.9 | 5.0 | 0.24 | 3.09 | DMRS 1998 |
| 1998 | JA09 | 98JA09AD20-1 | | 46.8 | 3.6 | 18.2 | | 9.4 | 0.9 | 0.1 | 1.2 | 6.5 | 3.7 | 2.9 | 1.6 | 1.4 | 2.2 | 3.6 | 0.2 | 4.2 | 99.1 | 9.4 | 0.11 | 7.80 | DMRS 1998 |
| 1998 | JA09 | 98JA09AD20-2 | | 46.3 | 3.0 | 18.3 | | 10.6 | 1.5 | 0.1 | 1.1 | 5.9 | 3.6 | 3.0 | 1.1 | 1.4 | 2.7 | 4.1 | 0.1 | 4.8 | 99.1 | 11.0 | 0.09 | 10.11 | DMRS 1998 |
| 1999 | JA09 | 99JA09AD34-1 | | 46.6 | 2.3 | 14.6 | | 9.4 | 0.0 | 0.5 | 2.0 | 7.2 | 3.8 | 3.5 | 2.4 | 1.4 | 4.0 | 5.4 | 0.7 | 6.9 | 99.2 | 8.4 | 0.19 | 4.21 | DMRS 1999 |
| 1999 | JA09 | 99JA09AD34-2 | | 44.3 | 2.7 | 17.2 | | 10.5 | 0.4 | 0.1 | 1.2 | 7.3 | 3.4 | 2.8 | 2.8 | 2.1 | 3.4 | 5.5 | 0.4 | 7.1 | 99.8 | 9.8 | 0.11 | 8.48 | DMRS 1999 |
| 1999 | JA09 | 99JA09AD34-3 | | 40.0 | 2.3 | 15.1 | | 7.0 | 0.4 | 0.1 | 2.1 | 13.5 | 3.5 | 1.9 | 6.2 | 1.8 | 3.8 | 5.5 | 1.0 | 7.4 | 99.2 | 6.7 | 0.24 | 3.20 | DMRS 1999 |
| 1999 | JA09 | 99JA09AD35-1 | Clinopyroxene olivine alkali dolerite | 45.5 | 2.1 | 13.4 | | 9.9 | 1.4 | 0.2 | 6.1 | 9.9 | 2.7 | 2.1 | 1.4 | 2.1 | 2.9 | 5.0 | >0.05 | 5.9 | 100.6 | 10.3 | 0.37 | 1.68 | DMRS 1999 |
| 1999 | JA09 | 99JA09AD35-2 | Clinopyroxene olivine alkali basalt | 45.1 | 2.4 | 15.1 | | 9.1 | 1.4 | 0.2 | 5.2 | 7.6 | 2.9 | 2.2 | 1.0 | 3.6 | 3.7 | 7.4 | 0.5 | 7.6 | 99.7 | 9.6 | 0.35 | 1.85 | DMRS 1999 |
| 2000 | JA09 | 00JA09AD54-1 | Olivine basalt | 47.1 | 2.3 | 18.3 | | 10.1 | 1.6 | 0.3 | 2.8 | 8.4 | 3.5 | 1.2 | 0.4 | 3.7 | 1.6 | 5.3 | <0.05 | 3.5 | 99.4 | 10.7 | 0.21 | 3.88 | DMRS 2000 |
| 2000 | JA09 | 00JA09AD54-2 | Olivine basalt | 39.7 | 3.0 | 17.3 | | 12.2 | 0.3 | 0.8 | 1.1 | 11.6 | 3.0 | 1.3 | 3.5 | 4.9 | 1.7 | 6.7 | 0.4 | 5.4 | 99.0 | 11.2 | 0.09 | 10.10 | DMRS 2000 |
| 2000 | JA09 | 00JA09AD58 | Clinopyroxene andesite | 46.6 | 3.4 | 16.6 | | 10.4 | 1.3 | 0.1 | 1.3 | 7.5 | 3.5 | 2.6 | 2.5 | 4.3 | 2.3 | 6.6 | <0.05 | 4.8 | 100.5 | 10.7 | 0.11 | 8.47 | DMRS 2000 |
| 2000 | JA09 | 00JA09CB69 | Aphyric basalt | 46.4 | 1.5 | 17.8 | | 10.0 | 1.0 | 0.1 | 2.1 | 8.8 | 3.5 | 1.4 | 0.3 | 4.4 | 2.2 | 6.6 | 0.8 | 5.5 | 98.4 | 10.0 | 0.18 | 4.70 | DMRS 2000 |
| 1989 | JA10 | 89JA10AD04-E | Amygdaloidal olivine basalt | 35.9 | 3.2 | 14.9 | | 9.7 | 3.7 | 0.2 | 4.8 | 11.2 | 1.4 | 1.2 | 1.3 | | | | | 12.1 | 99.5 | 12.4 | 0.28 | 2.59 | DMRS 1989 |
| 1999 | JA10 | 99JA10AD11 | Clinopyroxene olivine alkali basalt | 36.7 | 2.8 | 12.3 | | 9.6 | 3.7 | 0.2 | 5.5 | 13.5 | 1.0 | 1.2 | 0.8 | 3.4 | 5.0 | 8.4 | 3.0 | 11.6 | 98.8 | 12.4 | 0.31 | 2.24 | DMRS 1999 |
| 1999 | JA10 | 99JA10AD17 | Clinopyroxene olivine alkali basalt | 36.6 | 4.5 | 12.4 | | 8.4 | 5.3 | 0.2 | 8.0 | 14.6 | 3.4 | 2.3 | 0.8 | 1.0 | 1.0 | 2.0 | 0.9 | 2.6 | 99.1 | 12.9 | 0.38 | 1.61 | DMRS 1999 |
| 2000 | JA10 | 00JA10AD33 | Olivine alkali basalt | 28.1 | 3.6 | 10.6 | | 8.5 | 3.1 | 0.2 | 5.4 | 22.3 | 1.0 | 0.8 | 1.4 | 5.4 | 1.5 | 6.9 | 8.5 | 14.0 | 98.9 | 10.7 | 0.33 | 1.99 | DMRS 2000 |
| 2000 | JA10 | 00JA10AD34 | Olivine alkali basalt | 40.3 | 4.4 | 12.9 | | 10.6 | 2.2 | 0.2 | 4.3 | 8.6 | 2.1 | 2.6 | 1.3 | 8.2 | 3.8 | 12.0 | 0.6 | 9.5 | 99.0 | 11.7 | 0.27 | 2.72 | DMRS 2000 |
| 2000 | JA10 | 00JA10AD37 | Olivine alkali basalt | 41.6 | 3.3 | 16.6 | | 9.5 | 2.6 | 0.2 | 4.7 | 11.0 | 1.7 | 2.1 | 0.6 | 4.6 | 1.4 | 6.0 | 0.9 | 5.9 | 99.8 | 11.2 | 0.29 | 2.41 | DMRS 2000 |
| 2000 | JA10 | 00JA10AD41 | Olivine alkali basalt | 44.0 | 2.6 | 14.5 | | 8.3 | 4.4 | 0.2 | 6.6 | 11.2 | 3.2 | 1.3 | 0.4 | 2.2 | 0.6 | 2.8 | <0.05 | 2.3 | 98.8 | 11.8 | 0.36 | 1.78 | DMRS 2000 |
| 2002 | JA10 | 02JA10BMS02B | | 45.2 | 4.3 | 15.1 | | 7.6 | 1.9 | 0.1 | 5.4 | 8.6 | 3.7 | 1.5 | 0.8 | 2.7 | 1.7 | 4.4 | 0.3 | 4.8 | 99.0 | 8.8 | 0.38 | 1.61 | DMRS 2002 |
| 2001 | JA11 | 01JA11BM01A | Olivine basalt | 40.3 | 4.9 | 14.7 | | 14.0 | 1.6 | 0.3 | 4.8 | 6.8 | 2.7 | 2.2 | 1.6 | 2.8 | 2.4 | 5.2 | <0.01 | 5.8 | 99.7 | 14.2 | 0.25 | 2.95 | DMRS 2001 |
| 2001 | JA11 | 01JA11BM02A | Clinopyroxene basalt | 44.6 | 4.8 | 14.4 | | 10.4 | 3.3 | 0.2 | 5.0 | 7.6 | 3.3 | 1.7 | 0.8 | 2.1 | 1.2 | 3.2 | <0.01 | 3.5 | 99.5 | 12.7 | 0.28 | 2.53 | DMRS 2001 |
| 2005 | JA11 | 02JA11BMS06A | | | | | | | | | | | | | | | | | | | | | | | SOPET 2005 |
| 1989 | JA12 | 89JA12AD07-A | Olivine basalt | 40.9 | 2.8 | 12.2 | | 9.6 | 3.6 | 0.7 | 8.9 | 11.9 | 2.4 | 1.5 | 0.7 | | | | | 4.0 | 99.0 | 12.2 | 0.42 | 1.38 | DMRS 1989 |
| 2002 | JA12 | 02JA12BMS03A | | 37.9 | 3.6 | 13.2 | | 8.9 | 4.9 | 0.2 | 7.1 | 14.0 | 3.2 | 1.3 | 0.8 | 2.1 | 1.0 | 3.2 | 0.4 | 3.7 | 98.9 | 13.0 | 0.36 | 1.82 | DMRS 2002 |
| 2002 | JA12 | 02JA12BMS04A | | 41.2 | 1.8 | 15.2 | | 11.5 | 1.3 | 0.1 | 3.0 | 8.9 | 3.1 | 2.9 | 0.6 | 2.7 | 1.8 | 4.5 | 4.3 | 9.2 | 98.7 | 11.6 | 0.21 | 3.84 | DMRS 2002 |
| 2019 | JA12 | 19JA12#101BMS01A | Weathered dolerite | 33.2 | 3.5 | 10.6 | 10.8 | | | 0.3 | 5.4 | 21.1 | 1.5 | 1.5 | 8.9 | | | | | 4.6 | 101.2 | 9.7 | 0.36 | 1.79 | SRAPT 2019 |
| 2019 | JA12 | 19JA12#101BMS01B | Weathered dolerite | 39.7 | 4.4 | 13.1 | 7.8 | | | 0.5 | 4.7 | 16.0 | 1.5 | 2.0 | 6.7 | | | | | 4.8 | 101.0 | 7.0 | 0.40 | 1.50 | SRAPT 2019 |
| 2019 | JA12 | 19JA12#101BMS01C | Weathered dolerite | 35.8 | 3.5 | 10.5 | 11.2 | | | 0.4 | 7.0 | 18.2 | 1.4 | 1.3 | 5.7 | | | | | 3.3 | 98.1 | 10.0 | 0.41 | 1.44 | SRAPT 2019 |
| 2019 | JA12 | 19JA12#103BMS01C | Hyaloclastite | 37.8 | 2.6 | 12.4 | 12.8 | | | 0.5 | 2.5 | 12.5 | 1.8 | 1.7 | 8.0 | | | | | 7.9 | 100.3 | 11.5 | 0.18 | 4.66 | SRAPT 2019 |
| 2019 | JA12 | 19JA12#105BMS01A | Volcaniclastic tuff | 16.4 | 1.4 | 5.7 | 6.8 | | | 0.3 | 5.1 | 33.9 | 1.0 | 0.5 | 11.7 | | | | | 16.4 | 99.2 | 6.1 | 0.45 | 1.20 | SRAPT 2019 |
| 2019 | JA12 | 19JA12#105BMS01C | Volcaniclastic tuff | 22.1 | 1.8 | 7.1 | 8.2 | | | 0.3 | 6.9 | 27.0 | 1.0 | 0.6 | 2.8 | | | | | 22.4 | 100.1 | 7.4 | 0.48 | 1.07 | SRAPT 2019 |
| 2002 | JA13 | 02JA13BMS02B | | 42.0 | 2.9 | 16.1 | | 7.5 | 4.1 | 0.2 | 3.9 | 9.5 | 3.5 | 1.7 | 0.8 | 3.3 | 1.8 | 5.1 | 1.1 | 6.5 | 98.6 | 10.9 | 0.27 | 2.78 | DMRS 2002 |
| 1989 | JA14 | 89JA14AD06-B | Olivine basalt | 45.3 | 2.5 | 15.5 | | 4.8 | 5.9 | 0.2 | 8.3 | 8.0 | 2.9 | 1.9 | 0.6 | | | | | 4.0 | 99.9 | 10.3 | 0.45 | 1.23 | DMRS 1989 |
| 1998 | JA15 | 98JA15AD10CA01 | Basalt | 40.4 | 1.6 | 13.5 | | 10.8 | 0.2 | 0.3 | 4.2 | 10.9 | 3.0 | 1.8 | 4.7 | 2.4 | 3.2 | 5.6 | 0.8 | 7.3 | 98.5 | 9.8 | 0.30 | 2.34 | DMRS 1998 |
| 1998 | JA15 | 98JA15AD12CA01 | Basalt | 49.3 | 2.4 | 14.7 | | 8.5 | 2.0 | 0.1 | 4.0 | 6.4 | 3.0 | 4.1 | 0.6 | 1.2 | 1.8 | 3.0 | <0.01 | 3.7 | 98.8 | 9.7 | 0.29 | 2.42 | DMRS 1998 |
| 1998 | JA15 | 98JA15AD13CA01 | Basalt | 19.9 | 1.0 | 7.6 | | 9.1 | <0.01 | 0.5 | 1.7 | 27.7 | 1.2 | 2.3 | 17.5 | 3.1 | 3.0 | 6.1 | 2.6 | 10.1 | 98.6 | 8.2 | 0.17 | 4.86 | DMRS 1998 |
| 1998 | JA15 | 98JA15AD19CA01 | Hyaloclastite | 44.7 | 2.1 | 13.7 | | 10.1 | 0.3 | 0.1 | 4.8 | 1.7 | 3.1 | 3.8 | 0.3 | 4.3 | 7.7 | 11.9 | 0.2 | 14.3 | 98.7 | 9.4 | 0.34 | 1.95 | DMRS 1998 |
| 1989 | JA16 | 89JA16AD01 | Amygdaloidal pyroxene basalt | 37.4 | 3.6 | 14.2 | | 7.9 | 4.0 | 0.2 | 4.0 | 11.4 | 2.0 | 1.5 | 1.4 | | | | | 12.0 | 99.6 | 11.1 | 0.26 | 2.78 | DMRS 1989 |
| 1990 | JA17 | 90JA17AD01C | Augite aegirine olivine basalt | 37.4 | 3.4 | 13.0 | | 7.1 | 5.5 | 0.3 | 6.0 | 15.5 | 1.3 | 1.9 | 1.1 | | | | | 7.8 | 100.3 | 11.9 | 0.33 | 1.99 | DMRS 1990 |
| 2005 | JA17 | 05JA17AD05b1 | | 40.0 | 3.6 | 12.9 | | 7.9 | 5.8 | 0.2 | 8.0 | 12.5 | 2.8 | 1.1 | 0.6 | 1.0 | 1.5 | 2.4 | 0.5 | 2.9 | 98.3 | 12.9 | 0.53 | 1.60 | SOPET 2005 |
| 2005 | JA17 | 05JA17AD05b2 | | 42.0 | 4.2 | 15.3 | | 8.5 | 3.5 | 0.2 | 6.1 | 10.7 | 2.4 | 1.6 | 0.7 | 1.4 | 2.0 | 3.3 | 0.1 | 3.3 | 98.4 | 11.2 | 0.50 | 1.82 | SOPET 2005 |
| 2005 | JA17 | 05JA17AD07r1 | | 38.4 | 3.5 | 12.8 | | 9.7 | 3.7 | 0.3 | 7.7 | 13.9 | 2.1 | 0.9 | 0.9 | 1.9 | 2.8 | 4.7 | 0.1 | 4.9 | 98.9 | 12.5 | 0.52 | 1.61 | SOPET 2005 |
| 2005 | JA17 | 05JA17AD07r2 | | 53.0 | 0.2 | 20.6 | | 3.3 | 0.7 | 0.2 | 0.7 | 0.9 | 0.1 | 5.7 | 0.0 | 0.9 | 3.8 | 4.7 | 0.2 | 5.0 | 90.4 | 3.6 | 0.26 | 4.97 | SOPET 2005 |

Table 1 Continued.

| Year | Seamount | Sample ID | Rock type | (wt%) SiO$_2$ | TiO$_2$ | Al$_2$O$_3$ | Fe$_2$O$_3$t | Fe$_2$O$_3$ | FeO | MnO | MgO | CaO | Na$_2$O | K$_2$O | P$_2$O$_5$ | H$_2$O$^+$ | H$_2$O$^-$ | H$_2$O$_{total}$ | CO$_2$ | LOI | Total | FeO* | Mg# | FeO*/MgO | Project name |
|---|---|---|---|---|---|---|---|---|---|---|---|---|---|---|---|---|---|---|---|---|---|---|---|---|---|
| 2005 | JA17 | 05JA17AD07r3 | | 43.6 | 4.3 | 16.7 | | 8.1 | 2.0 | 0.1 | 4.5 | 10.5 | 2.4 | 1.9 | 0.8 | 1.5 | 1.7 | 3.2 | 0.1 | 4.1 | 98.9 | 9.3 | 0.46 | 2.06 | SOPET 2005 |
| 2005 | JA17 | 02JA17BMS01A | | | | | | | | | | | | | | | | | | | | | | | SOPET 2005 |
| 2018 | JA17 | 18JA17#145BMS01B | Altered basalt | 46.4 | 1.2 | 17.6 | 4.3 | | | 1.0 | 1.9 | 9.0 | 3.5 | 4.3 | 3.7 | 2.1 | 2.3 | 4.4 | | 8.3 | 101.1 | 3.8 | 0.33 | 2.01 | SRAPT 2018 |
| 2018 | JA17 | 18JA17#146BMS01C | Basalt | 42.8 | 3.4 | 16.4 | 11.7 | | | 0.7 | 5.1 | 9.8 | 2.7 | 1.9 | 1.1 | 2.3 | 3.4 | 5.7 | | 4.9 | 100.3 | 10.5 | 0.33 | 2.06 | SRAPT 2018 |
| 2018 | JA17 | 18JA17#147BMS01A | Basalt | 38.4 | 2.5 | 12.7 | 12.9 | | | 0.5 | 7.0 | 13.6 | 1.6 | 1.4 | 2.6 | 3.4 | 4.8 | 8.2 | | 6.9 | 99.9 | 11.6 | 0.38 | 1.64 | SRAPT 2018 |
| 2018 | JA17 | 18JA17#147BMS01B | Basalt | 39.5 | 2.8 | 14.8 | 11.8 | | | 0.7 | 6.6 | 12.3 | 4.0 | 1.6 | 1.3 | 2.2 | 3.7 | 5.9 | | 4.6 | 99.9 | 10.6 | 0.39 | 1.59 | SRAPT 2018 |
| 2018 | JA17 | 18JA17#147BMS01C | Basalt | 37.9 | 2.0 | 12.9 | 11.8 | | | 1.3 | 5.2 | 14.7 | 2.5 | 1.2 | 4.6 | 2.5 | 3.3 | 5.8 | | 6.1 | 100.1 | 10.6 | 0.33 | 2.02 | SRAPT 2018 |
| 2018 | JA17 | 18JA17#147BMS01D | Basalt | 44.9 | 2.2 | 15.1 | 12.1 | | | 0.2 | 5.7 | 11.3 | 3.6 | 1.7 | 0.7 | 1.2 | 2.0 | 3.2 | | 2.9 | 100.2 | 10.9 | 0.34 | 1.91 | SRAPT 2018 |
| 2019 | JA17 | 19JA17#142BMS01C | Fresh basalt gravel | 46.2 | 1.9 | 20.2 | 7.6 | | | 0.8 | 2.0 | 6.6 | 6.7 | 4.8 | 0.5 | | | | | 3.9 | 101.1 | 6.8 | 0.23 | 3.44 | SRAPT 2019 |
| 2019 | JA17 | 19JA17#150BMS01C | Basalt | 42.7 | 2.5 | 13.6 | 13.4 | | | 0.5 | 7.4 | 12.6 | 3.8 | 1.4 | 1.1 | | | | | 1.6 | 100.5 | 12.1 | 0.38 | 1.62 | SRAPT 2019 |
| 1990 | JA19 | 90JA19AD01C | Augite olivine basalt | 44.8 | 1.8 | 9.5 | | 4.9 | 7.0 | 0.4 | 16.9 | 6.8 | 1.7 | 2.3 | 0.4 | | | | | 3.1 | 99.4 | 11.4 | 0.60 | 0.67 | DMRS 1990 |
| 1990 | JA19 | 90JA19AD04D | Augite olivine basalt | 38.2 | 2.8 | 11.7 | | 7.1 | 4.5 | 0.3 | 7.4 | 12.8 | 1.5 | 2.8 | 0.9 | | | | | 10.4 | 100.4 | 10.9 | 0.41 | 1.46 | DMRS 1990 |
| 1990 | JA22 | 90JA22AD05D | Altered basalt | 42.2 | 3.2 | 13.3 | | 9.9 | 0.3 | 2.0 | 1.8 | 7.7 | 3.0 | 4.5 | 2.4 | | | | | 9.9 | 100.0 | 9.1 | 0.16 | 5.16 | DMRS 1990 |
| 1990 | JA22 | 90JA22AD11B | Augite olivine basalt | 39.1 | 1.6 | 10.7 | | 7.7 | 1.8 | 0.4 | 2.6 | 17.8 | 2.7 | 3.1 | 2.2 | | | | | 11.2 | 100.7 | 8.7 | 0.23 | 3.42 | DMRS 1990 |
| 2005 | MT472 | 05DSMT472AD01r1-1 | | 42.9 | 4.2 | 17.0 | | 8.8 | 2.2 | 0.2 | 1.8 | 9.1 | 2.8 | 1.7 | 2.2 | 2.5 | 2.2 | 4.7 | 0.4 | 5.3 | 98.1 | 10.1 | 0.24 | 5.66 | SOPET 2005 |
| 2005 | MT472 | 05DSMT472AD01r1-2 | | 43.8 | 4.3 | 17.2 | | 8.6 | 2.2 | 0.1 | 1.9 | 7.8 | 2.8 | 1.8 | 1.6 | 4.1 | 2.0 | 6.1 | 0.3 | 6.8 | 98.8 | 9.9 | 0.24 | 5.37 | SOPET 2005 |
| 2005 | MT472 | 05DSMT472AD01a3 | | 43.0 | 4.3 | 17.1 | | 8.7 | 2.4 | 0.2 | 1.8 | 8.8 | 2.7 | 1.7 | 1.9 | 2.5 | 2.2 | 4.7 | 0.5 | 5.3 | 97.9 | 10.3 | 0.24 | 5.65 | SOPET 2005 |
| 2005 | MT473 | MT473BMS02A-2 | | | | | | | | | | | | | | | | | | | | | | | SOPET 2005 |
| 2005 | MT474 | MT474BMS04A | | | | | | | | | | | | | | | | | | | | | | | SOPET 2005 |
| 2019 | Takuyo-Daigo | 19TAKUYO5BMS41B | Volcaniclastic tuff | 29.8 | 1.6 | 9.9 | 14.8 | | | 12.3 | 3.0 | 7.9 | 2.3 | 2.8 | 4.3 | | | | | 11.0 | 99.5 | 13.3 | 0.19 | 4.39 | SRAPT 2019 |
| 2019 | Takuyo-Daigo | 19TAKUYO5BMS50B | Basalt | 49.1 | 2.3 | 18.3 | 9.1 | | | 0.5 | 4.8 | 8.1 | 3.5 | 2.4 | 0.6 | | | | | 2.6 | 101.2 | 8.2 | 0.37 | 1.71 | SRAPT 2019 |
| 2019 | Takuyo-Daigo | 19TAKUYO5BMS57B | Basalt | 42.2 | 2.3 | 16.6 | 12.5 | | | 0.4 | 5.8 | 11.4 | 4.0 | 1.6 | 0.5 | | | | | 2.5 | 99.8 | 11.2 | 0.34 | 1.93 | SRAPT 2019 |
| 2019 | Takuyo-Daigo | 19TAKUYO5BMS57C | Basalt | 47.1 | 1.6 | 18.4 | 12.0 | | | 0.8 | 3.0 | 8.9 | 5.4 | 2.2 | 0.9 | | | | | 1.6 | 101.7 | 10.8 | 0.22 | 3.63 | SRAPT 2019 |
| 2019 | Takuyo-Daigo | 19TAKUYO5BMS58C | Basalt | 42.8 | 2.2 | 16.3 | 12.8 | | | 1.0 | 5.5 | 10.2 | 4.2 | 1.7 | 0.8 | | | | | 2.0 | 99.3 | 11.5 | 0.32 | 2.09 | SRAPT 2019 |
| 2019 | Takuyo-Daigo | 19TAKUYO5BMS59A | Basalt | 45.4 | 2.1 | 16.4 | 12.8 | | | 0.3 | 5.8 | 11.6 | 4.5 | 1.5 | 0.5 | | | | | 0.9 | 101.8 | 11.5 | 0.34 | 1.97 | SRAPT 2019 |
| 2019 | Takuyo-Daigo | 19TAKUYO5BMS59B | Porous basalt | 45.6 | 2.3 | 20.5 | 10.6 | | | 0.4 | 3.9 | 6.0 | 2.9 | 2.2 | 1.4 | | | | | 4.4 | 100.0 | 9.5 | 0.29 | 2.44 | SRAPT 2019 |
| 2019 | Takuyo-Daigo | 19TAKUYO5BMS52A | Basalt gravel | 43.0 | 2.2 | 14.6 | 14.5 | | | 0.7 | 7.7 | 11.1 | 2.5 | 1.1 | 1.0 | | | | | 3.0 | 101.3 | 13.0 | 0.37 | 1.68 | SRAPT 2019 |
| 2019 | Takuyo-Daigo | 19TAKUYO5BMS55C | Basalt gravel? | 40.6 | 2.0 | 13.1 | 13.7 | | | 0.3 | 8.9 | 11.8 | 2.1 | 1.3 | 1.4 | | | | | 3.1 | 98.2 | 12.3 | 0.42 | 1.39 | SRAPT 2019 |
| 2019 | Takuyo-Daigo | 19TAKUYO5BMS52A | Hyaloclastite | 36.4 | 1.9 | 13.2 | 12.7 | | | 0.4 | 6.3 | 15.8 | 2.4 | 1.7 | 0.6 | | | | | 10.5 | 101.7 | 11.4 | 0.36 | 1.81 | SRAPT 2019 |
| 2019 | Takuyo-Daigo | 19TAKUYO5BMS52B | Hyaloclastite | 42.8 | 2.2 | 15.3 | 15.6 | | | 0.7 | 5.4 | 4.3 | 3.0 | 3.5 | 1.1 | | | | | 7.2 | 101.0 | 14.0 | 0.28 | 2.61 | SRAPT 2019 |
| 2019 | Takuyo-Daigo | 19TAKUYO5BMS53B | Hyaloclastite | 37.8 | 2.6 | 14.2 | 15.8 | | | 0.6 | 5.6 | 6.4 | 3.3 | 3.2 | 0.5 | | | | | 11.4 | 101.1 | 14.2 | 0.28 | 2.55 | SRAPT 2019 |
| 2019 | Takuyo-Daigo | 19TAKUYO5BMS53D | Hyaloclastite | 27.3 | 2.3 | 12.6 | 11.1 | | | 0.5 | 2.0 | 19.9 | 2.4 | 2.1 | 4.2 | | | | | 17.0 | 101.2 | 10.0 | 0.17 | 4.97 | SRAPT 2019 |
| 2019 | Takuyo-Daigo | 19TAKUYO5BMS53E | Hyaloclastite | 40.2 | 3.0 | 16.2 | 15.5 | | | 0.1 | 4.2 | 2.5 | 3.8 | 3.7 | 1.0 | | | | | 9.4 | 99.5 | 13.9 | 0.23 | 3.33 | SRAPT 2019 |
| 2019 | Takuyo-Daigo | 19TAKUYO5BMS52A | Hyaloclastite including basalt gravel | 43.0 | 2.2 | 15.6 | 14.5 | | | 0.2 | 6.8 | 6.9 | 3.0 | 2.7 | 0.6 | | | | | 6.4 | 101.8 | 13.0 | 0.34 | 1.93 | SRAPT 2019 |
| 2019 | Takuyo-Daigo | 19TAKUYO5BMS53B | Hyaloclastite (calcite filling) | 33.4 | 1.6 | 14.5 | 10.9 | | | 1.2 | 4.2 | 12.9 | 1.9 | 1.7 | 0.4 | | | | | 17.8 | 100.4 | 9.8 | 0.30 | 2.33 | SRAPT 2019 |
| 2019 | Takuyo-Daigo | 19TAKUYO5BMS53D | Hyaloclastite (calcite filling) | 24.7 | 1.8 | 9.5 | 8.6 | | | 0.2 | 4.6 | 28.2 | 1.6 | 1.1 | 0.5 | | | | | 19.4 | 100.1 | 7.7 | 0.37 | 1.70 | SRAPT 2019 |
| 2020 | Takuyo-Daigo | 19TAKUYO5BMS53D_1a | Basalt | | 2.7 | 15.0 | 12.4 | | | 0.1 | 6.3 | | | | 1.8 | | | | | | | 0.4 | 0.95 | 0.06 | ESCRC 2020 |
| 2020 | Takuyo-Daigo | 19TAKUYO5BMS53D_1b | Basalt | | 2.9 | 16.0 | 14.1 | | | 0.1 | 8.0 | | | | 1.2 | | | | | | | 0.4 | 0.95 | 0.05 | ESCRC 2020 |
| 2020 | Takuyo-Daigo | 19TAKUYO5BMS53D_2a | Basalt | | 1.9 | 9.7 | 11.1 | | | 0.2 | 4.6 | | | | 0.6 | | | | | | | 0.3 | 0.94 | 0.07 | ESCRC 2020 |
| 2020 | Takuyo-Daigo | 19TAKUYO5BMS53D_2b | Basalt | | 1.6 | 9.4 | 10.1 | | | 0.2 | 3.7 | | | | 0.4 | | | | | | | 0.3 | 0.93 | 0.08 | ESCRC 2020 |
| 2020 | Takuyo-Daigo | 19TAKUYO5BMS53E_1a | Fe-rich basalt | | 2.0 | 11.4 | 11.3 | | | 0.0 | 3.3 | | | | 0.3 | | | | | | | 0.2 | 0.93 | 0.07 | ESCRC 2020 |
| 2020 | Takuyo-Daigo | 19TAKUYO5BMS53E_1b | Fe-rich basalt | | 2.0 | 11.5 | 12.9 | | | 0.1 | 3.8 | | | | 0.6 | | | | | | | 0.2 | 0.94 | 0.07 | ESCRC 2020 |
| 2020 | Takuyo-Daigo | 19TAKUYO5BMS53F_1a | Basalt | | 2.2 | 12.5 | 12.1 | | | 0.0 | 3.7 | | | | 0.4 | | | | | | | 0.3 | 0.94 | 0.07 | ESCRC 2020 |
| 2020 | Takuyo-Daigo | 19TAKUYO5BMS53F_1b | Basalt | | 2.1 | 11.4 | 12.8 | | | 0.1 | 3.9 | | | | 0.9 | | | | | | | 0.3 | 0.94 | 0.06 | ESCRC 2020 |
| 2020 | Takuyo-Daigo | 19TAKUYO5BMS53F_2a | Basalt including carbonate | | 1.4 | 7.7 | 7.1 | | | 0.1 | 4.1 | | | | 0.6 | | | | | | | 0.4 | 0.91 | 0.10 | ESCRC 2020 |
| 2020 | Takuyo-Daigo | 19TAKUYO5BMS53F_2b | Basalt including carbonate | | 2.5 | 13.9 | 12.4 | | | 0.2 | 6.7 | | | | 0.9 | | | | | | | 0.4 | 0.95 | 0.06 | ESCRC 2020 |
| 2020 | Takuyo-Daigo | 19TAKUYO5BMS53F_3a | Fe-rich basalt | | 1.5 | 8.4 | 9.8 | | | 0.2 | 3.8 | | | | 0.4 | | | | | | | 0.3 | 0.93 | 0.08 | ESCRC 2020 |
| 2020 | Takuyo-Daigo | 19TAKUYO5BMS53F_3b | Fe-rich basalt | | 1.6 | 9.0 | 10.2 | | | 0.2 | 3.4 | | | | 0.3 | | | | | | | 0.3 | 0.93 | 0.08 | ESCRC 2020 |

Total was calculated by using major element composition and LOI. FeO*: FeO+Fe$_2$O$_3$, Mg#: MgO/(MgO+FeO*)

DMRS: Deep-sea mineral resource surveys

SOPET: Survey on offshore petroleum exploration technology (basic survey on exploration technology for deep water petroleum resources)

SRAPT: Survey on resource assessment and production technology for the development of marine mineral resources

ESCRC: Environmental study in the area for exploration of cobalt-rich crusts

Table 2 Minor elemental compositions of basement rocks from seamounts in the JA area

| Year | Seamount | Sample ID | (ppm) V | Cr | Rb | Sr | Y | Zr | Nb | Ba | La | Ce | Pr | Nd | Sm | Eu | Gd | Tb | Dy | Ho | Er | Tm | Yb | Lu | Pb | Th | U | Project name |
|---|---|---|---|---|---|---|---|---|---|---|---|---|---|---|---|---|---|---|---|---|---|---|---|---|---|---|---|---|
| 1999 | JA01 | 99JA01AD12 | 284 | | 23 | 523 | 106 | 339 | 75 | 235 | 106.0 | 137.0 | 18.7 | 75.9 | 14.0 | 4.6 | 14.3 | 2.2 | 12.1 | 2.6 | 7.2 | 0.9 | 5.4 | 0.8 | | | | DMRS 1999 |
| 1999 | JA01 | 99JA01AD13 | 338 | | 28 | 564 | 38 | 227 | 42 | 247 | 40.2 | 73.2 | 8.9 | 37.3 | 7.9 | 2.8 | 7.8 | 1.3 | 6.8 | 1.4 | 3.8 | 0.5 | 3.0 | 0.4 | | | | DMRS 1999 |
| 1999 | JA01 | 99JA01AD18 | 295 | | 18 | 1300 | 35 | 369 | 92 | 214 | 68.6 | 126.0 | 13.8 | 54.6 | 10.4 | 3.5 | 9.2 | 1.4 | 6.9 | 1.2 | 3.2 | 0.4 | 2.2 | 0.3 | | | | DMRS 1999 |
| 1999 | JA01 | 99JA01AD23 | 189 | | 106 | 586 | 27 | 687 | 198 | 394 | 73.1 | 127.0 | 12.3 | 42.6 | 7.3 | 2.4 | 6.1 | 1.0 | 5.1 | 1.0 | 2.8 | 0.4 | 2.4 | 0.4 | | | | DMRS 1999 |
| | | | | | | | | | | | | | | | | | | | | | | | | | | | | |
| 2001 | JA02 | 01JA02BM02C | 260 | | 14 | 1470 | 42 | 236 | 85 | 807 | 87.5 | 158.0 | 18.7 | 76.8 | 13.6 | 4.6 | 12.4 | 1.8 | 9.1 | 1.6 | 3.9 | 0.4 | 2.9 | 0.4 | | | | DMRS 2001 |
| 2001 | JA02 | 01JA02BM03A | 297 | | 10 | 1450 | 31 | 269 | 94 | 516 | 61.4 | 112.0 | 13.3 | 55.2 | 10.1 | 3.5 | 9.3 | 1.3 | 6.8 | 1.2 | 2.9 | 0.4 | 2.2 | 0.3 | | | | DMRS 2001 |
| 2001 | JA02 | 01JA02BM05A | 312 | | 17 | 910 | 32 | 252 | 92 | 605 | 64.5 | 116.0 | 13.7 | 56.6 | 10.0 | 3.4 | 9.0 | 1.3 | 6.6 | 1.2 | 2.8 | 0.3 | 2.1 | 0.3 | | | | DMRS 2001 |
| 2002 | JA02 | 02JA02BMS06B | 224 | | 11 | 643 | 27 | 182 | 68 | 240 | 49.6 | 88.8 | 9.9 | 38.0 | 7.3 | 2.5 | 6.9 | 1.0 | 5.5 | 1.0 | 2.5 | 0.3 | 1.9 | 0.3 | | | | DMRS 2002 |
| 2005 | JA02 | 01JA02BMS05B | 290 | 528 | 26 | 573 | 26 | 171 | 48 | 315 | 28.0 | 56.9 | 7.1 | 30.8 | 6.9 | 2.2 | 6.2 | 1.0 | 5.3 | 0.9 | 2.3 | 0.3 | 1.9 | 0.3 | 1.9 | 2.9 | 0.7 | SOPET 2005 |
| 2005 | JA02 | 01JA02BMS02B | 251 | 309 | 12 | 1346 | 41 | 256 | 82 | 713 | 80.6 | 157.7 | 18.7 | 72.4 | 14.1 | 4.1 | 11.5 | 1.7 | 8.2 | 1.5 | 3.6 | 0.5 | 2.6 | 0.3 | 4.6 | 10.3 | 2.2 | SOPET 2005 |
| 2005 | JA02 | 02JA02BMS06B | 227 | 236 | 9 | 687 | 28 | 186 | 80 | 287 | 54.8 | 97.0 | 11.1 | 43.1 | 8.1 | 2.4 | 7.4 | 1.1 | 5.7 | 1.1 | 2.4 | 0.4 | 2.0 | 0.3 | 3.0 | 6.7 | 1.7 | SOPET 2005 |
| 2005 | JA02 | 02JA02BMS07A | 208 | 392 | 42 | 851 | 30 | 222 | 70 | 625 | 52.3 | 102.3 | 12.2 | 48.9 | 9.3 | 3.0 | 8.5 | 1.2 | 6.3 | 1.1 | 2.7 | 0.4 | 2.0 | 0.3 | 2.6 | 5.0 | 1.4 | SOPET 2005 |
| 2018 | JA02 | 18JA02#016BMS01A | 231 | 400 | 18 | 320 | 27 | | | 205 | 21.6 | 40.7 | 5.1 | 21.0 | 5.4 | 1.5 | 5.2 | 0.8 | 4.5 | 1.0 | 2.5 | 0.3 | 1.8 | 0.3 | 5.8 | 2.0 | 0.8 | SRAPT 2018 |
| 2018 | JA02 | 18JA02#016BMS01C | 227 | 290 | 17 | 342 | 36 | | | 289 | 29.1 | 36.2 | 5.5 | 24.9 | 5.7 | 1.6 | 6.4 | 0.9 | 5.2 | 1.1 | 2.8 | 0.4 | 2.3 | 0.3 | 4.6 | 1.8 | 0.8 | SRAPT 2018 |
| 2018 | JA02 | 18JA02#018BMS01A | 250 | 600 | 48 | 567 | 67 | | | 730 | 72.3 | 128.5 | 13.6 | 54.3 | 11.3 | 2.9 | 10.2 | 1.4 | 7.7 | 1.6 | 4.7 | 0.6 | 3.4 | 0.5 | 65.0 | 5.2 | 2.1 | SRAPT 2018 |
| 2018 | JA02 | 18JA02#018BMS01C | 315 | 690 | 33 | 736 | 41 | | | 478 | 43.8 | 90.9 | 9.4 | 39.9 | 9.1 | 2.7 | 8.6 | 1.3 | 6.9 | 1.3 | 3.4 | 0.5 | 2.8 | 0.4 | 45.1 | 4.2 | 1.7 | SRAPT 2018 |
| 2018 | JA02 | 18JA02#019BMS01A | 186 | 450 | 17 | 239 | 17 | | | 181 | 15.7 | 30.5 | 3.6 | 15.9 | 3.7 | 1.3 | 4.0 | 0.6 | 3.5 | 0.7 | 1.8 | 0.2 | 1.5 | 0.2 | 2.3 | 1.9 | 0.5 | SRAPT 2018 |
| 2018 | JA02 | 18JA02#020BMS01A | 229 | 330 | 21 | 349 | 28 | | | 298 | 29.9 | 50.4 | 6.1 | 25.9 | 5.7 | 1.7 | 6.0 | 0.8 | 4.7 | 0.9 | 2.6 | 0.3 | 1.8 | 0.3 | 5.1 | 2.7 | 0.9 | SRAPT 2018 |
| 2018 | JA02 | 18JA02#020BMS01B | 218 | 430 | 29 | 342 | 35 | | | 366 | 38.4 | 84.8 | 8.1 | 34.1 | 7.5 | 2.0 | 7.6 | 1.1 | 6.0 | 1.3 | 3.2 | 0.5 | 2.5 | 0.4 | 58.3 | 3.3 | 2.0 | SRAPT 2018 |
| 2018 | JA02 | 18JA02#020BMS01C | 237 | 350 | 26 | 333 | 31 | | | 324 | 33.8 | 90.9 | 7.2 | 30.4 | 7.0 | 2.0 | 6.9 | 1.1 | 5.7 | 1.2 | 3.1 | 0.4 | 2.4 | 0.4 | 58.6 | 3.2 | 1.4 | SRAPT 2018 |
| 2018 | JA02 | 18JA02#021BMS01B | 286 | 590 | 17 | 1355 | 41 | | | 616 | 68.7 | 112.0 | 14.2 | 55.6 | 10.0 | 2.8 | 9.0 | 1.3 | 6.4 | 1.3 | 3.5 | 0.5 | 2.9 | 0.4 | 9.3 | 6.2 | 1.2 | SRAPT 2018 |
| 2018 | JA02 | 18JA02#021BMS01C | 305 | 430 | 27 | 661 | 73 | | | 510 | 58.2 | 103.0 | 10.3 | 44.2 | 9.1 | 2.6 | 9.9 | 1.4 | 8.8 | 1.9 | 5.2 | 0.7 | 4.8 | 0.7 | 74.6 | 3.6 | 2.8 | SRAPT 2018 |
| 2018 | JA02 | 18JA02#033BMS01A | 183 | 480 | 31 | 524 | 195 | | | 165 | 131.0 | 90.5 | 15.7 | 70.3 | 13.8 | 3.7 | 19.5 | 2.7 | 17.1 | 4.0 | 11.3 | 1.4 | 9.3 | 1.3 | 95.6 | 2.0 | 2.5 | SRAPT 2018 |
| 2018 | JA02 | 18JA02#033BMS01B | 209 | 350 | 26 | 448 | 51 | | | 210 | 36.1 | 116.5 | 6.6 | 29.0 | 6.8 | 2.1 | 8.4 | 1.3 | 7.7 | 1.6 | 4.2 | 0.6 | 4.0 | 0.6 | 129.5 | 2.1 | 2.0 | SRAPT 2018 |
| 2018 | JA02 | 18JA02#034BMS01A | 150 | 290 | 23 | 454 | 49 | | | 103 | 41.0 | 44.6 | 7.6 | 32.2 | 7.2 | 2.1 | 7.8 | 1.1 | 6.7 | 1.3 | 3.4 | 0.5 | 3.1 | 0.5 | 12.3 | 1.7 | 2.4 | SRAPT 2018 |
| 2018 | JA02 | 18JA02#034BMS01B | 134 | 240 | 11 | 335 | 21 | | | 138 | 21.2 | 43.2 | 4.8 | 20.2 | 4.8 | 1.5 | 4.6 | 0.8 | 3.9 | 0.8 | 2.2 | 0.3 | 1.6 | 0.3 | 7.0 | 1.9 | 0.9 | SRAPT 2018 |
| 2018 | JA02 | 18JA02#034BMS01C | 136 | 340 | 28 | 558 | 131 | | | 170 | 88.1 | 48.8 | 12.3 | 54.4 | 10.5 | 3.0 | 14.1 | 1.9 | 12.2 | 2.8 | 8.3 | 1.2 | 7.0 | 1.0 | 15.7 | 2.3 | 2.4 | SRAPT 2018 |
| 2018 | JA02 | 18JA02#038BMS01A | 295 | 750 | 10 | 276 | 27 | | | 329 | 42.0 | 96.1 | 9.5 | 38.5 | 8.4 | 2.3 | 7.2 | 1.1 | 5.5 | 1.1 | 2.6 | 0.4 | 2.2 | 0.3 | 38.1 | 5.1 | 1.4 | SRAPT 2018 |
| | | | | | | | | | | | | | | | | | | | | | | | | | | | | |
| 1997 | JA03 | 97JA03AD19 | 386 | | 17 | 470 | 24 | 162 | 54 | 290 | 35.1 | 70.9 | 8.4 | 34.9 | 7.3 | 2.1 | 7.2 | 1.0 | 5.1 | 0.9 | 2.4 | 0.3 | 1.9 | 0.3 | | | | DMRS 1997 |
| 2002 | JA03 | 02JA03BMS04B-1 | 21 | | 170 | 863 | 27 | 484 | 135 | 1210 | 97.9 | 148.3 | 13.9 | 44.8 | 6.7 | 2.2 | 4.7 | 0.7 | 5.1 | 1.0 | 2.9 | 0.5 | 3.0 | 0.4 | | | | DMRS 2002 |
| 2005 | JA03 | 02JA03BMS04B-2 | 21 | 1 | 155 | 656 | 25 | 488 | 126 | 826 | 97.7 | 153.5 | 13.8 | 43.8 | 6.3 | 1.9 | 5.5 | 0.7 | 4.5 | 0.9 | 2.7 | 0.4 | 2.7 | 0.4 | 16.8 | 27.5 | 3.1 | SOPET 2005 |
| 2019 | JA03 | 19JA03#052BMS01C | 252 | 192 | 43 | 859 | | | | 560 | | | | | | | | | | | | | | | 77.1 | 9.8 | 2.9 | SRAPT 2019 |
| 2019 | JA03 | 19JA03#054BMS01C | 281 | 97 | 16 | 1165 | | | | 860 | | | | | | | | | | | | | | | 118.0 | 14.1 | 3.0 | SRAPT 2019 |
| 2019 | JA03 | 19JA03#062BMS01A | 304 | 382 | 22 | 1230 | | | | 940 | | | | | | | | | | | | | | | 17.2 | 6.7 | 1.7 | SRAPT 2019 |
| 2019 | JA03 | 19JA03#064BMS01A | 265 | 351 | 13 | 2310 | | | | 830 | | | | | | | | | | | | | | | 58.5 | 8.5 | 2.1 | SRAPT 2019 |
| 2019 | JA03 | 19JA03#064BMS01C | 287 | 472 | 16 | 1720 | | | | 900 | | | | | | | | | | | | | | | 10.0 | 7.4 | 1.7 | SRAPT 2019 |
| 2019 | JA03 | 19JA03#072BMS01B | 231 | 95 | 38 | 859 | | | | 540 | | | | | | | | | | | | | | | 51.6 | 10.4 | 3.0 | SRAPT 2019 |
| 2019 | JA03 | 19JA03#072BMS01D | 363 | 287 | 60 | 596 | | | | 1630 | | | | | | | | | | | | | | | 85.0 | 8.3 | 3.6 | SRAPT 2019 |
| | | | | | | | | | | | | | | | | | | | | | | | | | | | | |
| 2002 | JA05 | 02JA05BMS01B | 114 | | 45 | 1850 | 60 | 798 | 213 | 1840 | 146.5 | 283.6 | 31.6 | 122.2 | 21.0 | 6.5 | 16.0 | 2.1 | 12.5 | 2.1 | 5.5 | 0.7 | 4.3 | 0.6 | | | | DMRS 2002 |
| | | | | | | | | | | | | | | | | | | | | | | | | | | | | |
| 1997 | JA06 | 97JA06AD20 | 224 | | 31 | 665 | 53 | 226 | 77 | 471 | 64.4 | 76.8 | 9.9 | 39.0 | 7.6 | 2.4 | 8.2 | 1.1 | 5.7 | 1.2 | 3.2 | 0.5 | 2.6 | 0.4 | | | | DMRS 1997 |
| 2018 | JA06 | 18JA06#085BMS01B | 314 | 20 | 30 | 731 | 36 | | | 440 | 58.3 | 123.0 | 13.4 | 54.3 | 10.4 | 3.0 | 8.3 | 1.3 | 7.0 | 1.3 | 3.3 | 0.4 | 3.0 | 0.4 | 28.2 | 6.6 | 1.9 | SRAPT 2018 |
| 2018 | JA06 | 18JA06#086BMS02A | 280 | 540 | 29 | 557 | 27 | | | 304 | 43.4 | 88.6 | 10.8 | 42.3 | 8.2 | 2.3 | 6.7 | 1.0 | 5.3 | 1.0 | 2.4 | 0.3 | 2.1 | 0.3 | 3.9 | 4.6 | 1.3 | SRAPT 2018 |
| 2018 | JA06 | 18JA06#086BMS02B | 278 | 490 | 25 | 500 | 31 | | | 283 | 44.7 | 90.0 | 10.3 | 42.4 | 8.1 | 2.4 | 7.0 | 1.0 | 5.7 | 1.1 | 2.6 | 0.4 | 2.6 | 0.4 | 14.1 | 4.7 | 1.3 | SRAPT 2018 |
| 2018 | JA06 | 18JA06#089BMS01C | 411 | 2010 | 16 | 458 | 31 | | | 280 | 35.9 | 88.2 | 9.3 | 37.2 | 7.5 | 2.2 | 6.5 | 1.0 | 5.4 | 1.1 | 2.8 | 0.4 | 2.4 | 0.3 | 33.4 | 3.5 | 1.6 | SRAPT 2018 |
| 2018 | JA06 | 18JA06#089BMS01D | 320 | 1710 | 25 | 498 | 40 | | | 381 | 41.5 | 105.0 | 9.3 | 37.8 | 8.0 | 2.3 | 7.8 | 1.2 | 6.2 | 1.3 | 3.4 | 0.5 | 3.1 | 0.5 | 69.4 | 3.9 | 2.2 | SRAPT 2018 |
| 2018 | JA06 | 18JA06#093BMS01A | 287 | 420 | 23 | 660 | 39 | | | 355 | 56.2 | 108.0 | 12.6 | 50.9 | 9.6 | 2.6 | 7.3 | 1.2 | 6.6 | 1.2 | 3.3 | 0.5 | 2.8 | 0.4 | 15.1 | 6.1 | 2.0 | SRAPT 2018 |
| 2018 | JA06 | 18JA06#096BMS01A | 384 | 390 | 21 | 494 | 38 | | | 268 | 44.7 | 87.2 | 10.3 | 41.7 | 8.8 | 2.6 | 8.0 | 1.2 | 6.5 | 1.3 | 3.3 | 0.5 | 2.8 | 0.4 | 21.3 | 4.9 | 1.4 | SRAPT 2018 |
| 2018 | JA06 | 18JA06#096BMS01B | 323 | 480 | 30 | 643 | 141 | | | 480 | 122.0 | 107.0 | 15.3 | 62.7 | 10.5 | 3.0 | 12.4 | 1.7 | 10.6 | 2.5 | 7.5 | 1.0 | 6.3 | 1.0 | 42.5 | 4.7 | 2.6 | SRAPT 2018 |
| 2018 | JA06 | 18JA06#096BMS01C | 370 | 460 | 20 | 549 | 52 | | | 459 | 54.4 | 101.0 | 11.0 | 44.4 | 9.8 | 2.7 | 9.4 | 1.2 | 6.9 | 1.5 | 3.9 | 0.6 | 3.4 | 0.6 | 47.9 | 4.5 | 1.8 | SRAPT 2018 |
| 2018 | JA06 | 18JA06#100BMS01A | 345 | 210 | 15 | 778 | 44 | | | 414 | 65.7 | 133.5 | 14.5 | 60.6 | 12.3 | 3.1 | 10.2 | 1.4 | 7.7 | 1.4 | 3.6 | 0.5 | 2.7 | 0.4 | 42.8 | 6.3 | 1.6 | SRAPT 2018 |
| 2018 | JA06 | 18JA06#100BMS01B | 280 | 480 | 22 | 516 | 28 | | | 321 | 42.6 | 87.2 | 10.4 | 41.7 | 8.5 | 2.2 | 7.2 | 1.0 | 5.2 | 1.0 | 2.7 | 0.3 | 2.3 | 0.3 | 5.2 | 4.8 | 1.3 | SRAPT 2018 |
| 2018 | JA06 | 18JA06#100BMS01C | 258 | 330 | 24 | 709 | 34 | | | 507 | 57.0 | 132.5 | 12.3 | 48.8 | 9.5 | 2.6 | 8.4 | 1.2 | 6.4 | 1.3 | 3.5 | 0.5 | 2.9 | 0.4 | 48.6 | 6.8 | 2.1 | SRAPT 2018 |
| 2018 | JA06 | 18JA06#086BMS01A | 284 | 580 | 24 | 622 | 94 | | | 611 | 74.5 | 83.4 | 12.0 | 47.6 | 10.3 | 2.6 | 10.3 | 1.4 | 8.3 | 2.0 | 5.8 | 0.8 | 4.4 | 0.8 | 29.9 | 4.4 | 2.0 | SRAPT 2018 |
| 2018 | JA06 | 18JA06#087BMS01A | 338 | 270 | 25 | 844 | 53 | | | 418 | 63.5 | 151.0 | 12.8 | 51.8 | 10.3 | 2.9 | 9.0 | 1.3 | 7.3 | 1.5 | 4.0 | 0.5 | 3.5 | 0.5 | 78.8 | 5.2 | 2.2 | SRAPT 2018 |
| 2018 | JA06 | 18JA06#087BMS01B | 351 | 110 | 24 | 750 | 81 | | | 474 | 80.7 | 211.0 | 15.4 | 65.1 | 12.2 | 3.5 | 12.2 | 1.7 | 9.8 | 2.2 | 5.6 | 0.8 | 5.1 | 0.8 | 139.0 | 5.7 | 2.3 | SRAPT 2018 |

Table 2 Continued.

| Year | Seamount | Sample ID | (ppm) V | Cr | Rb | Sr | Y | Zr | Nb | Ba | La | Ce | Pr | Nd | Sm | Eu | Gd | Tb | Dy | Ho | Er | Tm | Yb | Lu | Pb | Th | U | Project name |
|---|---|---|---|---|---|---|---|---|---|---|---|---|---|---|---|---|---|---|---|---|---|---|---|---|---|---|---|---|
| 2018 | JA06 | 18JA06#087BMS01C | 333 | 90 | 29 | 797 | 36 | | | 412 | 53.5 | 114.0 | 13.0 | 52.3 | 10.6 | 2.9 | 9.3 | 1.3 | 7.0 | 1.3 | 3.7 | 0.5 | 2.9 | 0.4 | 22.5 | 5.5 | 1.5 | SRAPT 2018 |
| 2018 | JA06 | 18JA06#088BMS01C | 270 | 90 | 26 | 660 | 29 | | | 378 | 46.8 | 100.5 | 10.9 | 43.3 | 8.7 | 2.6 | 7.6 | 1.0 | 5.7 | 1.2 | 2.7 | 0.4 | 2.4 | 0.3 | 19.4 | 5.9 | 1.5 | SRAPT 2018 |
| 2018 | JA06 | 18JA06#091BMS01A | 264 | 380 | 27 | 687 | 35 | | | 399 | 59.1 | 140.0 | 13.1 | 52.9 | 9.5 | 2.8 | 9.0 | 1.3 | 6.7 | 1.3 | 3.6 | 0.5 | 2.8 | 0.4 | 66.1 | 6.9 | 2.0 | SRAPT 2018 |
| 2018 | JA06 | 18JA06#091BMS01B | 260 | 400 | 28 | 689 | 32 | | | 371 | 56.4 | 116.0 | 12.8 | 50.8 | 9.8 | 2.5 | 8.6 | 1.1 | 6.2 | 1.1 | 3.3 | 0.4 | 2.7 | 0.3 | 22.3 | 6.7 | 1.9 | SRAPT 2018 |
| 2018 | JA06 | 18JA06#091BMS01C | 250 | 420 | 29 | 648 | 30 | | | 358 | 54.3 | 113.0 | 12.4 | 49.1 | 10.0 | 2.5 | 8.0 | 1.1 | 6.0 | 1.1 | 2.8 | 0.4 | 2.5 | 0.3 | 17.1 | 6.9 | 1.7 | SRAPT 2018 |
| 2018 | JA06 | 18JA06#092BMS01C | 325 | 130 | 41 | 643 | 57 | | | 1045 | 55.1 | 86.2 | 12.0 | 49.1 | 10.1 | 2.7 | 8.7 | 1.2 | 8.0 | 1.7 | 4.6 | 0.6 | 4.0 | 0.5 | 12.5 | 4.6 | 1.9 | SRAPT 2018 |
| 1998 | JA09 | 98JA09AD18 | 105 | | 44 | 800 | 216 | 245 | 15 | 2030 | 148.0 | 83.0 | 14.5 | 59.0 | 10.0 | 2.7 | 11.0 | 1.8 | 11.0 | 2.7 | 8.9 | 1.4 | 8.0 | 1.4 | | | | DMRS 1998 |
| 1998 | JA09 | 98JA09AD20-1 | 328 | | 82 | 521 | 34 | 238 | 34 | 368 | 36.0 | 57.0 | 7.5 | 32.0 | 6.7 | 2.5 | 5.3 | 0.9 | 4.7 | 0.8 | 2.4 | 0.3 | 1.8 | 0.3 | | | | DMRS 1998 |
| 1998 | JA09 | 98JA09AD20-2 | 318 | | 46 | 469 | 22 | 206 | 30 | 453 | 26.0 | 49.0 | 6.6 | 28.0 | 5.8 | 2.0 | 4.6 | 0.8 | 4.1 | 0.7 | 2.0 | 0.3 | 1.5 | 0.2 | | | | DMRS 1998 |
| 1999 | JA09 | 99JA09AD34-1 | 96 | | 55 | 651 | 38 | 168 | 48 | 1110 | 85.2 | 145.0 | 15.3 | 58.4 | 10.6 | 3.4 | 8.6 | 1.2 | 5.7 | 1.0 | 2.5 | 0.3 | 1.6 | 0.2 | | | | DMRS 1999 |
| 1999 | JA09 | 99JA09AD34-2 | 139 | | 38 | 760 | 48 | 174 | 54 | 918 | 96.7 | 167.0 | 18.0 | 69.1 | 12.6 | 4.0 | 10.1 | 1.4 | 7.0 | 1.2 | 3.2 | 0.4 | 2.5 | 0.4 | | | | DMRS 1999 |
| 1999 | JA09 | 99JA09AD34-3 | 74 | | 34 | 868 | 30 | 145 | 46 | 848 | 87.9 | 153.0 | 16.5 | 62.5 | 11.3 | 3.6 | 8.8 | 1.2 | 5.7 | 0.9 | 2.1 | 0.3 | 1.4 | 0.2 | | | | DMRS 1999 |
| 1999 | JA09 | 99JA09AD35-1 | 204 | | 41 | 590 | 36 | 161 | 35 | 520 | 37.6 | 61.8 | 7.6 | 30.7 | 5.9 | 2.2 | 5.9 | 0.9 | 5.0 | 1.0 | 2.8 | 0.4 | 2.1 | 0.3 | | | | DMRS 1999 |
| 1999 | JA09 | 99JA09AD35-2 | 184 | | 40 | 562 | 31 | 176 | 38 | 591 | 39.3 | 65.2 | 7.6 | 30.8 | 6.1 | 2.1 | 5.7 | 0.9 | 4.6 | 0.9 | 2.4 | 0.3 | 1.6 | 0.2 | | | | DMRS 1999 |
| 2000 | JA09 | 00JA09AD54-1 | 204 | | 36 | 475 | 23 | 90 | 18 | 171 | 16.9 | 30.2 | 4.5 | 19.1 | 4.6 | 1.9 | 5.2 | 0.8 | 4.6 | 0.9 | 2.4 | 0.3 | 1.8 | 0.2 | | | | DMRS 2000 |
| 2000 | JA09 | 00JA09AD54-2 | 322 | | 34 | 744 | 157 | 178 | 48 | 452 | 146.0 | 83.0 | 23.4 | 98.8 | 18.7 | 5.9 | 21.0 | 3.4 | 20.4 | 4.4 | 12.9 | 1.7 | 10.7 | 1.6 | | | | DMRS 2000 |
| 2000 | JA09 | 00JA09AD58 | 209 | | 48 | 580 | 93 | 219 | 37 | 395 | 78.4 | 67.5 | 12.1 | 49.7 | 9.4 | 3.1 | 10.9 | 1.6 | 9.6 | 2.0 | 5.6 | 0.8 | 4.5 | 0.6 | | | | DMRS 2000 |
| 2000 | JA09 | 00JA09CB69 | 183 | | 40 | 317 | 17 | 55 | 12 | 130 | 12.8 | 21.4 | 2.9 | 13.6 | 3.4 | 1.3 | 3.4 | 0.6 | 3.4 | 0.6 | 1.6 | 0.2 | 1.1 | 0.2 | | | | DMRS 2000 |
| 1989 | JA10 | 89JA10AD04-E | | | | | | | | 358 | | | | | | | | | | | | | | | | | | DMRS 1989 |
| 1999 | JA10 | 99JA10AD11 | 294 | | 28 | 361 | 28 | 279 | 59 | 206 | 57.2 | 115.0 | 12.8 | 49.5 | 9.1 | 3.0 | 7.7 | 1.1 | 5.4 | 1.0 | 2.5 | 0.3 | 1.7 | 0.3 | | | | DMRS 1999 |
| 1999 | JA10 | 99JA10AD17 | 346 | | 46 | 972 | 33 | 315 | 101 | 640 | 80.4 | 168.0 | 19.2 | 75.2 | 13.0 | 4.2 | 10.0 | 1.4 | 6.9 | 1.2 | 3.2 | 0.4 | 2.6 | 0.3 | | | | DMRS 1999 |
| 2000 | JA10 | 00JA10AD33 | 269 | | 19 | 852 | 33 | 252 | 93 | 504 | 105.0 | 193.0 | 21.1 | 80.1 | 13.3 | 4.1 | 11.3 | 1.4 | 7.0 | 1.2 | 2.9 | 0.3 | 1.9 | 0.2 | | | | DMRS 2000 |
| 2000 | JA10 | 00JA10AD34 | 213 | | 56 | 657 | 36 | 261 | 114 | 710 | 87.7 | 161.0 | 17.7 | 69.3 | 12.1 | 3.8 | 10.4 | 1.4 | 6.7 | 1.1 | 2.8 | 0.3 | 1.8 | 0.2 | | | | DMRS 2000 |
| 2000 | JA10 | 00JA10AD37 | 300 | | 39 | 833 | 29 | 201 | 96 | 468 | 60.2 | 118.0 | 13.8 | 51.6 | 9.8 | 3.3 | 9.3 | 1.3 | 6.5 | 1.2 | 2.9 | 0.4 | 2.1 | 0.3 | | | | DMRS 2000 |
| 2000 | JA10 | 00JA10AD41 | 296 | | 45 | 576 | 25 | 175 | 51 | 458 | 39.4 | 77.7 | 9.2 | 35.3 | 6.9 | 2.3 | 7.0 | 1.0 | 5.5 | 1.1 | 2.7 | 0.4 | 2.1 | 0.3 | | | | DMRS 2000 |
| 2002 | JA10 | 02JA10BMS02B | 342 | | 27 | 870 | 36 | 372 | 75 | 912 | 69.7 | 138.1 | 16.1 | 63.2 | 11.9 | 3.9 | 10.2 | 1.4 | 7.9 | 1.4 | 3.5 | 0.4 | 2.6 | 0.4 | | | | DMRS 2002 |
| 2001 | JA11 | 01JA11BM01A | 330 | | 38 | 822 | 50 | 487 | 73 | 378 | 62.7 | 119.0 | 16.1 | 72.9 | 14.6 | 4.9 | 13.3 | 2.0 | 9.7 | 1.7 | 4.0 | 0.5 | 2.9 | 0.4 | | | | DMRS 2001 |
| 2001 | JA11 | 01JA11BM02A | 355 | | 36 | 579 | 42 | 383 | 55 | 342 | 41.3 | 88.0 | 11.8 | 55.7 | 11.9 | 4.1 | 11.6 | 1.8 | 9.0 | 1.6 | 3.8 | 0.5 | 2.9 | 0.4 | | | | DMRS 2001 |
| 2005 | JA11 | 02JA11BMS06A | | | | | | | | | | | | | | | | | | | | | | | | | | SOPET 2005 |
| 1989 | JA12 | 89JA12AD07-A | | | | | | | | 985 | | | | | | | | | | | | | | | | | | DMRS 1989 |
| 2002 | JA12 | 02JA12BMS03A | 427 | | 17 | 792 | 33 | 210 | 91 | 948 | 58.3 | 104.9 | 12.2 | 48.4 | 9.2 | 3.1 | 8.1 | 1.1 | 6.2 | 1.1 | 2.8 | 0.4 | 2.3 | 0.3 | | | | DMRS 2002 |
| 2002 | JA12 | 02JA12BMS04A | 160 | | 30 | 515 | 24 | 117 | 46 | 550 | 35.8 | 56.7 | 6.8 | 27.9 | 5.5 | 2.0 | 5.1 | 0.7 | 4.5 | 0.8 | 2.1 | 0.3 | 1.7 | 0.2 | | | | DMRS 2002 |
| 2019 | JA12 | 19JA12#101BMS01A | 216 | 369 | 33 | 1495 | | | | 400 | | | | | | | | | | | | | | | 10.9 | 5.1 | 4.4 | SRAPT 2019 |
| 2019 | JA12 | 19JA12#101BMS01B | 260 | 419 | 41 | 713 | | | | 500 | | | | | | | | | | | | | | | 10.3 | 7.1 | 4.8 | SRAPT 2019 |
| 2019 | JA12 | 19JA12#101BMS01C | 265 | 266 | 24 | 1015 | | | | 390 | | | | | | | | | | | | | | | 15.0 | 4.9 | 2.7 | SRAPT 2019 |
| 2019 | JA12 | 19JA12#103BMS01C | 210 | 153 | 39 | 586 | | | | 40 | | | | | | | | | | | | | | | 32.0 | 7.9 | 4.6 | SRAPT 2019 |
| 2019 | JA12 | 19JA12#105BMS01A | 91 | 352 | 11 | 666 | | | | 50 | | | | | | | | | | | | | | | 7.7 | 7.9 | 4.1 | SRAPT 2019 |
| 2019 | JA12 | 19JA12#105BMS01C | 170 | 292 | 11 | 289 | | | | 40 | | | | | | | | | | | | | | | 14.1 | 11.2 | 2.3 | SRAPT 2019 |
| 2002 | JA13 | 02JA13BMS02B | 188 | | 37 | 865 | 31 | 307 | 82 | 403 | 62.4 | 125.4 | 14.5 | 58.0 | 10.6 | 3.4 | 8.7 | 1.1 | 6.5 | 1.1 | 2.7 | 0.3 | 2.2 | 0.3 | | | | DMRS 2002 |
| 1989 | JA14 | 89JA14AD06-B | | | | | | | | 806 | | | | | | | | | | | | | | | | | | DMRS 1989 |
| 1998 | JA15 | 98JA15AD10CA01 | 147 | | 34 | 435 | 74 | 127 | 22 | 319 | 45.0 | 41.0 | 6.6 | 29.0 | 6.2 | 1.9 | 6.1 | 1.1 | 6.7 | 1.4 | 4.1 | 0.6 | 3.4 | 0.6 | | | | DMRS 1998 |
| 1998 | JA15 | 98JA15AD12CA01 | 215 | | 45 | 517 | 29 | 277 | 35 | 752 | 48.0 | 91.0 | 10.7 | 42.0 | 7.9 | 2.3 | 6.4 | 1.0 | 5.1 | 0.9 | 2.6 | 0.3 | 2.0 | 0.3 | | | | DMRS 1998 |
| 1998 | JA15 | 98JA15AD13CA01 | 132 | | 37 | 759 | 73 | 210 | 17 | 411 | 62.0 | 65.0 | 8.5 | 33.0 | 6.0 | 1.8 | 5.9 | 1.0 | 5.9 | 1.3 | 4.1 | 0.6 | 3.8 | 0.7 | | | | DMRS 1998 |
| 1998 | JA15 | 98JA15AD19CA01 | 61 | | 69 | 260 | 16 | 184 | 24 | 961 | 23.0 | 55.0 | 6.0 | 25.0 | 5.7 | 1.8 | 4.3 | 0.7 | 3.6 | 0.6 | 1.6 | 0.2 | 1.1 | 0.2 | | | | DMRS 1998 |
| 1989 | JA16 | 89JA16AD01 | | | | | | | | 895 | | | | | | | | | | | | | | | | | | DMRS 1989 |
| 1990 | JA17 | 90JA17AD01C | | | | | | | | | | | | | | | | | | | | | | | | | | DMRS 1990 |
| 2005 | JA17 | 05JA17AD05b1 | 294 | 636 | 14 | 787 | 29 | 220 | 83 | 560 | 52.8 | 107.1 | 12.3 | 48.7 | 9.4 | 2.8 | 7.8 | 1.2 | 5.9 | 1.1 | 2.8 | 0.4 | 2.1 | 0.3 | 2.4 | 6.0 | 1.4 | SOPET 2005 |
| 2005 | JA17 | 05JA17AD05b2 | 280 | 217 | 31 | 790 | 35 | 275 | 80 | 435 | 49.5 | 103.2 | 12.0 | 51.0 | 9.9 | 3.0 | 8.4 | 1.3 | 6.6 | 1.3 | 3.0 | 0.4 | 2.5 | 0.4 | 3.1 | 5.2 | 1.5 | SOPET 2005 |
| 2005 | JA17 | 05JA17AD07r1 | 306 | 355 | 16 | 808 | 36 | 267 | 120 | 170 | 77.9 | 144.2 | 16.5 | 65.1 | 11.1 | 3.4 | 9.5 | 1.3 | 6.9 | 1.3 | 3.2 | 0.4 | 2.5 | 0.4 | 4.0 | 9.5 | 1.5 | SOPET 2005 |
| 2005 | JA17 | 05JA17AD07r2 | 18 | 0 | 170 | 690 | 36 | 668 | 182 | 453 | 105.2 | 149.1 | 11.3 | 32.3 | 4.1 | 1.3 | 3.9 | 0.7 | 4.5 | 1.1 | 3.5 | 0.6 | 4.1 | 0.6 | 17.9 | 26.5 | 8.8 | SOPET 2005 |

Table 2 Continued.

| Year | Seamount | Sample ID | V (ppm) | Cr | Rb | Sr | Y | Zr | Nb | Ba | La | Ce | Pr | Nd | Sm | Eu | Gd | Tb | Dy | Ho | Er | Tm | Yb | Lu | Pb | Th | U | Project name |
|---|---|---|---|---|---|---|---|---|---|---|---|---|---|---|---|---|---|---|---|---|---|---|---|---|---|---|---|---|
| 2005 | JA17 | 05JA17AD07r3 | 294 | 2 | 36 | 824 | 36 | 353 | 75 | 448 | 51.8 | 104.6 | 13.0 | 55.5 | 10.6 | 3.4 | 9.8 | 1.4 | 7.2 | 1.4 | 3.4 | 0.5 | 2.7 | 0.4 | 4.0 | 5.6 | 1.7 | SOPET 2005 |
| 2005 | JA17 | 02JA17BMS01A | 207 | 10 | 39 | 1323 | 50 | 335 | 123 | 694 | 99.3 | 192.4 | 22.3 | 89.9 | 16.5 | 5.0 | 14.2 | 1.9 | 10.0 | 1.8 | 4.5 | 0.6 | 3.6 | 0.5 | 4.4 | 9.6 | 2.4 | SOPET 2005 |
| 2018 | JA17 | 18JA17#145BMS01B | 98 | 70 | 102 | 1080 | 125 | | | 913 | 147.5 | 195.0 | 24.4 | 92.3 | 15.0 | 4.0 | 15.8 | 2.2 | 13.2 | 3.2 | 9.3 | 1.3 | 8.6 | 1.2 | 51.7 | 17.8 | 4.9 | SRAPT 2018 |
| 2018 | JA17 | 18JA17#146BMS01C | 262 | 60 | 40 | 1070 | 38 | | | 611 | 68.9 | 151.5 | 16.4 | 64.8 | 13.1 | 3.6 | 10.9 | 1.4 | 7.9 | 1.5 | 4.1 | 0.5 | 3.0 | 0.4 | 31.0 | 7.2 | 2.2 | SRAPT 2018 |
| 2018 | JA17 | 18JA17#147BMS01A | 313 | 900 | 30 | 1060 | 66 | | | 669 | 67.9 | 103.0 | 11.1 | 42.9 | 8.8 | 2.5 | 9.0 | 1.2 | 6.9 | 1.7 | 4.1 | 0.5 | 3.6 | 0.5 | 36.1 | 5.6 | 2.5 | SRAPT 2018 |
| 2018 | JA17 | 18JA17#147BMS01B | 301 | 180 | 16 | 1325 | 47 | | | 848 | 94.4 | 180.0 | 19.3 | 73.9 | 12.9 | 3.6 | 11.3 | 1.6 | 8.3 | 1.6 | 4.4 | 0.6 | 3.7 | 0.6 | 33.7 | 9.6 | 3.0 | SRAPT 2018 |
| 2018 | JA17 | 18JA17#147BMS01C | 256 | 400 | 25 | 766 | 112 | | | 545 | 73.8 | 79.6 | 10.8 | 44.9 | 8.8 | 2.6 | 10.4 | 1.6 | 9.8 | 2.3 | 6.6 | 0.9 | 6.2 | 0.9 | 52.5 | 3.7 | 2.8 | SRAPT 2018 |
| 2018 | JA17 | 18JA17#147BMS01D | 242 | 310 | 39 | 1090 | 28 | | | 703 | 47.1 | 87.2 | 9.5 | 37.5 | 8.3 | 2.2 | 7.1 | 1.0 | 5.4 | 1.1 | 2.8 | 0.4 | 2.4 | 0.3 | 6.1 | 5.7 | 2.0 | SRAPT 2018 |
| 2019 | JA17 | 19JA17#142BMS01C | 153 | 5 | 76 | 2270 | | | | 1950 | | | | | | | | | | | | | | | 44.1 | 12.7 | 5.8 | SRAPT 2019 |
| 2019 | JA17 | 19JA17#150BMS01C | 231 | 167 | 36 | 1800 | | | | 960 | | | | | | | | | | | | | | | 23.5 | 8.2 | 3.0 | SRAPT 2019 |
| 1990 | JA19 | 90JA19AD01C | | | | | | | | | | | | | | | | | | | | | | | | | | DMRS 1990 |
| 1990 | JA19 | 90JA19AD04D | | | | | | | | | | | | | | | | | | | | | | | | | | DMRS 1990 |
| 1990 | JA22 | 90JA22AD05D | | | | | | | | | | | | | | | | | | | | | | | | | | DMRS 1990 |
| 1990 | JA22 | 90JA22AD11B | | | | | | | | | | | | | | | | | | | | | | | | | | DMRS 1990 |
| 2005 | MT472 | 05DSMT472AD01r1-1 | 241 | 136 | 29 | 627 | 82 | 312 | 42 | 219 | 63.1 | 71.7 | 15.9 | 76.5 | 16.6 | 5.2 | 18.2 | 2.7 | 14.2 | 2.8 | 7.2 | 1.0 | 5.4 | 0.8 | 6.0 | 2.8 | 1.1 | SOPET 2005 |
| 2005 | MT472 | 05DSMT472AD01r1-2 | 201 | 132 | 30 | 552 | 63 | 297 | 41 | 158 | 44.1 | 72.5 | 10.9 | 51.7 | 11.5 | 3.8 | 11.9 | 1.8 | 9.5 | 2.0 | 5.0 | 0.7 | 3.9 | 0.5 | 3.0 | 2.6 | 1.4 | SOPET 2005 |
| 2005 | MT472 | 05DSMT472AD01a3 | 230 | 149 | 30 | 638 | 76 | 301 | 43 | 195 | 58.2 | 70.5 | 13.8 | 65.7 | 14.4 | 4.5 | 15.3 | 2.3 | 12.4 | 2.5 | 6.2 | 0.9 | 4.7 | 0.7 | 5.0 | 2.7 | 1.0 | SOPET 2005 |
| 2005 | MT473 | MT473BMS02A-2 | 327 | 22 | 36 | 650 | 52 | 270 | 54 | 317 | 44.2 | 77.7 | 11.7 | 51.9 | 11.4 | 3.7 | 10.8 | 1.6 | 8.8 | 1.7 | 4.5 | 0.7 | 3.4 | 0.5 | 1.7 | 3.6 | 2.4 | SOPET 2005 |
| 2005 | MT474 | MT474BMS04A | | | | | | | | | | | | | | | | | | | | | | | | | | SOPET 2005 |
| 2019 | Takuyo-Daigo | 19TAKUYO5BMS41B | 244 | 221 | 52 | 652 | | | | 2250 | | | | | | | | | | | | | | | 304.0 | 2.8 | 4.1 | SRAPT 2019 |
| 2019 | Takuyo-Daigo | 19TAKUYO5BMS50B | 196 | 154 | 45 | 712 | | | | 530 | | | | | | | | | | | | | | | 21.4 | 10.6 | 2.1 | SRAPT 2019 |
| 2019 | Takuyo-Daigo | 19TAKUYO5BMS57B | 285 | 68 | 31 | 1075 | | | | 530 | | | | | | | | | | | | | | | 17.8 | 7.2 | 2.0 | SRAPT 2019 |
| 2019 | Takuyo-Daigo | 19TAKUYO5BMS57C | 136 | 3 | 52 | 933 | | | | 640 | | | | | | | | | | | | | | | 40.5 | 12.4 | 3.1 | SRAPT 2019 |
| 2019 | Takuyo-Daigo | 19TAKUYO5BMS58C | 224 | 57 | 45 | 737 | | | | 610 | | | | | | | | | | | | | | | 27.5 | 7.6 | 2.2 | SRAPT 2019 |
| 2019 | Takuyo-Daigo | 19TAKUYO5BMS59A | 231 | 50 | 37 | 774 | | | | 540 | | | | | | | | | | | | | | | 7.5 | 8.0 | 2.0 | SRAPT 2019 |
| 2019 | Takuyo-Daigo | 19TAKUYO5BMS59B | 215 | 62 | 27 | 793 | | | | 730 | | | | | | | | | | | | | | | 16.4 | 8.5 | 1.9 | SRAPT 2019 |
| 2019 | Takuyo-Daigo | 19TAKUYO5BMS52A | 247 | 234 | 16 | 821 | | | | 210 | | | | | | | | | | | | | | | 33.3 | 3.9 | 1.7 | SRAPT 2019 |
| 2019 | Takuyo-Daigo | 19TAKUYO5BMS55C | 226 | 328 | 23 | 622 | | | | 300 | | | | | | | | | | | | | | | 13.6 | 2.8 | 1.3 | SRAPT 2019 |
| 2019 | Takuyo-Daigo | 19TAKUYO5BMS52A | 157 | 198 | 26 | 449 | | | | 130 | | | | | | | | | | | | | | | 13.5 | 3.5 | 0.9 | SRAPT 2019 |
| 2019 | Takuyo-Daigo | 19TAKUYO5BMS52B | 154 | 236 | 55 | 316 | | | | 160 | | | | | | | | | | | | | | | 29.7 | 3.4 | 1.7 | SRAPT 2019 |
| 2019 | Takuyo-Daigo | 19TAKUYO5BMS53B | 191 | 127 | 49 | 197 | | | | 230 | | | | | | | | | | | | | | | 32.5 | 3.8 | 1.9 | SRAPT 2019 |
| 2019 | Takuyo-Daigo | 19TAKUYO5BMS53D | 196 | 128 | 32 | 3270 | | | | 130 | | | | | | | | | | | | | | | 25.7 | 3.9 | 3.3 | SRAPT 2019 |
| 2019 | Takuyo-Daigo | 19TAKUYO5BMS53E | 155 | 117 | 47 | 480 | | | | 240 | | | | | | | | | | | | | | | 10.0 | 4.0 | 2.2 | SRAPT 2019 |
| 2019 | Takuyo-Daigo | 19TAKUYO5BMS52A | 157 | 254 | 27 | 412 | | | | 130 | | | | | | | | | | | | | | | 8.2 | 3.3 | 1.1 | SRAPT 2019 |
| 2019 | Takuyo-Daigo | 19TAKUYO5BMS53B | 170 | 95 | 37 | 244 | | | | 370 | | | | | | | | | | | | | | | 69.3 | 3.4 | 1.5 | SRAPT 2019 |
| 2019 | Takuyo-Daigo | 19TAKUYO5BMS53D | 165 | 84 | 19 | 458 | | | | 240 | | | | | | | | | | | | | | | 9.7 | 2.8 | 0.7 | SRAPT 2019 |
| 2020 | Takuyo-Daigo | 19TAKUYO5BMS53D_1a | 271 | 217 | 26 | 487 | 23 | 189 | 58 | 150 | 36.1 | 72.5 | 8.5 | 36.0 | 7.1 | 2.4 | 7.6 | 1.0 | 5.1 | 0.9 | 2.4 | 0.3 | 1.9 | 0.3 | 2.4 | 4.4 | 1.8 | ESCRC 2020 |
| 2020 | Takuyo-Daigo | 19TAKUYO5BMS53D_1b | 274 | 220 | 36 | 458 | 23 | 207 | 63 | 148 | 37.9 | 78.0 | 8.8 | 36.5 | 7.4 | 2.5 | 7.6 | 1.1 | 5.3 | 1.0 | 2.5 | 0.3 | 1.9 | 0.2 | 2.8 | 4.8 | 2.0 | ESCRC 2020 |
| 2020 | Takuyo-Daigo | 19TAKUYO5BMS53D_2a | 153 | 118 | 28 | 129 | 13 | 124 | 39 | 87 | 23.8 | 48.6 | 5.6 | 22.7 | 4.4 | 1.5 | 4.6 | 0.6 | 3.2 | 0.6 | 1.5 | 0.2 | 1.1 | 0.1 | 1.4 | 2.9 | 1.2 | ESCRC 2020 |
| 2020 | Takuyo-Daigo | 19TAKUYO5BMS53D_2b | 153 | 115 | 31 | 109 | 11 | 111 | 35 | 65 | 17.8 | 35.0 | 4.3 | 17.5 | 3.5 | 1.2 | 3.5 | 0.5 | 2.6 | 0.5 | 1.3 | 0.2 | 1.0 | 0.1 | 1.3 | 2.5 | 1.0 | ESCRC 2020 |
| 2020 | Takuyo-Daigo | 19TAKUYO5BMS53E_1a | 139 | 89 | 50 | 228 | 29 | 180 | 50 | 185 | 55.8 | 71.9 | 10.9 | 43.8 | 8.1 | 2.5 | 8.7 | 1.1 | 5.9 | 1.1 | 3.0 | 0.4 | 2.3 | 0.3 | 18.4 | 3.8 | 1.7 | ESCRC 2020 |
| 2020 | Takuyo-Daigo | 19TAKUYO5BMS53E_1b | 140 | 106 | 47 | 327 | 55 | 169 | 52 | 180 | 59.5 | 61.5 | 11.3 | 47.1 | 9.3 | 2.7 | 10.8 | 1.5 | 8.7 | 1.8 | 5.1 | 0.7 | 4.1 | 0.6 | 20.2 | 4.0 | 1.9 | ESCRC 2020 |
| 2020 | Takuyo-Daigo | 19TAKUYO5BMS53F_1a | 139 | 91 | 46 | 248 | 29 | 189 | 47 | 176 | 57.6 | 75.8 | 10.5 | 42.3 | 7.7 | 2.3 | 8.2 | 1.1 | 5.7 | 1.1 | 2.9 | 0.4 | 2.3 | 0.3 | 17.2 | 3.6 | 1.6 | ESCRC 2020 |
| 2020 | Takuyo-Daigo | 19TAKUYO5BMS53F_1b | 127 | 105 | 41 | 302 | 56 | 162 | 45 | 155 | 56.8 | 59.2 | 10.2 | 43.2 | 8.4 | 2.5 | 10.0 | 1.4 | 8.0 | 1.7 | 5.1 | 0.6 | 3.9 | 0.6 | 17.9 | 3.5 | 1.6 | ESCRC 2020 |
| 2020 | Takuyo-Daigo | 19TAKUYO5BMS53F_2a | 145 | 96 | 17 | 395 | 12 | 99 | 30 | 153 | 20.6 | 38.5 | 4.7 | 19.7 | 4.0 | 1.4 | 4.1 | 0.6 | 2.9 | 0.5 | 1.4 | 0.2 | 0.9 | 0.1 | 1.1 | 2.3 | 0.6 | ESCRC 2020 |
| 2020 | Takuyo-Daigo | 19TAKUYO5BMS53F_2b | 269 | 179 | 37 | 573 | 21 | 178 | 53 | 368 | 33.5 | 67.6 | 8.0 | 33.2 | 6.8 | 2.3 | 7.0 | 1.0 | 4.8 | 0.9 | 2.3 | 0.3 | 1.8 | 0.2 | 1.9 | 4.1 | 1.1 | ESCRC 2020 |
| 2020 | Takuyo-Daigo | 19TAKUYO5BMS53F_3a | 146 | 108 | 28 | 121 | 14 | 115 | 40 | 90 | 24.9 | 49.9 | 5.8 | 23.8 | 4.6 | 1.6 | 4.9 | 0.6 | 3.3 | 0.6 | 1.5 | 0.2 | 1.1 | 0.2 | 1.5 | 2.9 | 1.3 | ESCRC 2020 |
| 2020 | Takuyo-Daigo | 19TAKUYO5BMS53F_3b | 165 | 127 | 35 | 114 | 12 | 115 | 39 | 77 | 20.5 | 40.4 | 4.9 | 20.1 | 4.1 | 1.4 | 4.3 | 0.6 | 3.1 | 0.5 | 1.4 | 0.2 | 1.1 | 0.1 | 1.6 | 3.0 | 1.2 | ESCRC 2020 |

DMRS: Deep-sea mineral resource surveys

SOPET: Survey on offshore petroleum exploration technology (basic survey on exploration technology for deep water petroleum resources)

SRAPT: Survey on resource assessment and production technology for the development of marine mineral resources

ESCRC: Environmental study in the area for exploration of cobalt-rich crusts

The decrease in $SiO_2$ is observed with the increase in LOI. The alteration reflects two stages of magmatic activity: hydrothermal alteration (recrystallization of hydrous minerals, increase in $H_2O^+$) and seafloor weathering (formation of clay minerals, increase in $H_2O^-$). With alteration, calcite crystallizes in the voids and $CO_2$ increases. For the samples with >1 % $P_2O_5$, the effect of phosphatization is considered. It is known that many elements, including alkali elements, are lost in hydrothermal alteration and alkali elements are added in seafloor weathering. In addition, with the increase of calcite and phosphate, elements such as Ca, Ba, Y, and REE are added. Careful interpretation is needed since the chemical composition of the rock changes from the original composition due to hydrothermal alteration and phosphatization.

Although $SiO_2$ of most samples are reduced due to increased LOI and CaO, these samples are classified as basalt. These basalts show a wide range of undifferentiated basalts with high MgO and Mg# (MgO/MgO+FeO*, FeO* = FeO+$Fe_2O_3$) to highly differentiated basalts with low MgO and Mg#. The high $Na_2O$+$K_2O$ (>3 %) and high $TiO_2$ (>2 %) relative to $SiO_2$ indicate the characteristics of alkaline rocks.

Figure 4 shows the Ti/1000-V diagram (after Shervais, 1982) and Figure 5 shows the Zr/4-2Nb-Y diagram (after Meschede, 1986). In the Ti/1000-V and Zr/4-2Nb-Y diagrams, the plots are in the oceanic island alkaline basalt region, although there is some variation. In the Zr/4-2Nb-Y diagram, samples with slightly higher Y values outside the oceanic island alkali basalt region are considered to be due to the increase in Y caused by phosphatization.

Figure 6 shows the Ba/Zr–Nb/Zr diagram. The Ba/Nb ratios of most of the samples are in the range of 4 to 10, which is similar to the basalts in the South Pacific Isotope and Thermal Anomaly (SOPITA) region where the seamounts in this area are thought to have been formed. The samples with Ba/Nb ratios higher than 10 are considered to have undergone Ba addition due to phosphatization. This is especially true for JA09 and JA15 Seamounts.

The MORB-normalized diagram is shown in Figure 7, and the REE chondrite-normalized diagram is shown in Figure 8. The reference values used for the normalization are those of Sun and McDonough (1989), and the figures are divided by seamounts. In the MORB normalized diagram, each seamount basically shows a smooth downward pattern enriched in incompatible elements. Rb, Ba, U, and K increase or decrease due to the influence of alteration, and the increase in Ba and Y may be due to phosphatization. For the samples with a large increase in Pb, MnO is also high, which may be due to the contamination of ferromanganese crusts. Ti-poor samples are found in JA02, JA03, JA05, JA09, JA15, and JA17 Seamounts. Since Ti is an element that is difficult to move during alteration, it may reflect the primary composition and may have been produced by different magmatic activities.

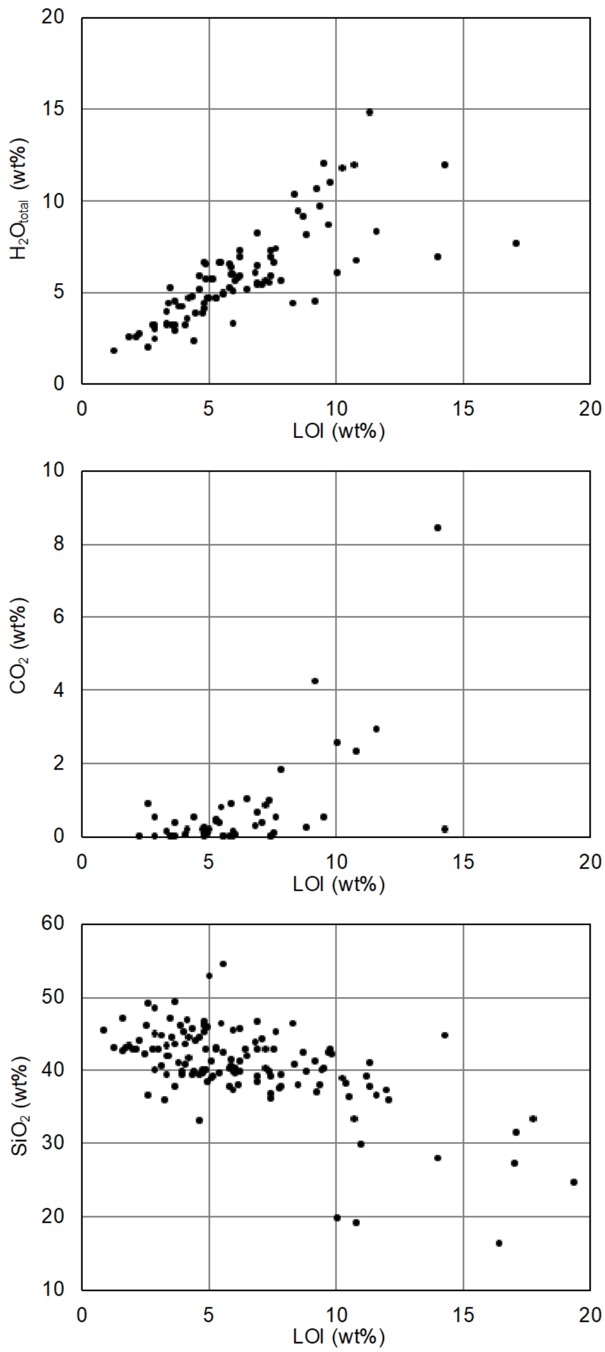


Fig. 2 $H_2O$, $CO_2$, and $SiO_2$ plots against LOI of seamount basement basalts.

The REE chondrite-normalization diagrams also show typical oceanic island alkaline basalt features enriched in LREEs for many samples. Two samples from the JA03 Seamount (02JA03BMS04B-1, 02JA03BMS04B-2) and one sample from the JA17 Seamount (05JAl7AD07r2) show a low MREE pattern that is different from the other samples. In the JA02 Seamount, JA09 Seamount, and MT472 Seamount, some samples show negative Ce anomalies. The negative Ce anomaly reflects the influence

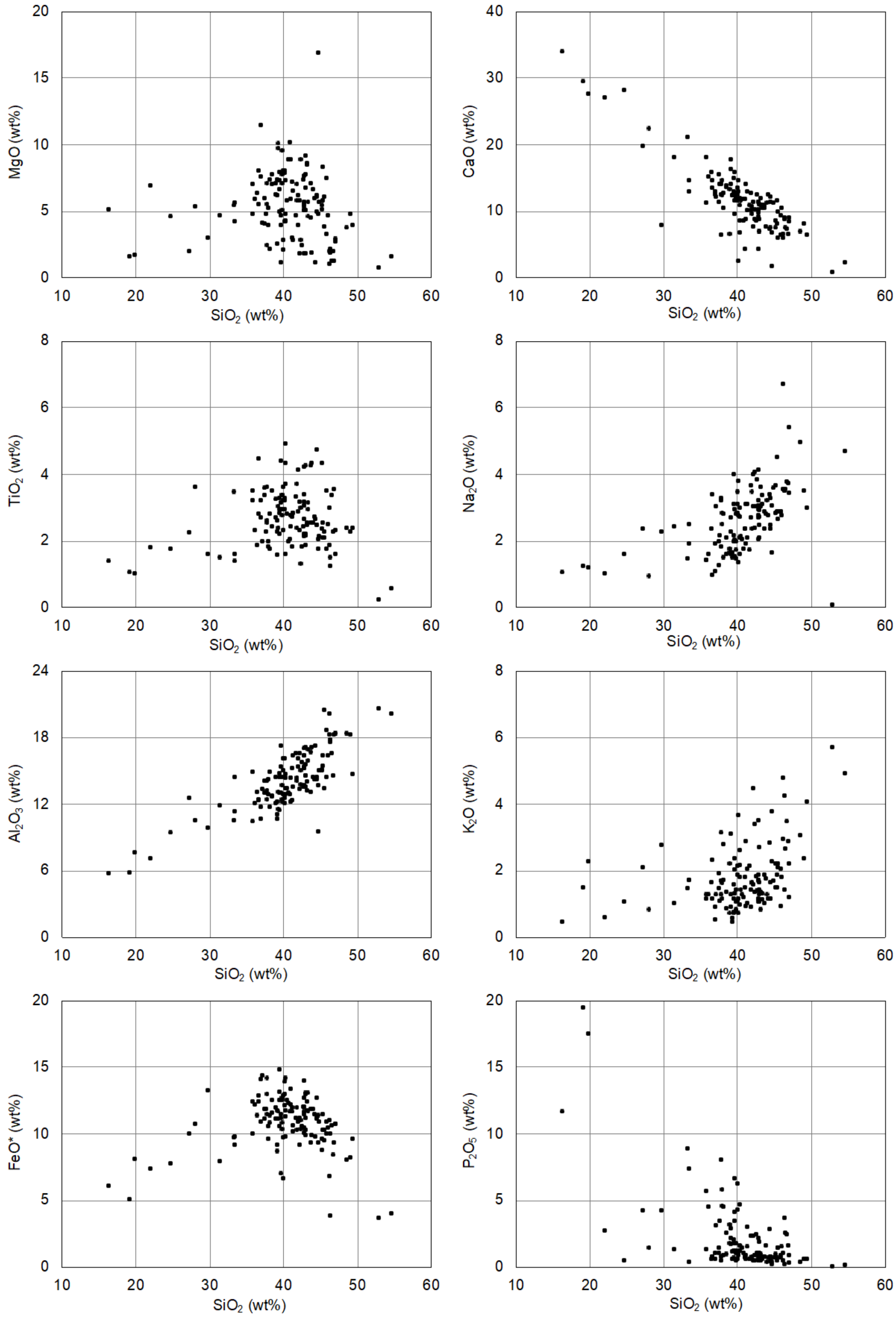


Fig. 3 Major elements plot against $SiO_2$ of seamount basement basalts.

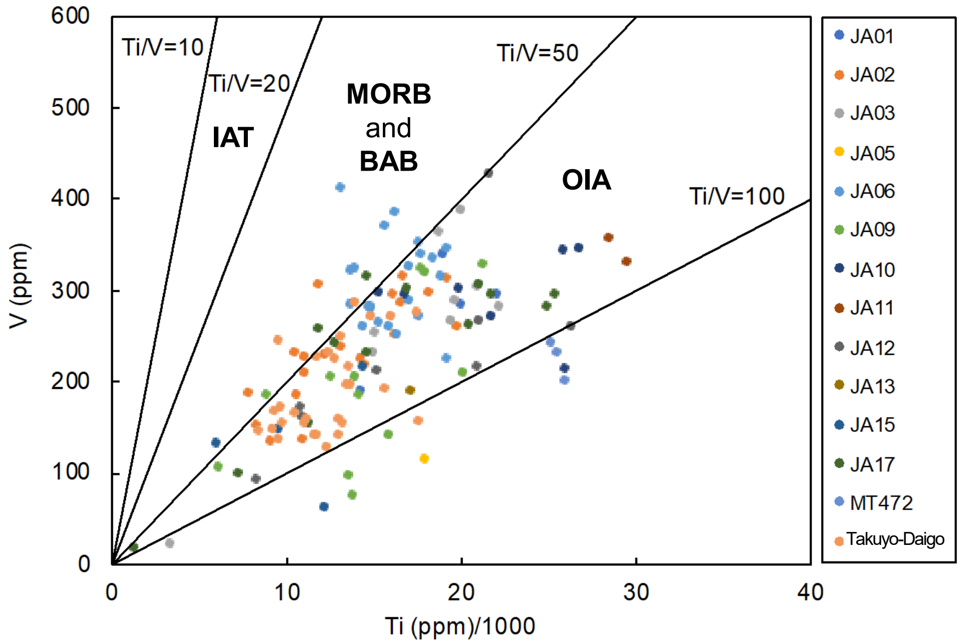


Fig. 4 Ti-V discrimination diagram for basalts (after Shervais, 1982). The fields are IAT-island arc tholeiite; MORB and BAB-mid-ocean ridge basalt and back-arc basin basalt; OIA-ocean island alkali basalt.

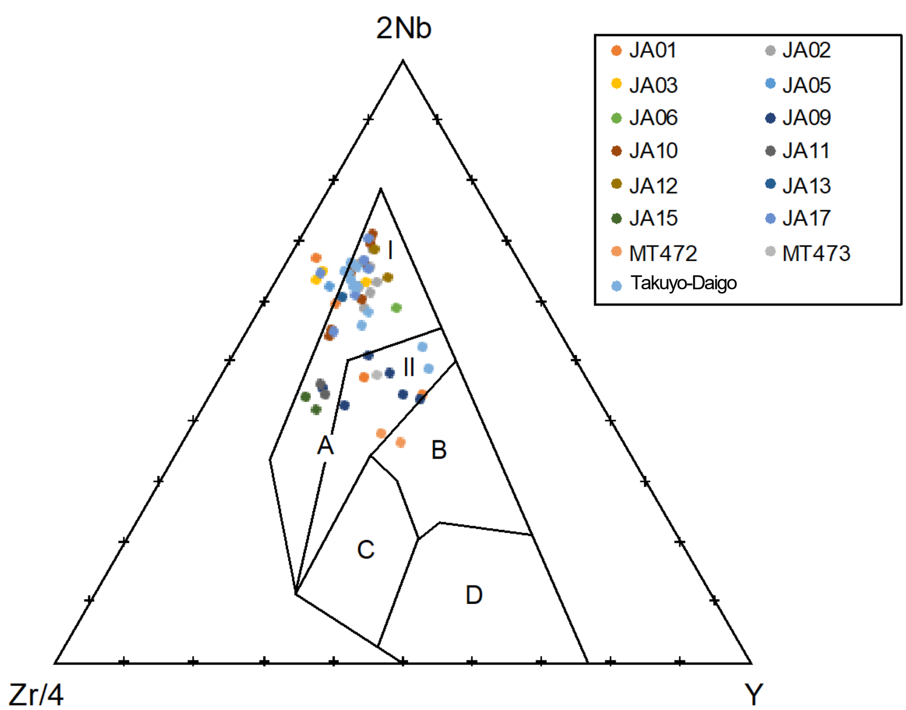


Fig. 5 Zr-Nb-Y discrimination diagram for basalts (after Meschede, 1986). Samples with $P_2O_5$>2 % were excluded because yttrium is increased by phosphatization. The fields are defined as follows: AI, within-plate alkali basalts; AII, within-plate alkali basalts and within-plate tholeiites; B, E-type MORB; C, within-plate tholeiites and volcanic-arc basalts; D, N-type MORB and volcanic-arc basalts.

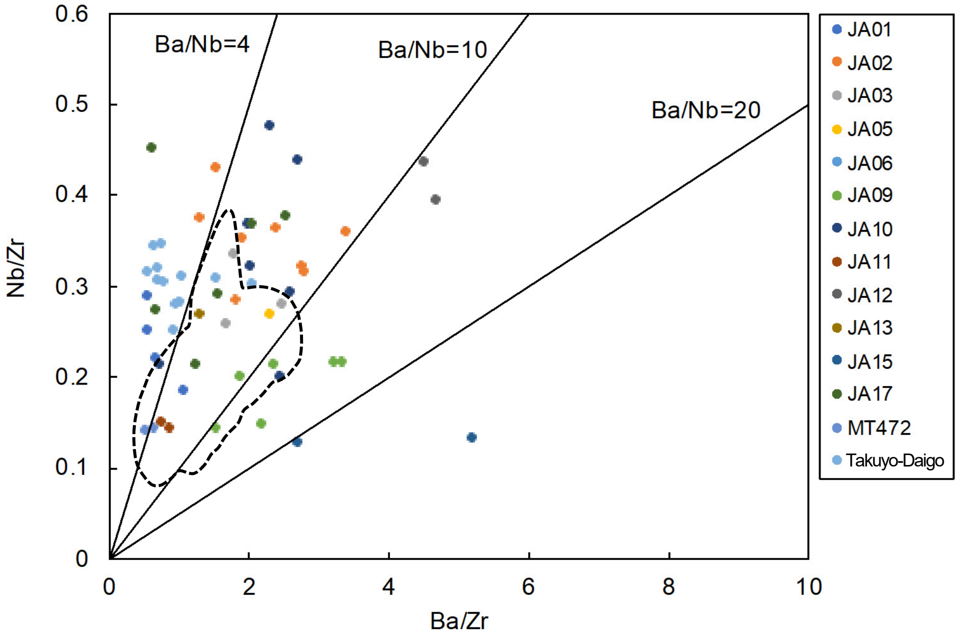


Fig. 6 Nb/Zr-Ba/Zr discrimination diagram for basalts. Samples with $P_2O_5$>2 % were excluded because barium is increased by phosphatization. The area enclosed by dashed line indicates SOPITA island chains (from Christie *et al.*, 1995).

of seawater and may be due to calcite crystallization, phosphatization, or limestone incorporation. On the other hand, some samples from JA02 Seamount and JA06 Seamount show positive Ce anomalies, suggesting contamination of ferromanganese crusts.

## 5. Formation age

The ages obtained from each seamount are summarized in Table 3. Below are the formation ages for the Marcus-Wake Seamount Group, Magellan Seamount Group, and Marshall Islands Seamount Group.

### 5. 1 Marcus-Wake Seamount Group

**(1) JA01 Seamount (Miami Guyot)**

Ar–Ar dating was performed on three samples with relatively little alteration, but no reliable age values were obtained from 99JA01AD12 and 99AD13K01. 99JA01AD18 yielded a plateau age of 85.7 ± 2.0 Ma. The stage-heating age spectra and inverse isochron diagrams are shown in Figure 9. The $^{40}Ar/^{39}Ar$ age measurement data are shown in Table 4. This age is slightly younger than the Ar–Ar age of 96.8 ± 1.2 Ma reported by Koppers *et al.* (2003).

**(2) JA02 Seamount (Lamont Guyot)**

Ar–Ar dating was carried out on three samples, but no plateau age was obtained for 01JA02BM02C due to alteration, and an isochron age value of 60.00 ± 16.92 Ma was obtained, which is not considered to be a valid result. A plateau age of 72.4 ± 1.4 Ma was obtained for 02JA02BM06B. Figure 10 shows the step heating age spectra and inverse isochron diagrams. The $^{40}Ar/^{39}Ar$ age measurement data are shown in Table 4. The ages obtained from the high-temperatures (9 to 12 steps) are much younger than those from the low-temperatures (1 to 8 steps) and the K/Ca ratios of each plateau decrease rapidly at high-temperatures, suggesting that the Ar–emitting mineral phases may differ between the high and low temperatures. In addition, the K/Ca ratio and $^{40}Ar^*$ (radiogenic $^{40}Ar$) are generally low, suggesting that the ages obtained are not from the source rock but from secondary mineral phases. A plateau age of 82.4 ± 0.5 Ma was obtained for 02JA02BMS07A, which is in harmony with the Ar–Ar ages (81.6 ± 1.2 Ma, 87.2 ± 0.6 Ma) reported by Koppers *et al.* (2003).

**(3) JA03 Seamount (Arnold Guyot)**

K–Ar dating was performed on one sample and Ar–Ar dating on two samples. The K–Ar age of 47.5 ± 1 Ma obtained from 97JA03AD19 is unreliable due to alteration. A plateau age of 98.4 ± 0.4 Ma was obtained from 02JA03BMS04B. The stage-heating age spectra and inverse isochron diagrams are shown in Fig. 11. The $^{40}Ar/^{39}Ar$ age measurement data are shown in Table 4. The K/Ca ratio of each plateau is very high, suggesting that the main source of Ar emission is alkali feldspar in matrix, which is K-rich and has a high K/Ca ratio. Ar–Ar dating was performed again on another part of the 02JA03BMS04B, yielding a whole rock age of 100.6 Ma and an isochron age of 93.6 Ma.

**(4) JA05 Seamount (Batiza Guyot)**

Ar–Ar dating was performed on one sample, and the stage-heating age spectra diagram yielded an age of 98.4

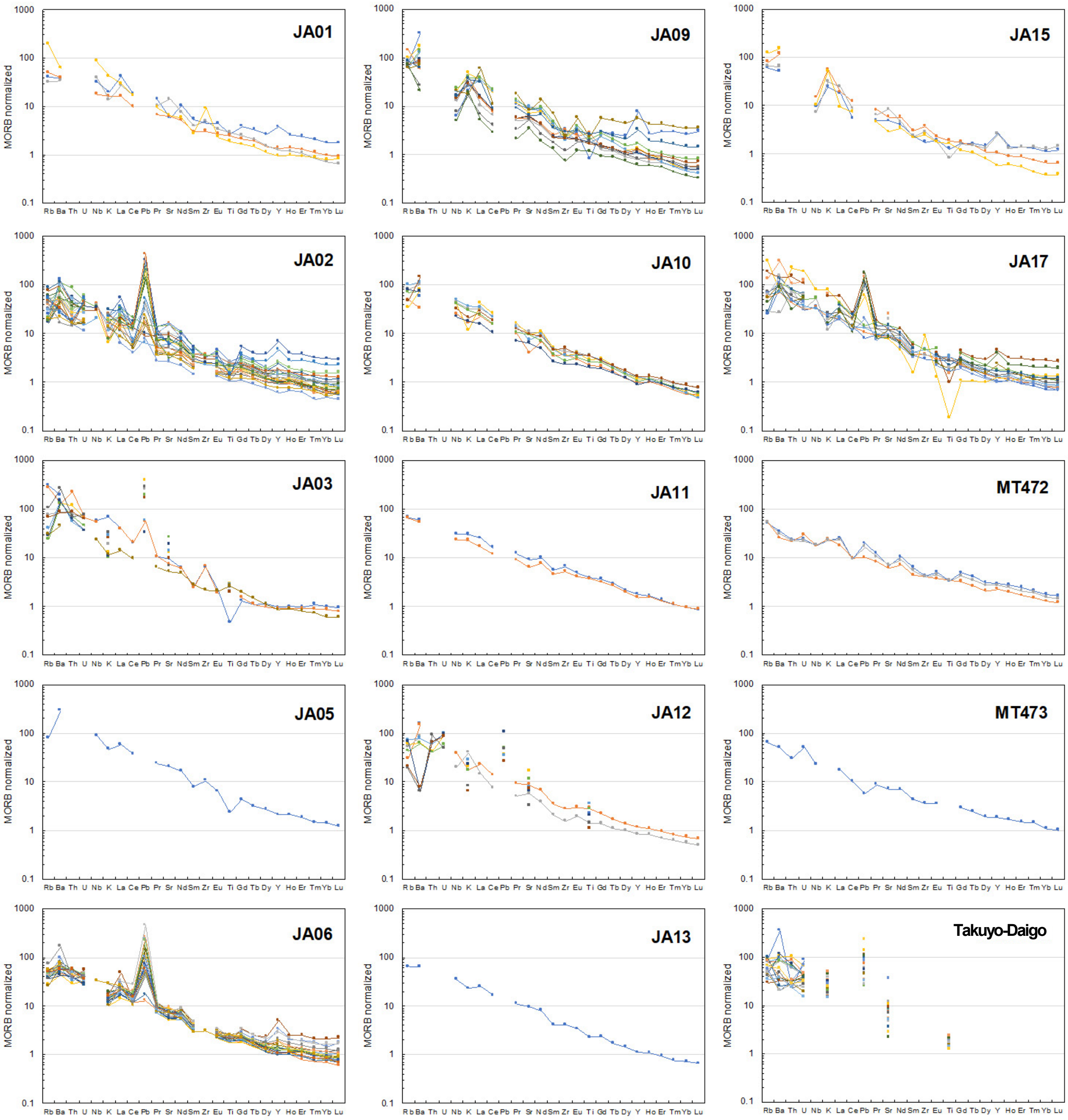


Fig. 7 MORB-normalized patterns of seamount basement basalts

± 0.4 Ma. However, the plateau age criterion is not met because there is no plateau greater than 50 % of $^{39}Ar$. The inverse isochron diagram cannot be used to verify the plateau age because no isochron can be drawn. The stage-heating age spectra and inverse isochron diagram are shown in Figure 12. The $^{40}Ar/^{39}Ar$ age measurement data are shown in Table 4.

**(5) JA06 Seamount (Xufu Guyot)**

K–Ar dating was carried out on two relatively unaltered samples, which yielded the ages of Late Cretaceous (80.0 ± 2 Ma, 86.5 ± 2 Ma), but the results are not reliable due to alteration.

**(6) JA11 Seamount (McDonnell Guyot)**

Ar–Ar dating was carried out on two samples. The obtained plateau ages are 109.4 ± 0.3 Ma and 116.43 ± 4.94 Ma (Late Cretaceous: Albian), which are reasonable results. Figure 13 shows the stage-heating age spectra diagram of 01JA11BMS02A. The $^{40}Ar/^{39}Ar$ age measurement data are

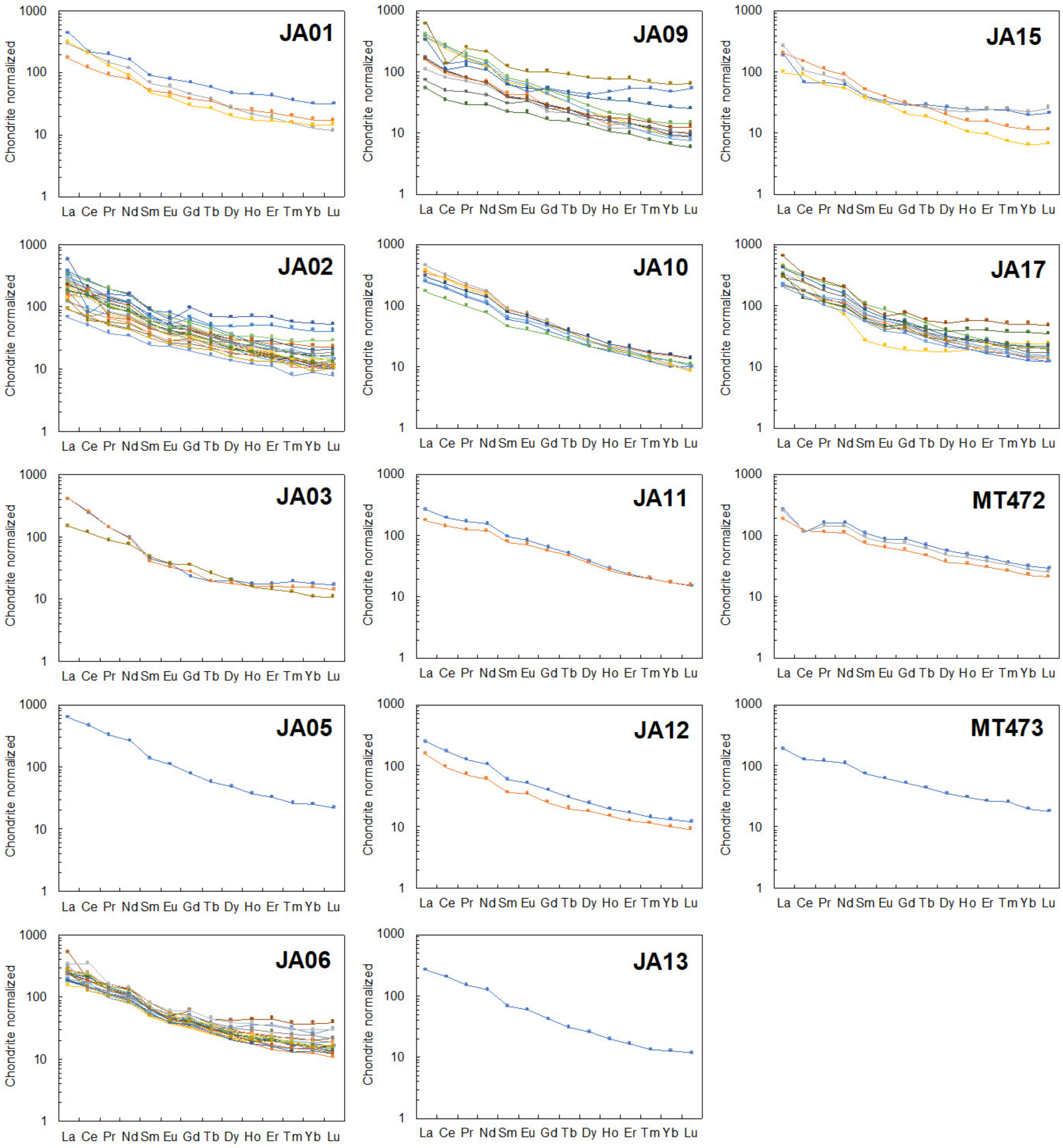


Fig. 8 REE patterns of seamount basement basalts

shown in Table 4.

**(7) JA12 Seamount (Zhinyu Guyot)**

K–Ar dating was performed on one sample and Ar–Ar dating on two samples. The K–Ar age of 72.4 ± 2.3 Ma obtained from 89JA12AD07-A is unreliable due to alteration. The stage-heating age spectra of 02JA12BMS03B gives an age of 85.6 ± 0.4 Ma. However, the plateau age criterion is not met because there is no plateau greater than 50 % of $^{39}$Ar. The inverse isochron diagram cannot be used to verify the plateau age because no isochron can be drawn. Figure 14 shows the stage-heating age spectra and inverse isochron diagram. The $^{40}$Ar/$^{39}$Ar age measurement data are shown in Table 4. A plateau age of 66.77 ± 0.17 Ma was obtained from 02JA12BMS04B.

**(8) JA17 Seamount (Scripps Guyot)**

K–Ar dating was performed on two samples and Ar–Ar dating on one sample. The K–Ar ages of 29.5 ± 1.9 Ma

Table 3 K–Ar/Ar–Ar ages of basement basalts from seamounts in the JA area

| Seamount | | Sample ID | Year | K-Ar age ± 1σ (Ma) | Ar-Ar age ± 1σ (Ma) Total integrated age | Inverse isochron age | $^{40}Ar/^{36}Ar$ intercept | Weighted mean plateau age | MSWD | $^{39}Ar$ (%) | Project name |
|---|---|---|---|---|---|---|---|---|---|---|---|
| **Marcus-Wake Seamount Group** | | | | | | | | | | | |
| JA01 | Miami | 99JA01AD12 | 1999 | | | - | | - | | | DMRS 1999 |
| | | 99JA01AD13 | 1999 | | | - | | - | | | DMRS 1999 |
| | | 99JA01AD18 | 1999 | | | - | | 85.7±2.0 | | 62.9 | DMRS 1999 |
| | | *Koppers et al. (2003)* | | | | | | *96.8±1.2 (2σ)* | | | |
| JA02 | Lamont | 01JA02BMS02C | 2001 | | | 60.00±16.92 | | - | | | DMRS 2001 |
| | | 02JA02BMS06B | 2002 | | | 72.53±1.36 | 294.4±7.0 | 72.4±1.4 | | 67.3 | DMRS 2002 |
| | | 02JA02BMS07A | 2005 | | 82.3±1.1 | 80±5 | 724±315 | 82.4±0.5 | 1.24 | 92.1 | SOPET 2005 |
| | | *Koppers et al. (2003)* | | | | | | *87.2±0.6 (2σ)* | | | |
| | | *Koppers et al. (2003)* | | | | | | *81.6±1.2 (2σ)* | | | |
| JA03 | Arnold | 97JA03AD19 | 1997 | 47.5±1 | | | | | | | DMRS 1997 |
| | | 02JA03BMS04B-1 | 2002 | | | 98.00±0.22 | 845.9±27.1 | 98.4±0.4 | | 60.0 | DMRS 2002 |
| | | 02JA03BMS04B-2 | 2005 | | 100.58±0.17 | - | | - | | | SOPET 2005 |
| JA04 | Maloney | *Koppers et al. (2003)* | | | | | | *100.8±0.6 (2σ)* | | | |
| | | *Koppers et al. (2003)* | | | | | | *97.7±0.6 (2σ)* | | | |
| JA05 | Batiza | 02JA05BMS01C | 2002 | | | - | | 98.8±0.4 | | 37.2 | DMRS 2002 |
| JA06 | Xufu | 97JA06AD13 | 1997 | 80.0±2 | | | | | | | DMRS 1997 |
| | | 97JA06AD20 | 1997 | 86.5±2 | | | | | | | DMRS 1997 |
| JA11 | McDonnell | 01JA11BMS02A | 2001 | | | 117.77±4.62 | | 116.43±4.94 | | 53.4 | DMRS 2001 |
| | | 02JA11BMS06A | 2005 | | 110.94±0.20 | 109.7±0.8 | 276±31 | 109.4±0.3 | 3.91 | 69.6 | SOPET 2005 |
| JA12 | Zhinyu | 89JA12AD07-A | 1989 | 72.4±2.3 | | | | | | | |
| | | 02JA12BMS03B | 2002 | | | - | | 85.6±0.4 | | 31.2 | DMRS 2002 |
| | | 02JA12BMS04B | 2005 | | 70.9±0.5 | 68.3±0.7 | -166±77 | 66.77±0.17 | 1.59 | 66.4 | SOPET 2005 |
| JA17 | Scripps | 90JA17AD01C | 1990 | 29.5±1.9 | | | | | | | DMRS 1990 |
| | | 91JA17AD10A | 1991 | 94.6±4.7 | | | | | | | DMRS 1991 |
| | | 02JA17BMS01A | 2005 | | 104.54±0.13 | 113±6 | -7200±8600 | 105.29±0.19 | 0.53 | 46.0 | SOPET 2005 |
| | | *Koppers et al. (2003)* | | | | | | *101.4±1.4 (2σ)* | | | |
| JA18 | Kimotsuki | 04MT474BMS04A | 2005 | | 152.6±1.3 | - | | - | | | DMRS 2005 |
| MT473 | Tsunogai | 04MT473BMS02A-1 | 2005 | | 79.24±0.21 | 85.3±1.5 | -747±770 | 84.4±0.3 | 0.60 | 37.9 | SOPET 2005 |
| | | 04MT473BMS02A-2 | 2005 | | 74.80±0.09 | 79.5±0.6 | 545±235 | 79.77±0.21 | 1.20 | 37.2 | SOPET 2005 |
| Takuyo-Daigo | | *NT09-02HPD#953-R11* | | | | | | *101.4±2.3* | | *83.0* | |
| | | *Tokumaru et al. (2015)* | | | | | | | | | |

Table 3 Continued.

| Seamount | | Sample ID | Year | K-Ar age ± 1σ (Ma) | Ar-Ar age ± 1σ (Ma) Total integrated age | Inverse isochron age | $^{40}Ar/^{36}Ar$ intercept | Weighted mean plateau age | MSWD | $^{39}Ar$ (%) | Project name |
|---|---|---|---|---|---|---|---|---|---|---|---|
| **Magellan Seamount Group** | | | | | | | | | | | |
| JA09 | Ioah (Fedorov) | 98JA09AD20-1 | 1998 | 70.8±3.5 | | | | | | | DMRS 1998 |
| | | 98JA09AD20-2 | 1998 | 71.5±3.6 | | | | | | | DMRS 1998 |
| | | 99JA09AD34 | 1999 | | | | | 86.8±1.0 | | 45.2 | DMRS 1999 |
| | | 99JA09AD35 | 1999 | | | | | 105±4 | | 48.6 | DMRS 1999 |
| | | 00JA09AD58 | 2000 | | | - | | 66.6±1.8 | | 33.8 | DMRS 2000 |
| | | 00JA09CB69 | 2000 | | | - | | - | | | DMRS 2000 |
| | | *Koppers et al. (2003)* | | | | | | *86.7±0.4 (2σ)* | | | |
| | | *Koppers et al. (2003)* | | | | | | *88.5±0.7 (2σ)* | | | |
| JA13 | Magoshichi | 89JA13AD03-D | 1989 | 66.9±2.2 | | | | | | | DMRS 1989 |
| JA14 | Govorov | 89JA14AD06-E | 1989 | 86.8±3.0 | | | | | | | DMRS 1989 |
| JA15 | Pegas | 98JA15AD10 | 1998 | 56.0±2.8 | | | | | | | DMRS 1998 |
| | | 98JA15AD13 | 1998 | 68.7±3.4 | | | | | | | DMRS 1998 |
| JA19 | Hemler | 90JA19AD01C | 1990 | 79.6±2.6 | | | | | | | DMRS 1990 |
| | | 90JA19AD04C | 1990 | 78.1±2.5 | | | | | | | DMRS 1990 |
| | | *Koppers et al. (2003)* | | | | | | *100.1±0.8 (2σ)* | | | |
| JA22 | Butakov | 90JA22AD05C | 1990 | 53.3±1.9 | | | | | | | DMRS 1990 |
| | | 90JA22AD11B | 1990 | 69.9±2.3 | | | | | | | DMRS 1990 |
| **Marshall Islands Seamount Group** | | | | | | | | | | | |
| JA10 | Rykachev | 89JA10AD04-E | 1989 | 43.6±2.8 | | | | | | | DMRS 1989 |
| | | 99JA10AD11 | 1999 | | | - | | - | | | DMRS 1999 |
| | | 99JA10AD17 | 1999 | | | - | | - | | | DMRS 1999 |
| | | 00JA10AD34 | 2000 | | | 79.8±4.0 | 367±10 | 82.7±3.1 | 3.74 | 83.8 | DMRS 2000 |
| | | 00JA10AD37 | 2000 | | | 91.5±1.8 | 412±21 | 91.8±0.7 | 1.1 | | DMRS 2000 |
| | | 00JA10AD41 | 2000 | | | 89.5±2.7 | 457±41 | 88.5±1.2 | 1.6 | | DMRS 2000 |
| JA16 | Changpogo | 89JA16AD01 | 1989 | 54.1±2.1 | | | | | | | DMRS 1989 |

Total integrated ages were calculated using sum of the total gas released.
MSWD: mean square of weighted deviates ((SUMS/(n-2))^0.5) in York (1969).
DMRS: Deep-sea mineral resource exploration
SOPET: Survey on offshore petroleum development technology (geological structure survey and analysis of resources for basic survey on exploration technology of petroleum resources in deep sea)

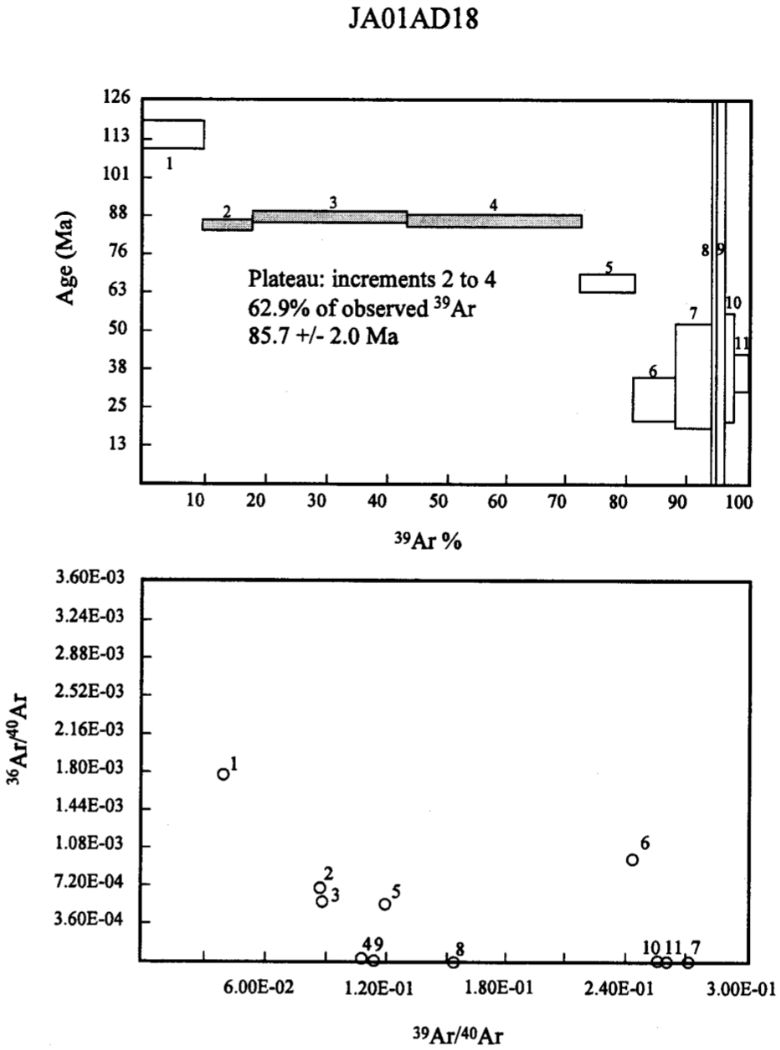


Fig. 9 Step heating age spectra and inverse isochron diagrams for Ar–Ar dating (JA01 Seamount)

and 94.6 ± 4.7 Ma are unreliable due to the effects of alteration. A plateau age of 105.29 ± 0.19 Ma was obtained from 02JA17BMS01A, which is consistent with the Ar–Ar age of 101.4 ± 1.4 Ma reported by Koppers *et al.* (2003). The $^{40}Ar/^{39}Ar$ age measurement data are shown in Table 4.

**(9) JA18 Seamount (Kimotsuki Seamount)**

Ar–Ar dating was carried out on one sample, but no plateau age was obtained. The $^{40}Ar/^{39}Ar$ age measurement data are shown in Table 4.

**(10) MT473 Seamount (Tsunogai Seamount)**

Ar–Ar dating was carried out on two samples and yielded plateau ages of 79.77 ± 0.21 Ma and 84.4 ± 0.3 Ma. The $^{40}Ar/^{39}Ar$ age measurement data are shown in Table 4.

## 5. 2 Magellan Seamount Group

**(1) JA09 Seamount (Ioah/Fedorov Guyot)**

K–Ar dating was performed on two samples and Ar–Ar dating on four samples. The ages obtained from 98JA09AD20 are 70.8 ± 3.5 Ma and 71.5 ± 3.5 Ma, corresponding to the Late Cretaceous (Maastrichtian), but it is likely that some of the Ar in the rocks was lost due to weathering and alteration, resulting in slightly younger ages. The Ar–Ar ages obtained from relatively less altered samples (99JA09AD34 and 99JA09AD35) are 86.8 ± 1.0 Ma and 105 ± 4 Ma, respectively, corresponding to the Late Cretaceous (Coniacian) and Middle Cretaceous (Albian). There is a large gap between these ages, suggesting that there were two distinct periods of volcanic activity. The Ar–Ar age from 00JA09AD58 is 66.6 ± 1.8 Ma and corresponds to the Late Cretaceous (Maastrichtian), but is unreliable because $^{39}Ar$ only accounts for 33.8 %. No plateau age was obtained from 00JA09CB69 due to alteration. Koppers *et al.* (2003) reported Ar–Ar ages of 86.7 ± 0.4 Ma and 88.5 ± 0.7 Ma. The stage-heating age spectra and inverse isochron diagrams of 99JA09AD34, 99JA09AD35, 00JA09AD58, and 00JA09CB69 are shown in Figure 15. The $^{40}Ar/^{39}Ar$ age measurement data are shown in Table 4.

**(2) JA13 Seamount (Magoshichi Guyot)**

K–Ar dating was carried out on one sample and yielded an age of 66.9 ± 2.2 Ma, but the results are not reliable

Table 4 $^{40}Ar/^{39}Ar$ age measurement data

**sample ID: JA01AD12**

| Temp. (K) | $^{36}Ar/^{40}Ar$ | $^{39}Ar/^{40}Ar$ | $\%^{39}Ar$ | $\%^{40}Ar^*$ | Age (Ma) |
|---|---|---|---|---|---|
| 800 | 1.292E+00 ± 1.419E+03 | 9.651E-02 ± 1.512E+02 | 0.00 | 0.00 | |
| 900 | 4.622E+00 ± 2.457E+03 | 1.225E-01 ± 8.085E+01 | 0.01 | 0.00 | |
| 1000 | 1.446E-02 ± 9.086E-03 | 1.932E-04 ± 5.046E-02 | 0.02 | 0.00 | |
| 1100 | 1.611E+00 ± 4.305E+02 | 1.766E+01 ± 4.721E+03 | 1.75 | 0.00 | |
| 1200 | 6.413E-03 ± 2.575E-03 | 1.179E-01 ± 3.354E-02 | 11.82 | 0.00 | |
| 1400 | 4.557E-04 ± 1.369E-03 | 1.301E-01 ± 6.455E-03 | 57.74 | 86.48 | 62.97 ± 29.11 |
| 1600 | 0.000E+00 ± 4.432E-03 | 5.650E-02 ± 2.023E-02 | 67.43 | 100.00 | 162.94 ± 211.40 |
| 1800 | 2.153E-04 ± 6.041E-04 | 2.576E-01 ± 2.940E-03 | 100.00 | 93.52 | 34.68 ± 6.56 |

**sample ID: JA01AD13**

| Temp. (K) | $^{36}Ar/^{40}Ar$ | $^{39}Ar/^{40}Ar$ | $\%^{39}Ar$ | $\%^{40}Ar^*$ | Age (Ma) |
|---|---|---|---|---|---|
| 800 | 1.169E-02 ± 1.508E+01 | 9.651E-02 ± 1.429E+02 | 0.01 | 0.00 | |
| 900 | 0.000E+00 ± 3.673E+00 | 1.514E-01 ± 9.151E+01 | 0.03 | 0.00 | |
| 1000 | 5.617E+00 ± 2.051E+03 | 1.537E-01 ± 6.104E+01 | 0.06 | 0.00 | |
| 1100 | 3.312E+00 ± 8.407E+02 | 1.360E-01 ± 3.844E+01 | 0.09 | 0.00 | |
| 1200 | 1.216E-02 ± 9.179E-03 | 6.037E-02 ± 4.528E-02 | 6.00 | 0.00 | |
| 1400 | 1.344E-03 ± 1.466E-03 | 1.180E-01 ± 1.087E-02 | 50.92 | 60.25 | 48.53 ± 33.80 |
| 1600 | 0.000E+00 ± 5.775E-03 | 2.339E-02 ± 2.633E-02 | 61.59 | 100.00 | 370.97 ± 685.40 |
| 1800 | 1.716E-03 ± 2.319E-03 | 2.373E-01 ± 6.468E-03 | 100.00 | 49.24 | 19.90 ± 27.53 |

**sample ID: JA01AD18**

| Temp. (K) | $^{36}Ar/^{40}Ar$ | $^{39}Ar/^{40}Ar$ | $\%^{39}Ar$ | $\%^{40}Ar^*$ | Age (Ma) |
|---|---|---|---|---|---|
| 800 | 1.745E-03 ± 6.814E-05 | 3.957E-02 ± 1.625E-04 | 9.32 | 48.41 | 114.16 ± 4.66 |
| 900 | 6.965E-04 ± 4.402E-05 | 8.816E-02 ± 4.256E-04 | 17.60 | 79.38 | 84.75 ± 1.46 |
| 1000 | 5.843E-04 ± 5.528E-05 | 8.936E-02 ± 2.951E-04 | 43.22 | 82.70 | 87.04 ± 1.73 |
| 1100 | 2.476E-05 ± 9.053E-05 | 1.086E-01 ± 4.642E-04 | 72.26 | 99.21 | 85.92 ± 2.31 |
| 1200 | 5.481E-04 ± 1.345E-04 | 1.204E-01 ± 4.744E-07 | 81.30 | 83.75 | 65.83 ± 3.09 |
| 1300 | 9.753E-04 ± 5.836E-04 | 2.437E-01 ± 1.340E-03 | 87.96 | 71.09 | 27.92 ± 6.72 |
| 1400 | 0.000E+00 ± 1.656E-03 | 2.705E-01 ± 7.494E-03 | 93.75 | 100.00 | 35.31 ± 17.11 |
| 1500 | 0.000E+00 ± 3.726E-03 | 1.564E-01 ± 1.499E-02 | 94.35 | 100.00 | 61.30 ± 66.50 |
| 1600 | 0.000E+00 ± 4.476E-03 | 1.142E+01 ± 1.988E-02 | 96.05 | 100.00 | 82.50 ± 107.50 |
| 1700 | 0.000E+00 ± 1.592E-03 | 2.564E+01 ± 6.876E-03 | 97.80 | 100.00 | 37.23 ± 17.35 |
| 1800 | 0.000E+00 ± 5.601E-04 | 2.607E-01 ± 3.505E-03 | 100.00 | 100.00 | 36.61 ± 6.01 |

**sample ID: JA09AD34**

| Temp. (K) | $^{36}Ar/^{40}Ar$ | $^{39}Ar/^{40}Ar$ | $\%^{39}Ar$ | $\%^{40}Ar^*$ | Age (Ma) |
|---|---|---|---|---|---|
| 800 | 2.164E-03 ± 1.709E-04 | 3.034E-02 ± 1.354E-03 | 2.11 | 36.04 | 110.96 ± 16.53 |
| 900 | 2.231E-04 ± 9.177E-05 | 1.135E-01 ± 2.456E-03 | 9.11 | 93.35 | 77.59 ± 2.80 |
| 1000 | 1.582E-04 ± 3.470E-05 | 1.017E-01 ± 1.154E-03 | 26.78 | 95.28 | 88.10 ± 1.40 |
| 1100 | 2.478E-05 ± 2.508E-05 | 1.083E-01 ± 8.329E-04 | 54.30 | 99.21 | 86.22 ± 0.96 |
| 1200 | 3.811E-05 ± 5.119E-05 | 1.143E-01 ± 8.930E-04 | 75.29 | 98.82 | 81.43 ± 1.40 |
| 1400 | 2.361E-06 ± 2.557E-05 | 1.311E-01 ± 5.542E-04 | 96.44 | 99.86 | 71.97 ± 0.67 |
| 1600 | 2.999E-04 ± 3.395E-04 | 1.502E-01 ± 1.525E-03 | 97.62 | 91.07 | 57.50 ± 6.26 |
| 1800 | 1.840E-04 ± 1.456E-04 | 1.514E-01 ± 4.541E-04 | 100.00 | 94.49 | 59.18 ± 2.66 |

Table 4 Continued.

**sample ID: JA09AD35**

| Temp. (K) | $^{36}Ar/^{40}Ar$ | $^{39}Ar/^{40}Ar$ | $\%^{39}Ar$ | $\%^{40}Ar^*$ | Age (Ma) |
|---|---|---|---|---|---|
| 800 | 7.499E-04 ± 2.233E-04 | 8.064E-02 ± 2.909E-03 | 2.60 | 77.81 | 90.66 ± 8.37 |
| 900 | 2.747E-04 ± 1.160E-04 | 8.414E-02 ± 1.759E-03 | 9.33 | 91.84 | 102.23 ± 4.32 |
| 1000 | 1.551E-04 ± 3.928E-05 | 8.179E-02 ± 1.179E-03 | 27.22 | 95.38 | 109.01 ± 2.06 |
| 1100 | 2.231E-05 ± 3.071E-05 | 8.972E-02 ± 1.066E-03 | 51.19 | 99.30 | 103.62 ± 1.56 |
| 1200 | 2.200E-05 ± 5.254E-05 | 9.972E-02 ± 1.245E-03 | 69.27 | 99.30 | 93.50 ± 1.86 |
| 1400 | 0.000E+00 ± 3.375E-05 | 1.057E-01 ± 9.426E-04 | 94.07 | 100.00 | 88.90 ± 1.20 |
| 1600 | 2.937E-04 ± 1.820E-04 | 1.154E-01 ± 1.216E-03 | 97.33 | 91.27 | 74.63 ± 4.39 |
| 1800 | 5.233E-05 ± 2.276E-04 | 1.031E-01 ± 3.097E-04 | 100.00 | 98.40 | 89.68 ± 5.99 |

**sample ID: JA10AD11**

| Temp. (K) | $^{36}Ar/^{40}Ar$ | $^{39}Ar/^{40}Ar$ | $\%^{39}Ar$ | $\%^{40}Ar^*$ | Age (Ma) |
|---|---|---|---|---|---|
| 800 | 1.705E+00 ± 2.664E+03 | 4.577E-02 ± 1.140E+02 | 0.00 | 0.00 | |
| 900 | 6.525E+00 ± 4.845E+03 | 9.449E-02 ± 8.521E+01 | 0.01 | 0.00 | |
| 1000 | 6.466E-03 ± 2.077E-03 | 4.608E-03 ± 1.353E-02 | 0.67 | 0.00 | |
| 1100 | 2.353E-03 ± 1.405E-03 | 7.936E-02 ± 1.484E-02 | 17.49 | 30.45 | 36.60 ± 51.16 |
| 1200 | 1.592E-03 ± 1.176E-03 | 7.257E-02 ± 6.582E-02 | 45.99 | 52.92 | 68.93 ± 45.32 |
| 1400 | 0.000E+00 ± 1.235E-03 | 9.778E-02 ± 6.128E-03 | 87.23 | 100.00 | 95.95 ± 34.58 |
| 1600 | 0.000E+00 ± 2.173E-02 | 4.537E-02 ± 9.573E-02 | 89.07 | 100.00 | 200.00 ± 1275.00 |
| 1800 | 0.000E+00 ± 2.427E-03 | 2.128E-01 ± 1.025E-02 | 100.00 | 100.00 | 44.75 ± 31.74 |

**sample ID: JA10AD17**

| Temp. (K) | $^{36}Ar/^{40}Ar$ | $^{39}Ar/^{40}Ar$ | $\%^{39}Ar$ | $\%^{40}Ar^*$ | Age (Ma) |
|---|---|---|---|---|---|
| 800 | 1.813E+01 ± 4.456E+04 | 3.430E-03 ± 1.278E+02 | 0.00 | 0.00 | |
| 900 | 1.526E+01 ± 2.801E+04 | 3.859E+00 ± 7.083E+05 | 3.46 | 0.00 | |
| 1000 | 4.390E-02 ± 8.598E-02 | 3.065E-01 ± 5.957E-01 | 6.07 | 0.00 | |
| 1100 | 2.723E-03 ± 4.652E-03 | 2.003E-02 ± 6.367E-03 | 9.51 | 19.53 | 91.58 ± 629.00 |
| 1200 | 3.119E-03 ± 3.299E-04 | 1.239E-02 ± 1.201E-03 | 15.04 | 7.82 | 59.81 ± 73.98 |
| 1400 | 2.270E-03 ± 5.674E-04 | 9.274E-02 ± 2.372E-03 | 55.68 | 32.90 | 33.86 ± 17.13 |
| 1600 | 0.000E+00 ± 3.492E-03 | 6.275E-02 ± 1.590E-02 | 94.07 | 100.00 | 147.30 ± 150.30 |
| 1800 | 0.000E+00 ± 2.827E-03 | 1.852E-01 ± 6.565E-03 | 100.00 | 100.00 | 51.32 ± 42.27 |

**sample ID: 01JA02BM02C**

| Temp. (K) | $^{36}Ar/^{40}Ar$ | $^{39}Ar/^{40}Ar$ | $\%^{39}Ar$ | $\%^{40}Ar^*$ | Age (Ma) |
|---|---|---|---|---|---|
| 900 | 4.973E-03 ± 1.104E-02 | 1.320E-01 ± 2.445E-03 | 10.34 | 0.00 | |
| 1200 | 3.490E-03 ± 2.066E-03 | 3.505E-02 ± 2.831E-03 | 12.13 | 6.28 | |
| 1400 | 7.160E-04 ± 7.670E-04 | 1.249E-01 ± 2.606E-03 | 50.88 | 78.72 | 56.53 ± 16.13 |
| 1823 | 2.921E-03 ± 1.791E-03 | 2.204E-01 ± 8.985E-03 | 100.00 | 13.64 | 5.63 ± 21.81 |

**sample ID: 01JA11BM02A**

| Temp. (K) | $^{36}Ar/^{40}Ar$ | $^{39}Ar/^{40}Ar$ | $\%^{39}Ar$ | $\%^{40}Ar^*$ | Age (Ma) |
|---|---|---|---|---|---|
| 900 | 2.290E-04 ± 8.520E-04 | 6.776E-02 ± 2.189E-02 | 4.06 | 93.18 | 121.14 ± 33.74 |
| 1100 | 7.920E-04 ± 5.940E-04 | 6.401E-01 ± 1.825E-03 | 16.83 | 76.56 | 105.79 ± 23.78 |
| 1300 | 7.200E-05 ± 1.330E-04 | 7.383E-02 ± 6.210E-04 | 53.39 | 97.81 | 116.62 ± 5.11 |
| 1500 | 1.430E-04 ± 9.500E-05 | 9.203E-02 ± 2.042E-03 | 80.02 | 95.72 | 92.34 ± 3.31 |
| 1823 | 4.280E-04 ± 3.460E-04 | 7.120E-02 ± 6.630E-04 | 100.00 | 87.29 | 108.35 ± 12.51 |

Table 4 Continued.

**sample ID: 00JA09AD58**

| Temp. (K) | $^{36}Ar/^{40}Ar$ | $^{39}Ar/^{40}Ar$ | $\%^{39}Ar$ | $\%^{40}Ar^*$ | Age (Ma) |
|---|---|---|---|---|---|
| 900 | 1.425E-03 ± 1.496E-05 | 2.792E-02 ± 1.535E-04 | 28.07 | 57.89 | 126.41 ± 2.71 |
| 1000 | 6.677E-05 ± 1.873E-05 | 5.896E-02 ± 3.056E-04 | 51.86 | 98.00 | 102.03 ± 2.13 |
| 1100 | 9.378E-05 ± 2.962E-05 | 6.988E-02 ± 3.142E-04 | 66.16 | 97.19 | 85.78 ± 1.88 |
| 1300 | 1.358E-04 ± 3.759E-05 | 8.770E-02 ± 2.450E-04 | 87.53 | 95.95 | 67.82 ± 1.55 |
| 1500 | 3.850E-04 ± 5.266E-05 | 8.477E-02 ± 1.939E-04 | 97.86 | 88.58 | 64.83 ± 1.70 |
| 1823 | 4.717E-04 ± 1.718E-04 | 8.488E-02 ± 4.263E-04 | 100.00 | 86.02 | 62.91 ± 3.87 |

**sample ID: 00JA09CB69**

| Temp. (K) | $^{36}Ar/^{40}Ar$ | $^{39}Ar/^{40}Ar$ | $\%^{39}Ar$ | $\%^{40}Ar^*$ | Age (Ma) |
|---|---|---|---|---|---|
| 900 | 1.438E-03 ± 2.750E-05 | 2.534E-02 ± 1.571E-04 | 30.27 | 57.49 | 137.84 ± 3.40 |
| 1000 | 1.750E-04 ± 8.436E-05 | 7.339E-02 ± 6.035E-04 | 46.58 | 94.80 | 78.80 ± 2.66 |
| 1100 | 3.985E-05 ± 6.480E-05 | 8.697E-01 ± 4.370E-04 | 60.46 | 98.78 | 70.36 ± 1.95 |
| 1300 | 1.202E-04 ± 7.984E-05 | 1.171E-01 ± 4.752E-04 | 88.13 | 96.39 | 51.29 ± 1.61 |
| 1500 | 4.576E-04 ± 8.664E-05 | 8.524E-02 ± 4.363E-04 | 94.70 | 86.44 | 62.95 ± 2.23 |
| 1823 | 5.337E-04 ± 2.237E-04 | 8.535E-02 ± 4.273E-04 | 100.00 | 84.19 | 61.26 ± 4.89 |

**sample ID: 00JA10AD34**

| Temp. (K) | $^{36}Ar/^{40}Ar$ | $^{39}Ar/^{40}Ar$ | $\%^{39}Ar$ | $\%^{40}Ar^*$ | Age (Ma) |
|---|---|---|---|---|---|
| 900 | 2.304E-03 ± 2.767E-05 | 1.206E-02 ± 1.537E-04 | 15.27 | 31.91 | 159.78 ± 5.79 |
| 1000 | 7.961E-04 ± 1.567E-04 | 5.166E-02 ± 7.085E-04 | 24.61 | 76.46 | 91.13 ± 5.84 |
| 1100 | 4.174E-04 ± 8.654E-05 | 6.354E-02 ± 2.487E-04 | 60.05 | 87.64 | 85.08 ± 2.96 |
| 1300 | 1.417E-04 ± 8.386E-03 | 7.542E-02 ± 4.063E-03 | 99.09 | 95.78 | 78.49 ± 2.55 |
| 1500 | 0.000E+00 ± 1.334E-03 | 5.204E-02 ± 5.953E-03 | 99.99 | 100.00 | 117.47 ± 46.73 |
| 1823 | 4.880E-03 ± 1.062E-03 | 9.566E-04 ± 2.353E-03 | 100.00 | 0.00 | |

**sample ID: 00JA10AD37**

| Temp. (K) | $^{36}Ar/^{40}Ar$ | $^{39}Ar/^{40}Ar$ | $\%^{39}Ar$ | $\%^{40}Ar^*$ | Age (Ma) |
|---|---|---|---|---|---|
| 800 | 1.313E-03 ± 6.891E-05 | 3.069E-02 ± 6.814E-04 | 4.88 | 61.18 | 121.69 ± 5.57 |
| 900 | 3.619E-04 ± 3.246E-05 | 5.746E-02 ± 4.240E-04 | 20.84 | 89.28 | 95.56 ± 2.23 |
| 1000 | 3.889E-05 ± 9.165E-06 | 6.638E-02 ± 1.815E-04 | 51.66 | 98.82 | 91.66 ± 1.82 |
| 1100 | 2.505E-05 ± 1.430E-05 | 6.632E-02 ± 9.300E-05 | 76.16 | 99.23 | 92.11 ± 1.84 |
| 1300 | 0.000E+00 ± 9.724E-05 | 7.578E-02 ± 4.579E-03 | 98.54 | 100.00 | 81.49 ± 2.83 |
| 1500 | 0.000E+00 ± 6.604E-04 | 6.797E-02 ± 2.352E-03 | 99.75 | 100.00 | 90.61 ± 17.60 |
| 1700 | 2.477E-03 ± 5.806E-04 | 3.752E-02 ± 1.935E-03 | 99.99 | 26.79 | 44.54 ± 28.31 |
| 1823 | 8.212E-03 ± 2.537E-03 | 4.589E-03 ± 3.598E-03 | 100.00 | 0.00 | |

**sample ID: 00JA10AD41**

| Temp. (K) | $^{36}Ar/^{40}Ar$ | $^{39}Ar/^{40}Ar$ | $\%^{39}Ar$ | $\%^{40}Ar^*$ | Age (Ma) |
|---|---|---|---|---|---|
| 900 | 6.763E-04 ± 4.190E-05 | 4.786E-02 ± 5.244E-04 | 20.68 | 80.00 | 102.59 ± 2.80 |
| 1000 | 2.329E-04 ± 5.225E-05 | 6.062E-02 ± 5.218E-04 | 33.78 | 93.09 | 94.47 ± 2.53 |
| 1100 | 1.019E-04 ± 3.088E-05 | 6.225E-02 ± 2.940E-04 | 49.20 | 96.96 | 95.79 ± 2.11 |
| 1300 | 0.000E+00 ± 6.493E-05 | 6.987E-02 ± 2.875E-04 | 92.08 | 100.00 | 88.21 ± 2.41 |
| 1500 | 0.000E+00 ± 2.501E-04 | 6.283E-02 ± 1.116E-03 | 98.92 | 100.00 | 97.82 ± 7.48 |
| 1823 | 2.142E-04 ± 3.601E-04 | 5.988E-02 ± 1.176E-03 | 100.00 | 93.64 | 96.17 ± 10.96 |

Table 4 Continued.

**sample ID: 02JA02BMS06B**

| Temp. (K) | $^{36}Ar/^{40}Ar$ | $^{37}Ar/^{40}Ar$ | $^{38}Ar/^{40}Ar$ | $^{39}Ar/^{40}Ar$ | K/Ca | $\%^{39}Ar$ | $\%^{40}Ar^*$ | Age (Ma) |
|---|---|---|---|---|---|---|---|---|
| 460 | 1.840E-03 | 5.815E-02 | 8.978E-05 | 3.453E-02 | 0.290 | 10.2 | 45.6 | 72.2 ± 1.7 |
| 500 | 1.817E-03 | 1.020E-01 | 9.872E-05 | 3.656E-02 | 0.180 | 19.2 | 46.3 | 69.3 ± 1.9 |
| 540 | 1.658E-03 | 2.184E-01 | 1.351E-04 | 3.752E-02 | 0.084 | 27.2 | 51.0 | 74.3 ± 2.1 |
| 580 | 1.559E-03 | 3.987E-01 | 2.948E-04 | 4.038E-02 | 0.050 | 35.7 | 54.0 | 73.1 ± 2.0 |
| 620 | 1.099E-03 | 5.201E-01 | 1.649E-04 | 4.997E-02 | 0.047 | 45.4 | 67.5 | 73.8 ± 1.6 |
| 660 | 5.085E-04 | 5.230E-01 | 6.519E-04 | 6.519E-02 | 0.061 | 55.4 | 85.0 | 71.3 ± 1.5 |
| 700 | 7.169E-04 | 3.680E-01 | 3.555E-04 | 5.925E-02 | 0.079 | 61.4 | 78.8 | 72.7 ± 2.5 |
| 740 | 9.689E-04 | 2.008E-01 | 1.205E-05 | 5.237E-02 | 0.130 | 64.8 | 71.4 | 74.5 ± 4.4 |
| 780 | 1.473E-03 | 1.751E-01 | 2.051E-04 | 4.661E-02 | 0.130 | 67.3 | 56.5 | 66.4 ± 5.8 |
| 850 | 1.444E-03 | 3.674E-01 | 0.000E+00 | 6.335E-02 | 0.084 | 69.4 | 57.4 | 49.8 ± 7.2 |
| 920 | 1.505E-03 | 7.867E-01 | 8.584E-04 | 1.010E-01 | 0.063 | 72.7 | 55.6 | 30.5 ± 4.5 |
| 1100 | 4.659E-04 | 1.106E+01 | 7.248E-04 | 1.294E-01 | 0.006 | 100.0 | 86.2 | 36.8 ± 0.7 |

**sample ID: 02JA03BMS04B**

| Temp. (K) | $^{36}Ar/^{40}Ar$ | $^{37}Ar/^{40}Ar$ | $^{38}Ar/^{40}Ar$ | $^{39}Ar/^{40}Ar$ | K/Ca | $\%^{39}Ar$ | $\%^{40}Ar^*$ | Age (Ma) |
|---|---|---|---|---|---|---|---|---|
| 460 | 8.117E-04 | 1.185E-03 | 0.000E+00 | 2.306E-02 | 9.500 | 2.6 | 76.0 | 174.9 ± 0.6 |
| 520 | 2.212E-04 | 1.783E-03 | 0.000E+00 | 4.514E-02 | 12.000 | 7.2 | 93.5 | 111.9 ± 0.3 |
| 580 | 2.167E-05 | 1.587E-03 | 0.000E+00 | 5.417E-02 | 17.000 | 19.4 | 99.4 | 99.4 ± 0.2 |
| 640 | 1.099E-05 | 1.407E-03 | 0.000E+00 | 5.495E-02 | 19.000 | 36.7 | 99.7 | 98.3 ± 0.2 |
| 670 | 1.098E-05 | 1.449E-03 | 0.000E+00 | 5.490E-02 | 19.000 | 47.6 | 99.7 | 98.4 ± 0.2 |
| 700 | 1.096E-05 | 1.562E-03 | 0.000E+00 | 5.481E-02 | 17.000 | 55.6 | 99.7 | 98.6 ± 0.2 |
| 730 | 5.493E-06 | 1.697E-03 | 0.000E+00 | 5.493E-02 | 16.000 | 61.9 | 99.8 | 98.5 ± 0.2 |
| 760 | 1.654E-05 | 1.891E-03 | 0.000E+00 | 5.515E-02 | 14.000 | 67.2 | 99.5 | 97.8 ± 0.2 |
| 790 | 1.669E-05 | 2.443E-03 | 0.000E+00 | 5.565E-02 | 11.000 | 71.0 | 99.4 | 96.9 ± 0.3 |
| 820 | 1.690E-05 | 3.307E-03 | 0.000E+00 | 5.633E-02 | 8.300 | 73.8 | 99.4 | 95.7 ± 0.3 |
| 850 | 2.271E-05 | 4.133E-03 | 0.000E+00 | 5.678E-02 | 6.700 | 76.6 | 99.3 | 94.9 ± 0.3 |
| 870 | 2.280E-05 | 4.627E-03 | 1.083E-05 | 5.699E-02 | 6.000 | 79.0 | 99.4 | 94.6 ± 0.3 |
| 930 | 1.159E-05 | 9.213E-03 | 0.000E+00 | 5.794E-02 | 3.100 | 83.9 | 99.6 | 93.3 ± 0.2 |
| 1000 | 1.724E-05 | 1.831E-02 | 0.000E+00 | 5.748E-02 | 1.500 | 93.0 | 99.5 | 93.9 ± 0.2 |
| 1080 | 5.576E-05 | 3.831E-02 | 0.000E+00 | 5.576E-02 | 0.710 | 100.0 | 98.3 | 95.6 ± 0.2 |

Table 4 Continued.

**sample ID: 02JA05BMS01C**

| Temp. (K) | $^{36}Ar/^{40}Ar$ | $^{37}Ar/^{40}Ar$ | $^{38}Ar/^{40}Ar$ | $^{39}Ar/^{40}Ar$ | K/Ca | $\%^{39}Ar$ | $\%^{40}Ar^*$ | Age (Ma) |
|---|---|---|---|---|---|---|---|---|
| 460 | 1.064E-04 | 4.571E-03 | 0.000E+00 | 5.068E-02 | 5.400 | 4.3 | 96.9 | 103.3 ± 0.3 |
| 520 | 3.649E-05 | 3.216E-03 | 0.000E+00 | 5.213E-02 | 7.900 | 12.7 | 98.9 | 102.5 ± 0.2 |
| 580 | 1.623E-05 | 1.785E-03 | 0.000E+00 | 5.410E-02 | 15.000 | 27.9 | 99.5 | 99.5 ± 0.2 |
| 640 | 1.639E-05 | 1.465E-03 | 0.000E+00 | 5.465E-02 | 18.000 | 41.7 | 99.5 | 98.5 ± 0.2 |
| 700 | 2.712E-05 | 1.974E-03 | 0.000E+00 | 5.424E-02 | 13.000 | 50.4 | 99.2 | 98.9 ± 0.2 |
| 770 | 3.781E-05 | 3.376E-03 | 0.000E+00 | 5.401E-02 | 7.800 | 57.6 | 98.9 | 99.1 ± 0.2 |
| 840 | 2.717E-05 | 6.754E-03 | 0.000E+00 | 5.434E-02 | 3.900 | 65.1 | 99.2 | 98.7 ± 0.2 |
| 910 | 2.223E-05 | 1.594E-02 | 0.000E+00 | 5.558E-02 | 1.700 | 72.9 | 99.3 | 96.8 ± 0.2 |
| 970 | 2.818E-05 | 3.019E-02 | 0.000E+00 | 5.637E-02 | 0.910 | 82.2 | 99.2 | 95.4 ± 0.2 |
| 1040 | 9.645E-05 | 2.513E-01 | 0.000E+00 | 5.674E-02 | 0.110 | 94.4 | 97.2 | 92.8 ± 0.2 |
| 1100 | 1.519E-04 | 5.011E-01 | 0.000E+00 | 5.425E-02 | 0.053 | 100.0 | 95.4 | 95.3 ± 0.2 |

**sample ID: 02JA12BMS03B**

| Temp. (K) | $^{36}Ar/^{40}Ar$ | $^{37}Ar/^{40}Ar$ | $^{38}Ar/^{40}Ar$ | $^{39}Ar/^{40}Ar$ | K/Ca | $\%^{39}Ar$ | $\%^{40}Ar^*$ | Age (Ma) |
|---|---|---|---|---|---|---|---|---|
| 460 | 2.591E-04 | 2.898E-02 | 0.000E+00 | 6.025E-02 | 1.000 | 9.0 | 92.4 | 83.2 ± 0.3 |
| 520 | 1.255E-04 | 3.219E-02 | 0.000E+00 | 6.275E-02 | 0.960 | 22.1 | 96.2 | 83.2 ± 0.2 |
| 570 | 6.345E-05 | 3.579E-02 | 0.000E+00 | 6.345E-02 | 0.870 | 36.6 | 98.1 | 83.9 ± 0.2 |
| 610 | 3.799E-05 | 3.247E-02 | 0.000E+00 | 6.332E-02 | 0.960 | 49.4 | 98.9 | 84.7 ± 0.2 |
| 640 | 1.261E-05 | 2.802E-02 | 0.000E+00 | 6.306E-02 | 1.100 | 59.3 | 99.6 | 85.7 ± 0.3 |
| 670 | 3.147E-05 | 2.701E-02 | 2.455E-05 | 6.294E-02 | 1.100 | 67.4 | 99.1 | 85.6 ± 0.3 |
| 710 | 4.376E-05 | 2.650E-02 | 0.000E+00 | 6.251E-02 | 1.200 | 74.5 | 98.7 | 85.6 ± 0.3 |
| 760 | 5.002E-05 | 2.810E-02 | 1.063E-04 | 6.252E-02 | 1.100 | 80.6 | 98.5 | 85.4 ± 0.4 |
| 820 | 6.355E-05 | 4.322E-02 | 0.000E+00 | 6.355E-02 | 0.720 | 84.8 | 98.1 | 83.7 ± 0.5 |
| 920 | 1.095E-04 | 1.784E-01 | 6.060E-05 | 7.302E-02 | 0.200 | 88.7 | 96.7 | 72.1 ± 0.5 |
| 1020 | 2.788E-04 | 8.221E-01 | 5.166E-04 | 8.200E-02 | 0.049 | 92.5 | 91.7 | 61.0 ± 0.6 |
| 1100 | 1.936E-04 | 5.858E+00 | 6.292E-04 | 6.914E-02 | 0.006 | 100.0 | 94.3 | 74.2 ± 0.4 |

Table 4 Continued.

| Laser output (W) | $^{40}$Ar (±1s) | $^{39}$Ar (±1s) | $^{38}$Ar (±1s) | $^{37}$Ar (±1s) | $^{36}$Ar (±1s) | days after irradiation | K/Ca | $^{40}$Ar* (%) | $^{39}$Ar$_K$ fraction (%) | $^{40}$Ar*/$^{39}$Ar$_K$ (±1s) | Age (±1s) (Ma) | adoption as plateau |
|---|---|---|---|---|---|---|---|---|---|---|---|---|
| **sample ID: MT474BMS04A (JA18)** | | | | | | | | | | | | |
| J= 0.003097 | | | | | | | | | | | | |
| 0.50W | 1.04681 ± 0.00338 | 0.008849 ± 0.000035 | 0.000433 ± 0.000024 | 0.00481 ± 0.00023 | 0.002228 ± 0.000021 | 198.1 | 1.083 | 37.1 | 9.2 | 43.89 ± 0.80 | 229.94 ± 4.01 | n |
| 0.72W | 2.21677 ± 0.01335 | 0.017747 ± 0.000108 | 0.000969 ± 0.000032 | 0.01008 ± 0.00045 | 0.005163 ± 0.000033 | 198.2 | 1.035 | 31.2 | 18.5 | 38.95 ± 0.96 | 205.45 ± 4.84 | n |
| 0.89W | 1.66381 ± 0.00803 | 0.009663 ± 0.000052 | 0.000793 ± 0.000034 | 0.00625 ± 0.00028 | 0.004467 ± 0.000019 | 198.2 | 0.910 | 20.7 | 10.1 | 35.59 ± 1.02 | 188.64 ± 5.18 | n |
| 1.1W | 0.57634 ± 0.00526 | 0.002753 ± 0.000033 | 0.000226 ± 0.000022 | 0.00348 ± 0.00022 | 0.001637 ± 0.000017 | 198.2 | 0.465 | 16.1 | 2.9 | 33.65 ± 2.67 | 178.85 ± 13.53 | n |
| 1.4W | 0.06215 ± 0.00028 | 0.001284 ± 0.000009 | 0.000033 ± 0.000012 | 0.00118 ± 0.00023 | 0.000062 ± 0.000003 | 198.2 | 0.640 | 70.5 | 1.3 | 34.13 ± 0.76 | 181.26 ± 3.90 | n |
| 1.8W | 0.27011 ± 0.00033 | 0.009674 ± 0.000043 | 0.000086 ± 0.000017 | 0.00731 ± 0.00029 | 0.000001 ± 0.000004 | 198.8 | 0.779 | 99.9 | 10.1 | 27.89 ± 0.18 | 149.46 ± 1.00 | n |
| 2.33W | 0.34135 ± 0.00060 | 0.015651 ± 0.000047 | 0.000076 ± 0.000021 | 0.01956 ± 0.00047 | 0.000001 ± 0.000002 | 198.8 | 0.471 | 99.9 | 16.4 | 21.79 ± 0.09 | 117.82 ± 0.57 | n |
| 2.9W | 0.38573 ± 0.00195 | 0.020254 ± 0.000139 | 0.000077 ± 0.000017 | 0.08744 ± 0.00121 | 0.000001 ± 0.000004 | 198.9 | 0.136 | 99.9 | 21.2 | 19.03 ± 0.17 | 103.31 ± 0.97 | n |
| 3.6W | 0.17625 ± 0.00063 | 0.009808 ± 0.000039 | 0.000008 ± 0.000014 | 0.36025 ± 0.00217 | 0.000018 ± 0.000007 | 199.0 | 0.016 | 97.0 | 10.3 | 17.44 ± 0.23 | 94.90 ± 1.24 | n |
| | | | | | | | | | | | **no plateau** | |

| Laser output (W) | $^{40}$Ar (±1s) | $^{39}$Ar (±1s) | $^{38}$Ar (±1s) | $^{37}$Ar (±1s) | $^{36}$Ar (±1s) | days after irradiation | K/Ca | $^{40}$Ar* (%) | $^{39}$Ar$_K$ fraction (%) | $^{40}$Ar*/$^{39}$Ar$_K$ (±1s) | Age (±1s) (Ma) | adoption as plateau |
|---|---|---|---|---|---|---|---|---|---|---|---|---|
| **sample ID: 02JA12BB04B** | | | | | | | | | | | | |
| J= 0.0030270 | | | | | | | | | | | | |
| 0.50W | 0.10533 ± 0.00079 | 0.00160 ± 0.00002 | 0.000045 ± 0.000010 | 0.00765 ± 0.00032 | 0.000211 ± 0.000005 | 227.0 | 0.123 | 40.9 | 0.1 | 26.87 ± 1.08 | 141.06 ± 5.48 | n |
| 0.8W | 0.35461 ± 0.00287 | 0.00550 ± 0.00005 | 0.000125 ± 0.000013 | 0.00632 ± 0.00035 | 0.000695 ± 0.000010 | 227.0 | 0.512 | 42.1 | 0.4 | 27.14 ± 0.78 | 142.46 ± 3.97 | n |
| 1.15W | 0.45720 ± 0.00698 | 0.00733 ± 0.00011 | 0.000224 ± 0.000020 | 0.00695 ± 0.00055 | 0.000940 ± 0.000017 | 227.0 | 0.621 | 39.3 | 0.5 | 24.48 ± 1.23 | 128.97 ± 6.25 | n |
| 1.55W | 0.77435 ± 0.01329 | 0.01381 ± 0.00024 | 0.000354 ± 0.000022 | 0.00990 ± 0.00056 | 0.001673 ± 0.000016 | 227.1 | 0.821 | 36.1 | 1.0 | 20.26 ± 1.08 | 107.39 ± 5.55 | n |
| 1.9W | 0.84662 ± 0.01281 | 0.01945 ± 0.00029 | 0.000309 ± 0.000045 | 0.01276 ± 0.00068 | 0.001720 ± 0.000022 | 227.2 | 0.896 | 40.0 | 1.4 | 17.39 ± 0.78 | 92.57 ± 4.08 | n |
| 2.25W | 1.08345 ± 0.01309 | 0.03497 ± 0.00042 | 0.000436 ± 0.000042 | 0.01911 ± 0.00070 | 0.001897 ± 0.000020 | 227.2 | 1.076 | 48.3 | 2.6 | 14.95 ± 0.45 | 79.86 ± 2.36 | n |
| 2.52W | 1.11840 ± 0.01351 | 0.04675 ± 0.00057 | 0.000374 ± 0.000051 | 0.02484 ± 0.00082 | 0.001586 ± 0.000013 | 227.2 | 1.107 | 58.1 | 3.4 | 13.90 ± 0.35 | 74.35 ± 1.82 | n |
| 2.78W | 1.59213 ± 0.01456 | 0.10385 ± 0.00096 | 0.000233 ± 0.000079 | 0.05479 ± 0.00106 | 0.000514 ± 0.000010 | 227.2 | 1.115 | 90.5 | 7.6 | 13.87 ± 0.19 | 74.19 ± 1.03 | n |
| 2.97W | 3.07162 ± 0.03080 | 0.22694 ± 0.00228 | 0.000059 ± 0.000336 | 0.12570 ± 0.00207 | 0.000143 ± 0.000009 | 228.9 | 1.062 | 98.6 | 16.6 | 13.35 ± 0.19 | 71.46 ± 1.03 | n |
| 3.1W | 2.57277 ± 0.05420 | 0.19512 ± 0.00413 | -0.000096 ± 0.000419 | 0.12935 ± 0.00267 | 0.000068 ± 0.000008 | 228.9 | 0.887 | 99.2 | 14.2 | 13.08 ± 0.39 | 70.07 ± 2.07 | y |
| 3.26W | 2.84366 ± 0.04563 | 0.21839 ± 0.00352 | -0.000263 ± 0.000333 | 0.19612 ± 0.00393 | 0.000080 ± 0.000008 | 229.0 | 0.655 | 99.2 | 15.9 | 12.91 ± 0.30 | 69.18 ± 1.56 | y |
| 3.41W | 4.02234 ± 0.03347 | 0.32369 ± 0.00272 | -0.000373 ± 0.000293 | 0.41792 ± 0.00517 | 0.000080 ± 0.000007 | 229.0 | 0.456 | 99.4 | 23.6 | 12.35 ± 0.15 | 66.23 ± 0.80 | y |
| 3.56W | 0.68409 ± 0.00092 | 0.05394 ± 0.00009 | -0.000174 ± 0.000032 | 0.07496 ± 0.00074 | 0.000025 ± 0.000004 | 229.0 | 0.423 | 98.9 | 3.9 | 12.55 ± 0.03 | 67.26 ± 0.27 | y |
| 3.85W | 0.43228 ± 0.00125 | 0.03426 ± 0.00010 | -0.000095 ± 0.000024 | 0.06887 ± 0.00088 | 0.000024 ± 0.000004 | 229.1 | 0.293 | 98.4 | 2.5 | 12.41 ± 0.06 | 66.53 ± 0.39 | y |
| 4.75W | 0.60771 ± 0.00124 | 0.04839 ± 0.00010 | -0.000120 ± 0.000032 | 0.17575 ± 0.00228 | 0.000031 ± 0.000007 | 229.1 | 0.162 | 98.5 | 3.5 | 12.37 ± 0.06 | 66.30 ± 0.36 | y |
| 6.2W | 0.46347 ± 0.00096 | 0.03656 ± 0.00014 | -0.000073 ± 0.000039 | 0.32655 ± 0.00240 | 0.000037 ± 0.000005 | 229.1 | 0.066 | 97.7 | 2.7 | 12.38 ± 0.07 | 66.36 ± 0.41 | y |
| | | | | | | | | | | **Plateau Age** | **66.77 ± 0.17** | |

| Laser output (W) | $^{40}$Ar (±1s) | $^{39}$Ar (±1s) | $^{38}$Ar (±1s) | $^{37}$Ar (±1s) | $^{36}$Ar (±1s) | days after irradiation | K/Ca | $^{40}$Ar* (%) | $^{39}$Ar$_K$ fraction (%) | $^{40}$Ar*/$^{39}$Ar$_K$ (±1s) | Age (±1s) (Ma) | adoption as plateau |
|---|---|---|---|---|---|---|---|---|---|---|---|---|
| **sample ID: MT473BMS02A-1** | | | | | | | | | | | | |
| J= 0.0031040 | | | | | | | | | | | | |
| 0.9W | 3.19226 ± 0.03840 | 0.20748 ± 0.00250 | -0.00034 ± 0.00023 | 0.05258 ± 0.00134 | 0.000061 ± 0.000005 | 229.8 | 2.321 | 99.4 | 11.1 | 15.30 ± 0.26 | 83.70 ± 1.42 | y |
| 1.02W | 2.97001 ± 0.02323 | 0.19343 ± 0.00152 | -0.00028 ± 0.00017 | 0.07180 ± 0.00092 | 0.000029 ± 0.000002 | 229.8 | 1.585 | 99.7 | 10.4 | 15.31 ± 0.17 | 83.76 ± 0.94 | y |
| 1.14W | 2.36620 ± 0.01187 | 0.15226 ± 0.00078 | -0.00013 ± 0.00009 | 0.09415 ± 0.00116 | 0.000020 ± 0.000003 | 229.9 | 0.951 | 99.8 | 8.2 | 15.50 ± 0.11 | 84.79 ± 0.64 | y |
| 1.3W | 2.35598 ± 0.00187 | 0.15226 ± 0.00023 | -0.00020 ± 0.00004 | 0.13395 ± 0.00189 | 0.000028 ± 0.000004 | 229.9 | 0.669 | 99.7 | 8.2 | 15.42 ± 0.03 | 84.35 ± 0.29 | y |
| 1.55W | 3.07132 ± 0.00863 | 0.20295 ± 0.00063 | -0.00003 ± 0.00012 | 0.21227 ± 0.00129 | 0.000029 ± 0.000006 | 230.0 | 0.562 | 99.7 | 10.9 | 15.09 ± 0.06 | 82.59 ± 0.42 | n |
| 1.82W | 2.55746 ± 0.00565 | 0.17107 ± 0.00038 | -0.00011 ± 0.00009 | 0.18145 ± 0.00156 | 0.000036 ± 0.000004 | 230.0 | 0.555 | 99.6 | 9.2 | 14.89 ± 0.05 | 81.50 ± 0.35 | n |
| 2.13W | 3.62409 ± 0.01708 | 0.25277 ± 0.00121 | 0.00001 ± 0.00017 | 0.21893 ± 0.00133 | 0.000063 ± 0.000003 | 230.0 | 0.679 | 99.5 | 13.6 | 14.26 ± 0.10 | 78.16 ± 0.56 | n |
| 2.35W | 1.98127 ± 0.00339 | 0.14097 ± 0.00027 | -0.00005 ± 0.00003 | 0.07876 ± 0.00078 | 0.000030 ± 0.000003 | 230.1 | 1.053 | 99.6 | 7.6 | 13.99 ± 0.04 | 76.70 ± 0.30 | n |
| 2.65W | 1.28049 ± 0.00374 | 0.09372 ± 0.00029 | -0.00004 ± 0.00007 | 0.04238 ± 0.00092 | 0.000011 ± 0.000003 | 230.1 | 1.301 | 99.7 | 5.0 | 13.63 ± 0.06 | 74.74 ± 0.38 | n |
| 3.1W | 1.42942 ± 0.00662 | 0.10919 ± 0.00051 | -0.00009 ± 0.00007 | 0.05112 ± 0.00115 | 0.000015 ± 0.000004 | 230.1 | 1.257 | 99.7 | 5.9 | 13.05 ± 0.09 | 71.64 ± 0.51 | n |
| 3.7W | 1.17649 ± 0.00415 | 0.09504 ± 0.00036 | -0.00009 ± 0.00005 | 0.04773 ± 0.00068 | 0.000019 ± 0.000004 | 230.2 | 1.171 | 99.5 | 5.1 | 12.32 ± 0.06 | 67.70 ± 0.40 | n |
| 4.6W | 1.05250 ± 0.00382 | 0.09207 ± 0.00039 | -0.00021 ± 0.00006 | 0.05154 ± 0.00093 | 0.000012 ± 0.000003 | 230.2 | 1.051 | 99.7 | 4.9 | 11.39 ± 0.06 | 62.70 ± 0.39 | n |
| | | | | | | | | | | **Plateau Age** | **84.35 ± 0.25** | |

Table 4 Continued.

| Laser output (W) | $^{40}Ar$ (±1s) | $^{39}Ar$ (±1s) | $^{38}Ar$ (±1s) | $^{37}Ar$ (±1s) | $^{36}Ar$ (±1s) | days after irradiation | K/Ca | $^{40}Ar^*$ (%) | $^{39}Ar_K$ fraction (%) | $^{40}Ar^*/^{39}Ar_K$ (±1s) | Age (±1s) (Ma) | adoption as plateau |
|---|---|---|---|---|---|---|---|---|---|---|---|---|
| **sample ID: 02JA17BMS01A** | | | | | | | | | | | | |
| J= 0.0031170 | | | | | | | | | | | | |
| 0.8W | 0.3937 ± 0.00562 | 0.01877 ± 0.00028 | 0.00003 ± 0.00003 | 0.01233 ± 0.00062 | 0.000309 ± 0.000007 | 230.2 | 0.896 | 76.8 | 1.6 | 16.10 ± 0.40 | 88.34 ± 2.14 | n |
| 0.95W | 0.3910 ± 0.00519 | 0.02018 ± 0.00027 | -0.00003 ± 0.00004 | 0.01328 ± 0.00050 | 0.000276 ± 0.000008 | 230.2 | 0.894 | 79.2 | 1.7 | 15.34 ± 0.35 | 84.29 ± 1.89 | n |
| 1.12W | 0.3818 ± 0.00311 | 0.02067 ± 0.00017 | 0.00000 ± 0.00003 | 0.01195 ± 0.00057 | 0.000239 ± 0.000005 | 231.8 | 1.018 | 81.5 | 1.8 | 15.06 ± 0.20 | 82.75 ± 1.13 | n |
| 1.3W | 0.5943 ± 0.00379 | 0.02601 ± 0.00018 | 0.00028 ± 0.00002 | 0.01304 ± 0.00049 | 0.000053 ± 0.000004 | 231.9 | 1.173 | 97.4 | 2.2 | 22.24 ± 0.22 | 120.94 ± 1.18 | n |
| 1.55W | 1.7198 ± 0.00881 | 0.08138 ± 0.00042 | 0.00051 ± 0.00006 | 0.02408 ± 0.00086 | 0.000038 ± 0.000005 | 232.0 | 1.988 | 99.3 | 7.0 | 21.00 ± 0.15 | 114.36 ± 0.88 | n |
| 1.73W | 2.2665 ± 0.00888 | 0.11370 ± 0.00046 | 0.00026 ± 0.00004 | 0.02365 ± 0.00074 | 0.000028 ± 0.000004 | 232.1 | 2.828 | 99.6 | 9.8 | 19.86 ± 0.11 | 108.37 ± 0.67 | n |
| 1.89W | 2.2545 ± 0.00566 | 0.11607 ± 0.00030 | 0.00003 ± 0.00007 | 0.02553 ± 0.00060 | 0.000019 ± 0.000003 | 232.1 | 2.674 | 99.7 | 10.0 | 19.37 ± 0.07 | 105.78 ± 0.48 | y |
| 2.06W | 2.1515 ± 0.00432 | 0.11165 ± 0.00026 | -0.00007 ± 0.00004 | 0.02830 ± 0.00093 | 0.000024 ± 0.000003 | 232.1 | 2.321 | 99.7 | 9.7 | 19.21 ± 0.06 | 104.89 ± 0.44 | y |
| 2.22W | 1.5056 ± 0.00409 | 0.07752 ± 0.00023 | -0.00008 ± 0.00006 | 0.02526 ± 0.00094 | 0.000015 ± 0.000003 | 232.1 | 1.805 | 99.7 | 6.7 | 19.36 ± 0.08 | 105.73 ± 0.52 | y |
| 2.43W | 1.4080 ± 0.00116 | 0.07254 ± 0.00007 | -0.00008 ± 0.00003 | 0.02760 ± 0.00099 | 0.000015 ± 0.000004 | 232.2 | 1.546 | 99.7 | 6.3 | 19.35 ± 0.03 | 105.65 ± 0.34 | y |
| 2.7W | 1.4854 ± 0.00419 | 0.07711 ± 0.00023 | -0.00001 ± 0.00006 | 0.03670 ± 0.00069 | 0.000017 ± 0.000005 | 232.2 | 1.236 | 99.7 | 6.7 | 19.20 ± 0.08 | 104.84 ± 0.53 | y |
| 3.02W | 1.4604 ± 0.00515 | 0.07639 ± 0.00030 | -0.00005 ± 0.00005 | 0.04501 ± 0.00120 | 0.000015 ± 0.000004 | 232.2 | 0.998 | 99.7 | 6.6 | 19.06 ± 0.10 | 104.11 ± 0.62 | y |
| 3.4W | 1.7308 ± 0.00153 | 0.09160 ± 0.00012 | -0.00009 ± 0.00003 | 0.08418 ± 0.00130 | 0.000010 ± 0.000005 | 232.9 | 0.640 | 99.8 | 7.9 | 18.86 ± 0.03 | 103.07 ± 0.35 | n |
| 3.85W | 2.0075 ± 0.00202 | 0.10761 ± 0.00013 | 0.00001 ± 0.00005 | 0.16458 ± 0.00171 | 0.000010 ± 0.000004 | 232.9 | 0.385 | 99.9 | 9.3 | 18.63 ± 0.03 | 101.82 ± 0.34 | n |
| 4.4W | 1.5946 ± 0.00209 | 0.08555 ± 0.00013 | -0.00002 ± 0.00004 | 0.19408 ± 0.00103 | 0.000014 ± 0.000004 | 232.9 | 0.259 | 99.7 | 7.4 | 18.59 ± 0.04 | 101.63 ± 0.36 | n |
| 5.08W | 1.1088 ± 0.00124 | 0.05937 ± 0.00014 | -0.00008 ± 0.00003 | 0.22895 ± 0.00220 | 0.000022 ± 0.000006 | 233.0 | 0.153 | 99.4 | 5.1 | 18.57 ± 0.06 | 101.49 ± 0.43 | n |
| | | | | | | | | | | **Plateau Age** | **105.29 ± 0.19** | |

| Laser output (W) | $^{40}Ar$ (±1s) | $^{39}Ar$ (±1s) | $^{38}Ar$ (±1s) | $^{37}Ar$ (±1s) | $^{36}Ar$ (±1s) | days after irradiation | K/Ca | $^{40}Ar^*$ (%) | $^{39}Ar_K$ fraction (%) | $^{40}Ar^*/^{39}Ar_K$ (±1s) | Age (±1s) (Ma) | adoption as plateau |
|---|---|---|---|---|---|---|---|---|---|---|---|---|
| **sample ID: 02JA11BMS06A** | | | | | | | | | | | | |
| J= 0.002966 | | | | | | | | | | | | |
| 0.75W | 0.5752 ± 0.00341 | 0.00706 ± 0.00005 | 0.00025 ± 0.00002 | 0.00862 ± 0.00075 | 0.001246 ± 0.000014 | 233.0 | 0.482 | 36.0 | 0.6 | 29.31 ± 0.77 | 150.40 ± 3.81 | n |
| 0.9W | 0.5588 ± 0.00452 | 0.00739 ± 0.00007 | 0.00019 ± 0.00001 | 0.00662 ± 0.00078 | 0.001195 ± 0.000012 | 233.0 | 0.657 | 36.8 | 0.6 | 27.85 ± 0.81 | 143.20 ± 4.03 | n |
| 1.15W | 0.8618 ± 0.00656 | 0.01252 ± 0.00010 | 0.00031 ± 0.00002 | 0.01113 ± 0.00088 | 0.001868 ± 0.000018 | 233.1 | 0.661 | 36.0 | 1.0 | 24.75 ± 0.71 | 127.80 ± 3.54 | n |
| 1.3W | 1.1809 ± 0.00113 | 0.01893 ± 0.00003 | 0.00038 ± 0.00005 | 0.00011 ± 0.00463 | 0.001175 ± 0.000100 | 237.8 | 101.1 | 70.6 | 1.5 | 44.04 ± 1.56 | 221.51 ± 7.41 | n |
| 1.55W | 2.2474 ± 0.01150 | 0.04648 ± 0.00024 | 0.00083 ± 0.00004 | 0.00011 ± 0.00465 | 0.004074 ± 0.000025 | 237.8 | 248.0 | 46.4 | 3.7 | 22.45 ± 0.31 | 116.31 ± 1.61 | n |
| 1.72W | 3.8073 ± 0.00954 | 0.15704 ± 0.00040 | 0.00046 ± 0.00006 | 0.05757 ± 0.00119 | 0.001766 ± 0.000011 | 237.9 | 1.605 | 86.3 | 12.5 | 20.92 ± 0.08 | 108.61 ± 0.53 | y |
| 1.89W | 9.1398 ± 0.01098 | 0.42957 ± 0.00073 | 0.00010 ± 0.00010 | 0.12751 ± 0.00190 | 0.000030 ± 0.000005 | 237.9 | 1.982 | 99.9 | 34.1 | 21.26 ± 0.04 | 110.30 ± 0.39 | y |
| 2.01W | 6.1058 ± 0.00325 | 0.29023 ± 0.00060 | -0.00014 ± 0.00008 | 0.11542 ± 0.00083 | 0.000030 ± 0.000004 | 238.1 | 1.479 | 99.9 | 23.0 | 21.01 ± 0.05 | 109.05 ± 0.39 | y |
| 2.08W | 1.8336 ± 0.00185 | 0.08968 ± 0.00013 | -0.00006 ± 0.00005 | 0.05381 ± 0.00086 | 0.000011 ± 0.000004 | 238.2 | 0.980 | 99.8 | 7.1 | 20.41 ± 0.04 | 106.03 ± 0.37 | n |
| 2.21W | 1.0178 ± 0.00075 | 0.04970 ± 0.00005 | 0.00001 ± 0.00004 | 0.03419 ± 0.00082 | 0.000010 ± 0.000004 | 238.2 | 0.855 | 99.7 | 3.9 | 20.42 ± 0.03 | 106.09 ± 0.36 | n |
| 2.45W | 1.0323 ± 0.00045 | 0.05134 ± 0.00006 | -0.00007 ± 0.00003 | 0.03736 ± 0.00075 | 0.000006 ± 0.000004 | 238.3 | 0.808 | 99.8 | 4.1 | 20.07 ± 0.03 | 104.32 ± 0.35 | n |
| 2.85W | 1.1739 ± 0.00166 | 0.05924 ± 0.00019 | 0.00000 ± 0.00004 | 0.05468 ± 0.00081 | 0.000001 ± 0.000004 | 238.2 | 0.637 | 100.0 | 4.7 | 19.81 ± 0.07 | 103.01 ± 0.48 | n |
| 3.55W | 0.7773 ± 0.01256 | 0.04046 ± 0.00084 | -0.00010 ± 0.00006 | 0.05842 ± 0.00246 | 0.000012 ± 0.000005 | 238.9 | 0.407 | 99.5 | 3.2 | 19.12 ± 0.50 | 99.52 ± 2.57 | n |
| | | | | | | | | | | **Plateau Age** | **109.44 ± 0.25** | |

Table 4 Continued.

| Laser output (W) | $^{40}Ar$ (±1s) | $^{39}Ar$ (±1s) | $^{38}Ar$ (±1s) | $^{37}Ar$ (±1s) | $^{36}Ar$ (±1s) | days after irradiation | K/Ca | $^{40}Ar^*$ (%) | $^{39}Ar_K$ fraction (%) | $^{40}Ar^*/^{39}Ar_K$ (±1s) | Age (±1s) (Ma) | adoption as plateau |
|---|---|---|---|---|---|---|---|---|---|---|---|---|
| **sample ID: 02JA03BMS04B-2** | | | | | | | | | | | | |
| J= 0.0029690 | | | | | | | | | | | | |
| 0.75W | 0.6129 ± 0.00267 | 0.01647 ± 0.00009 | 0.00016 ± 0.00003 | 0.0011 ± 0.0005 | 0.000589 ± 0.000005 | 238.9 | 8.599 | 71.6 | 0.6 | 26.64 ± 0.24 | 137.32 ± 1.24 | n |
| 0.92W | 0.8740 ± 0.00556 | 0.02278 ± 0.00017 | 0.00020 ± 0.00003 | 0.0032 ± 0.0005 | 0.000846 ± 0.000013 | 239.0 | 4.240 | 71.4 | 0.8 | 27.40 ± 0.36 | 141.11 ± 1.82 | n |
| 1.15W | 1.0866 ± 0.00942 | 0.02779 ± 0.00025 | 0.00020 ± 0.00003 | 0.0036 ± 0.0007 | 0.000985 ± 0.000013 | 239.0 | 4.524 | 73.2 | 0.9 | 28.62 ± 0.45 | 147.15 ± 2.24 | n |
| 1.3W | 1.4555 ± 0.01449 | 0.03715 ± 0.00038 | 0.00024 ± 0.00004 | 0.0040 ± 0.0007 | 0.001189 ± 0.000016 | 239.1 | 5.526 | 75.9 | 1.3 | 29.72 ± 0.51 | 152.57 ± 2.54 | n |
| 1.64W | 1.5985 ± 0.01511 | 0.04407 ± 0.00042 | 0.00026 ± 0.00005 | 0.0054 ± 0.0006 | 0.001062 ± 0.000011 | 239.1 | 4.778 | 80.4 | 1.5 | 29.15 ± 0.45 | 149.75 ± 2.25 | n |
| 1.74W | 1.8964 ± 0.01619 | 0.06380 ± 0.00056 | 0.00012 ± 0.00006 | 0.0050 ± 0.0008 | 0.000770 ± 0.000007 | 239.1 | 7.543 | 88.0 | 2.2 | 26.16 ± 0.34 | 134.93 ± 1.75 | n |
| 1.84W | 2.1616 ± 0.01215 | 0.09422 ± 0.00053 | 0.00012 ± 0.00005 | 0.0050 ± 0.0007 | 0.000331 ± 0.000008 | 239.2 | 11.128 | 95.5 | 3.2 | 21.90 ± 0.18 | 113.67 ± 0.96 | n |
| 1.93W | 2.7384 ± 0.01428 | 0.13927 ± 0.00075 | -0.00005 ± 0.00011 | 0.0055 ± 0.0007 | 0.000093 ± 0.000004 | 239.2 | 14.763 | 99.0 | 4.7 | 19.46 ± 0.15 | 101.35 ± 0.80 | n |
| 2.01W | 6.9663 ± 0.04185 | 0.36355 ± 0.00240 | -0.00030 ± 0.00017 | 0.0099 ± 0.0008 | 0.000047 ± 0.000005 | 239.2 | 21.692 | 99.8 | 12.3 | 19.12 ± 0.17 | 99.63 ± 0.91 | n |
| 2.06W | 12.4168 ± 0.00561 | 0.66136 ± 0.00129 | -0.00062 ± 0.00011 | 0.0201 ± 0.0004 | 0.000068 ± 0.000004 | 240.8 | 19.339 | 99.8 | 22.3 | 18.74 ± 0.04 | 97.71 ± 0.34 | n |
| 2.09W | 5.5968 ± 0.00309 | 0.31529 ± 0.00023 | -0.00047 ± 0.00007 | 0.0143 ± 0.0009 | 0.000046 ± 0.000003 | 240.9 | 12.990 | 99.8 | 10.6 | 17.71 ± 0.02 | 92.44 ± 0.28 | n |
| 2.13W | 3.8877 ± 0.00099 | 0.21564 ± 0.00009 | -0.00028 ± 0.00005 | 0.0107 ± 0.0005 | 0.000038 ± 0.000003 | 240.9 | 11.903 | 99.7 | 7.3 | 17.98 ± 0.01 | 93.80 ± 0.28 | y |
| 2.19W | 1.9379 ± 0.00272 | 0.10586 ± 0.00016 | -0.00009 ± 0.00004 | 0.0055 ± 0.0005 | 0.000017 ± 0.000004 | 241.0 | 11.299 | 99.7 | 3.6 | 18.26 ± 0.04 | 95.25 ± 0.34 | y |
| 2.36W | 1.4966 ± 0.00212 | 0.08171 ± 0.00017 | -0.00006 ± 0.00003 | 0.0036 ± 0.0005 | 0.000019 ± 0.000004 | 241.1 | 13.181 | 99.6 | 2.8 | 18.25 ± 0.05 | 95.18 ± 0.37 | y |
| 2.82W | 2.0911 ± 0.00128 | 0.11612 ± 0.00013 | -0.00026 ± 0.00005 | 0.0107 ± 0.0005 | 0.000021 ± 0.000003 | 241.1 | 6.377 | 99.7 | 3.9 | 17.96 ± 0.02 | 93.70 ± 0.30 | y |
| 3.6W | 4.1056 ± 0.00179 | 0.23766 ± 0.00025 | -0.00037 ± 0.00010 | 0.0501 ± 0.0008 | 0.000035 ± 0.000004 | 241.2 | 2.793 | 99.7 | 8.0 | 17.23 ± 0.02 | 90.01 ± 0.28 | n |
| 4.5W | 7.6555 ± 0.00439 | 0.42316 ± 0.00092 | -0.00076 ± 0.00011 | 0.1439 ± 0.0016 | 0.000048 ± 0.000003 | 241.2 | 1.729 | 99.8 | 14.3 | 18.06 ± 0.04 | 94.22 ± 0.34 | n |
| | | | | | | | | | | | **no plateau** | |

| Laser output (W) | $^{40}Ar$ (±1s) | $^{39}Ar$ (±1s) | $^{38}Ar$ (±1s) | $^{37}Ar$ (±1s) | $^{36}Ar$ (±1s) | days after irradiation | K/Ca | $^{40}Ar^*$ (%) | $^{39}Ar_K$ fraction (%) | $^{40}Ar^*/^{39}Ar_K$ (±1s) | Age (±1s) (Ma) | adoption as plateau |
|---|---|---|---|---|---|---|---|---|---|---|---|---|
| **sample ID: 02JA02BMS07A** | | | | | | | | | | | | |
| J= 0.0029720 | | | | | | | | | | | | |
| 0.8W | 1.0044 ± 0.00314 | 0.04307 ± 0.00092 | 0.00037 ± 0.00007 | 0.02438 ± 0.00059 | 0.000976 ± 0.000004 | 241.9 | 1.039 | 71.3 | 7.9 | 16.62 ± 0.36 | 86.98 ± 1.87 | n |
| 1W | 1.9655 ± 0.00573 | 0.12028 ± 0.00173 | 0.00050 ± 0.00014 | 0.04017 ± 0.00048 | 0.000168 ± 0.000005 | 241.9 | 1.761 | 97.5 | 21.9 | 15.93 ± 0.23 | 83.44 ± 1.22 | y |
| 1.25W | 1.4725 ± 0.00844 | 0.08737 ± 0.00242 | -0.00001 ± 0.00016 | 0.02955 ± 0.00066 | 0.000113 ± 0.000003 | 242.0 | 1.739 | 97.7 | 15.9 | 16.47 ± 0.47 | 86.22 ± 2.40 | y |
| 1.55W | 1.0375 ± 0.00430 | 0.06471 ± 0.00028 | 0.00007 ± 0.00006 | 0.02898 ± 0.00086 | 0.000071 ± 0.000004 | 242.0 | 1.314 | 98.0 | 11.8 | 15.71 ± 0.10 | 82.33 ± 0.55 | y |
| 1.92W | 1.1102 ± 0.00739 | 0.07197 ± 0.00415 | 0.00005 ± 0.00028 | 0.03570 ± 0.00083 | 0.000053 ± 0.000005 | 242.0 | 1.186 | 98.6 | 13.1 | 15.21 ± 0.88 | 79.75 ± 4.54 | y |
| 2.45W | 1.1817 ± 0.00786 | 0.07774 ± 0.00433 | -0.00015 ± 0.00029 | 0.05669 ± 0.00071 | 0.000042 ± 0.000004 | 242.1 | 0.807 | 98.9 | 14.2 | 15.04 ± 0.84 | 78.89 ± 4.33 | y |
| 3.2W | 1.2963 ± 0.00099 | 0.08322 ± 0.00201 | -0.00010 ± 0.00014 | 0.23013 ± 0.00163 | 0.000115 ± 0.000005 | 242.1 | 0.213 | 97.4 | 15.2 | 15.17 ± 0.37 | 79.54 ± 1.90 | y |
| | | | | | | | | | | **Plateau Age** | **82.4 ± 0.5** | |

| Laser output (W) | $^{40}Ar$ (±1s) | $^{39}Ar$ (±1s) | $^{38}Ar$ (±1s) | $^{37}Ar$ (±1s) | $^{36}Ar$ (±1s) | days after irradiation | K/Ca | $^{40}Ar^*$ (%) | $^{39}Ar_K$ fraction (%) | $^{40}Ar^*/^{39}Ar_K$ (±1s) | Age (±1s) (Ma) | adoption as plateau |
|---|---|---|---|---|---|---|---|---|---|---|---|---|
| **sample ID: MT473BMS02A-2** | | | | | | | | | | | | |
| J= 0.0031100 | | | | | | | | | | | | |
| 0.60W | 2.8529 ± 0.01174 | 0.19033 ± 0.00079 | -0.00016 ± 0.00011 | 0.03165 ± 0.00161 | 0.000114 ± 0.000005 | 294.8 | 3.537 | 98.8 | 7.7 | 14.81 ± 0.09 | 81.25 ± 0.53 | y |
| 0.82W | 3.0234 ± 0.00880 | 0.20838 ± 0.00063 | -0.00041 ± 0.00009 | 0.05165 ± 0.00192 | 0.000034 ± 0.000005 | 294.9 | 2.373 | 99.7 | 8.5 | 14.46 ± 0.06 | 79.36 ± 0.40 | y |
| 0.94W | 2.7555 ± 0.00858 | 0.18850 ± 0.00062 | -0.00026 ± 0.00007 | 0.06621 ± 0.00200 | 0.000017 ± 0.000004 | 295.0 | 1.675 | 99.8 | 7.7 | 14.59 ± 0.07 | 80.06 ± 0.43 | y |
| 1.08W | 3.0301 ± 0.01126 | 0.20879 ± 0.00081 | -0.00029 ± 0.00009 | 0.09904 ± 0.00262 | 0.000024 ± 0.000003 | 295.0 | 1.240 | 99.8 | 8.5 | 14.48 ± 0.08 | 79.46 ± 0.48 | y |
| 1.24W | 3.1841 ± 0.01215 | 0.22345 ± 0.00087 | -0.00019 ± 0.00010 | 0.15990 ± 0.00337 | 0.000026 ± 0.000004 | 295.0 | 0.822 | 99.8 | 9.1 | 14.22 ± 0.08 | 78.05 ± 0.48 | n |
| 1.39W | 2.3703 ± 0.00358 | 0.16827 ± 0.00028 | -0.00014 ± 0.00007 | 0.15387 ± 0.00437 | 0.000024 ± 0.000005 | 295.1 | 0.643 | 99.7 | 6.8 | 14.04 ± 0.03 | 77.13 ± 0.29 | n |
| 1.58W | 3.7568 ± 0.01094 | 0.27627 ± 0.00081 | -0.00013 ± 0.00010 | 0.26278 ± 0.00306 | 0.000031 ± 0.000003 | 295.1 | 0.618 | 99.8 | 11.2 | 13.57 ± 0.06 | 74.55 ± 0.37 | n |
| 1.79W | 3.4979 ± 0.00738 | 0.26653 ± 0.00057 | -0.00021 ± 0.00010 | 0.21067 ± 0.00232 | 0.000035 ± 0.000006 | 295.2 | 0.744 | 99.7 | 10.8 | 13.08 ± 0.04 | 71.96 ± 0.30 | n |
| 2.0W | 2.5349 ± 0.00255 | 0.19840 ± 0.00026 | -0.00011 ± 0.00008 | 0.11007 ± 0.00173 | 0.000033 ± 0.000004 | 295.2 | 1.060 | 99.6 | 8.1 | 12.73 ± 0.02 | 70.04 ± 0.24 | n |
| 2.28W | 2.2710 ± 0.00252 | 0.18283 ± 0.00022 | -0.00015 ± 0.00006 | 0.07857 ± 0.00246 | 0.000045 ± 0.000005 | 295.2 | 1.369 | 99.4 | 7.4 | 12.35 ± 0.02 | 67.99 ± 0.23 | n |
| 2.62W | 2.0961 ± 0.00106 | 0.17213 ± 0.00026 | -0.00023 ± 0.00006 | 0.06716 ± 0.00178 | 0.000092 ± 0.000004 | 296.2 | 1.508 | 98.7 | 7.0 | 12.02 ± 0.02 | 66.20 ± 0.22 | n |
| 3.22W | 2.1085 ± 0.00213 | 0.17440 ± 0.00026 | -0.00039 ± 0.00006 | 0.07875 ± 0.00181 | 0.000094 ± 0.000004 | 296.2 | 1.303 | 98.7 | 7.1 | 11.93 ± 0.02 | 65.73 ± 0.23 | n |
| | | | | | | | | | | **Plateau Age** | **79.77 ± 0.21** | |

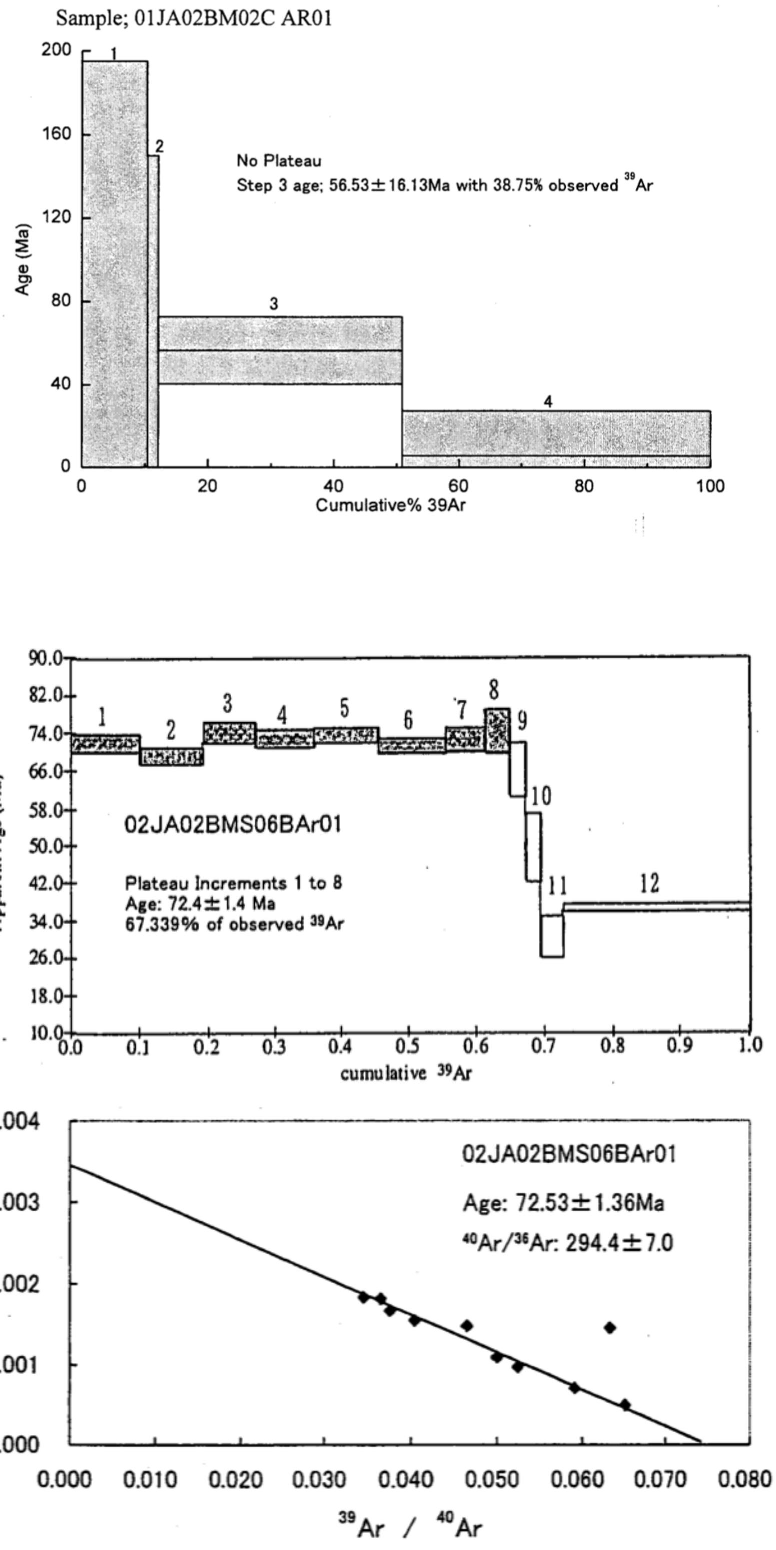


Fig. 10 Step heating age spectra and inverse isochron diagrams for Ar–Ar dating (JA02 Seamount)

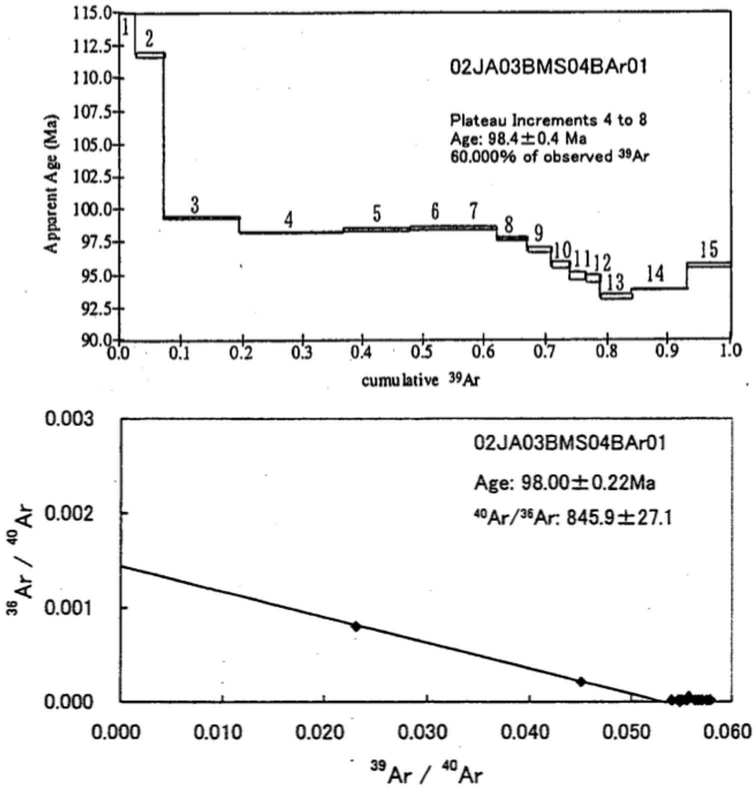


Fig. 11 Step heating age spectra and inverse isochron diagrams for Ar–Ar dating (JA03 Seamount)

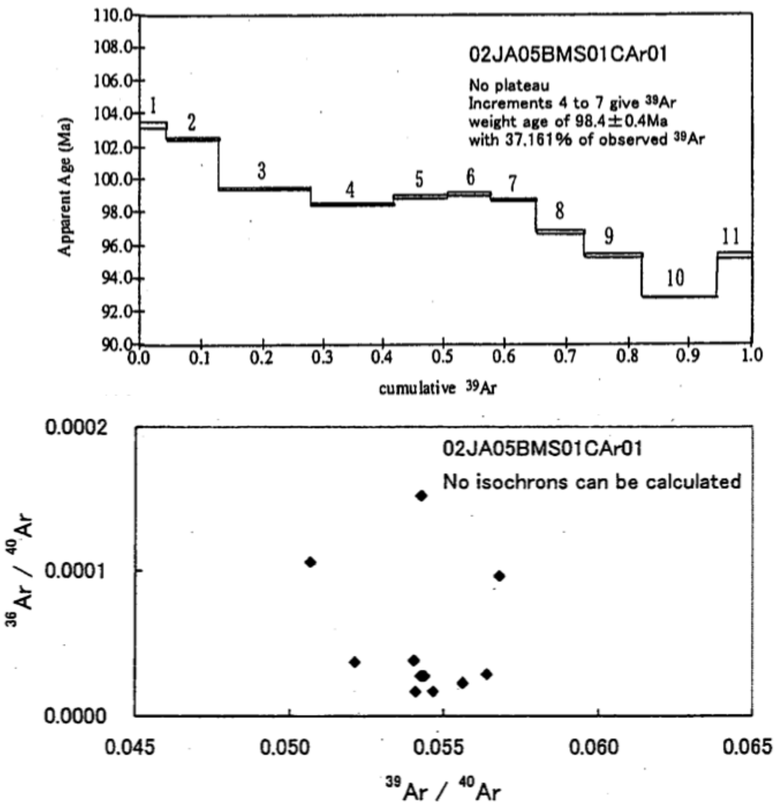


Fig. 12 Step heating age spectra and inverse isochron diagrams for Ar–Ar dating (JA05 Seamount)

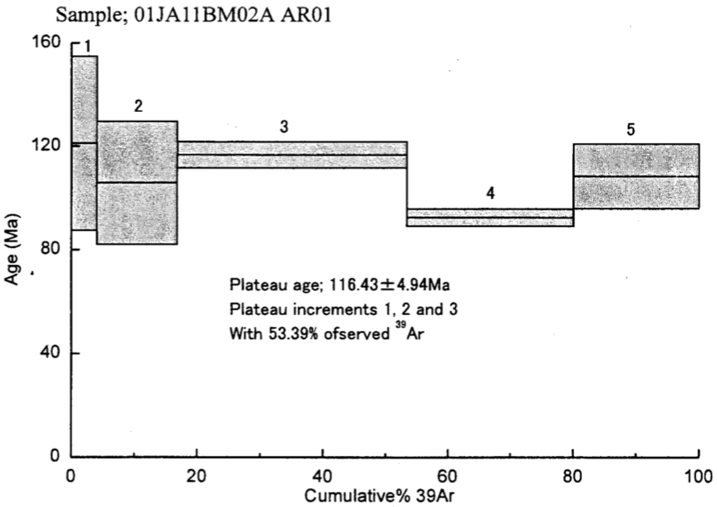


Fig. 13 Step heating age spectra diagram for Ar–Ar dating (JA11 Seamount)

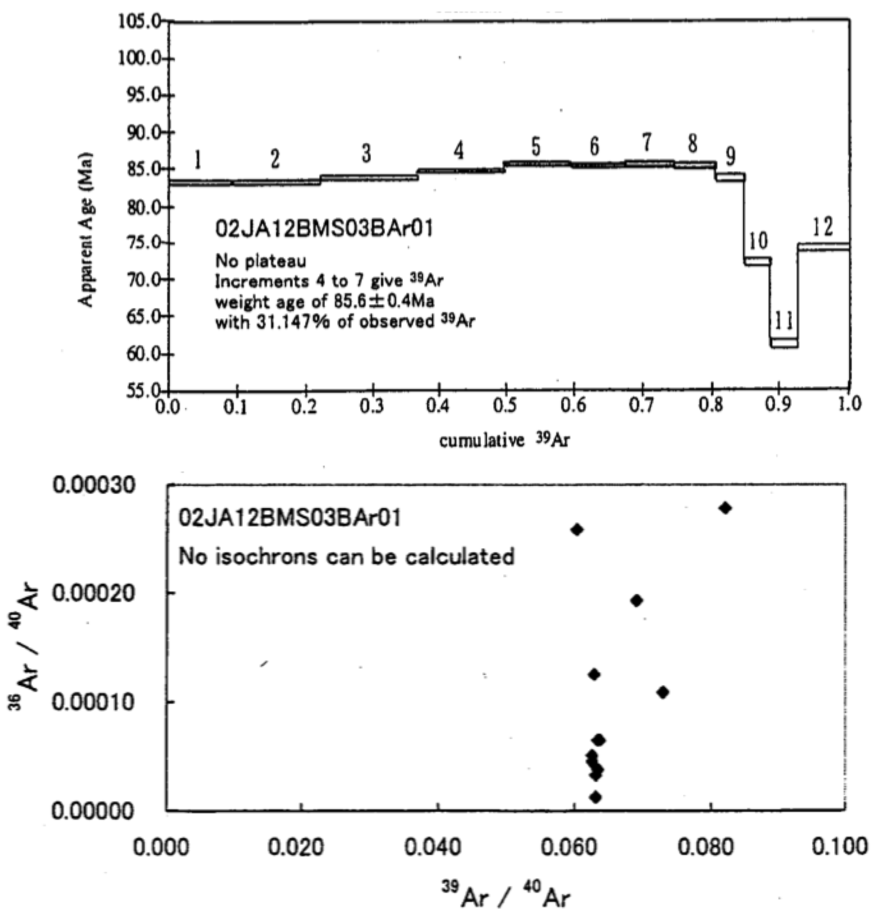


Fig. 14 Step heating age spectra and inverse isochron diagrams for Ar–Ar dating (JA12 Seamount)

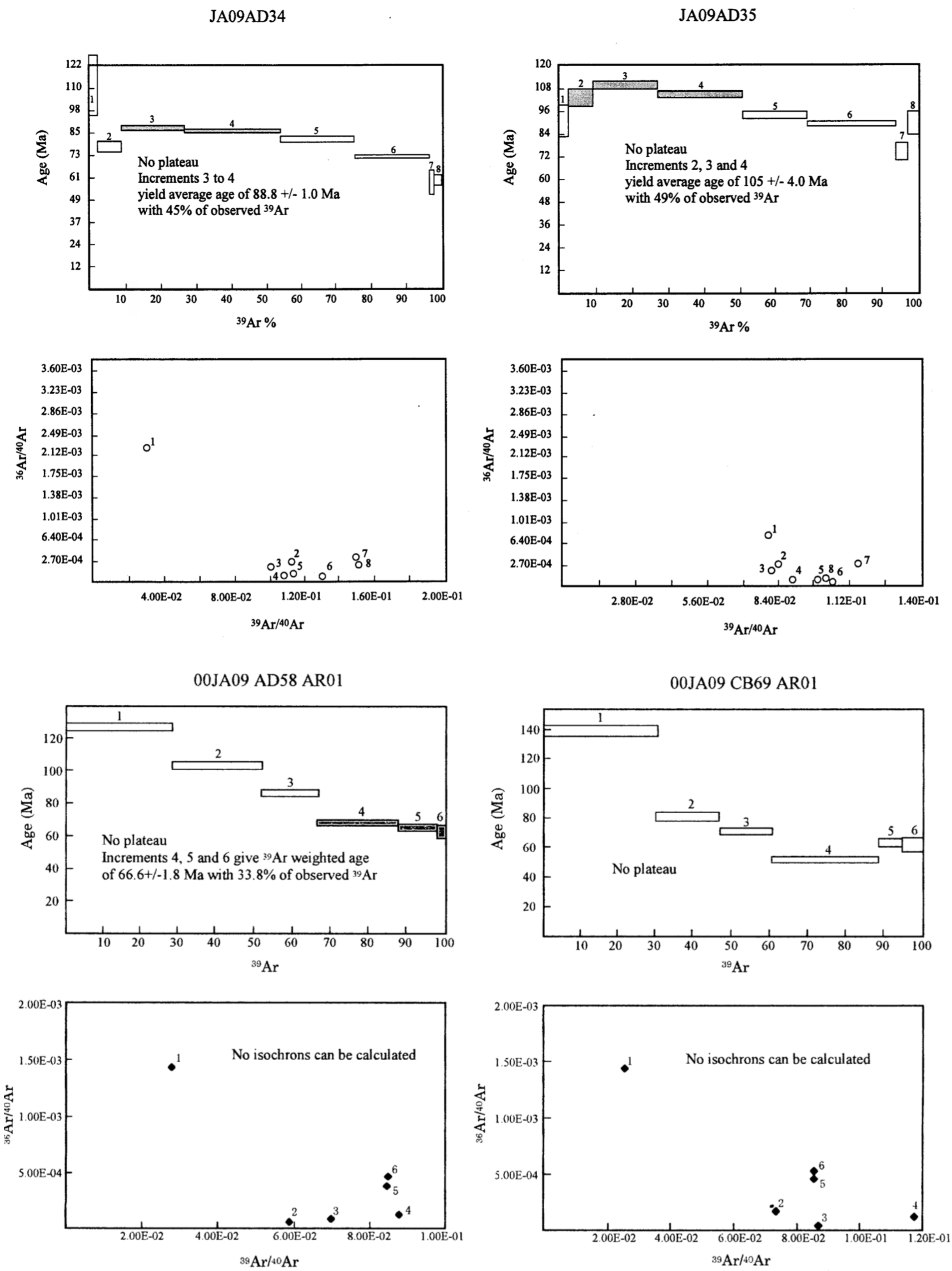


Fig. 15 Step heating age spectra and inverse isochron diagrams for Ar–Ar dating (JA09 Seamount)

due to alteration.

**(3) JA14 Seamount (Govorov Guyot)**

K–Ar dating was carried out on one sample and yielded an age of 86.8 ± 3.0 Ma, but the results are not reliable due to alteration.

**(4) JA15 Seamount (Pegas Guyot)**

K–Ar dating was carried out on two samples with a slightly higher degree of alteration. The obtained ages are 56.0 ± 2.8 Ma and 68.7 ± 3.4 Ma, corresponding to the Early Eocene to Late Cretaceous (Maastrichtian). However, these ages may be slightly young due to the loss of some Ar in the rocks through weathering and alteration after the magma solidified. This is supported by the facts that fossils from the Late Cretaceous (88–85 Ma) have been found in this seamount, and previous studies suggesting that the Magellan Seamounts were formed during the Aptian at the end of the Early Cretaceous (Smith *et al.*, 1989, Abrams *et al.*, 1993).

**(5) JA19 Seamount (Hemler Guyot)**

K–Ar dating was performed on two samples and yielded ages of 78.1 ± 2.5 Ma and 79.6 ± 2.6 Ma (Late Cretaceous), but the results are unreliable due to alteration. Ar–Ar age of 100.1 ± 0.8 Ma was reported by Koppers *et al.* (2003).

**(6) JA22 Seamount (Butakov Guyot)**

K–Ar dating was carried out on two samples, yielding ages of 53.3 ± 1.9 Ma and 69.9 ± 2.3 Ma, but the results are unreliable due to alteration.

### 5. 3 Marshall Islands Seamount Group

**(1) JA10 Seamount (Rykachev Guyot)**

K–Ar dating was performed on one sample and Ar–Ar dating on five samples. The K–Ar age of 43.6 ± 2.8 Ma obtained from 89JA10AD04-E is unreliable due to alteration. No reliable Ar–Ar ages were obtained from 99JA10AD11 and 99JA10AD17. An age of 82.7 ± 3.1 Ma (Late Cretaceous: Campanian) was obtained from 00JA10AD34 but is unreliable due to lack of agreement within the 95 % confidence limits. Plateau ages of 91.8 ± 0.7 Ma (Middle Cretaceous: Cenomanian) and 88.5 ± 1.2 Ma (Middle Cretaceous: Turonian) were obtained from 00JA10AD37 and 00JA10AD41, respectively, suggesting that the basement basalts of JA10 Seamount were formed during the Middle Cretaceous. Figure 16 shows the stage-heating age spectra and inverse isochron diagrams of 00JA10AD34, 00JA10AD37, and 00JA10AD41. The $^{40}Ar/^{39}Ar$ age measurement data are shown in Table 4.

**(2) JA16 Seamount (Changpogo Seamount)**

K–Ar dating was carried out on one sample with a slightly higher degree of alteration and yielded an age of 54.1 ± 2.1 Ma (Early Eocene to Late Cretaceous: Maastrichtian), but the reliability is low due to alteration.

## 6. Summary

The basement basalts of seamounts in the Northwest Pacific show characteristics of ocean island alkaline basalts similar to those of the basalts from the SOPITA region in the South Pacific, although many samples have been affected by alteration and phosphatization. The K–Ar ages of the basalts are likely to be younger than their actual ages due to alteration. On the other hand, Ar–Ar dating is more resilient to alteration than K–Ar dating, the plateau ages obtained by Ar–Ar dating are considered to be reliable. The basement basalts of JA01, JA02, JA03, JA11, JA12, JA17, and MT473 Seamounts in the Marcus Wake Seamount Group have Ar–Ar plateau ages of 67–116 Ma, the basement basalts of JA09 Seamount in the Magellan Seamount Group have Ar–Ar plateau ages of 87 Ma and 105 Ma, and the basement basalts of JA10 Seamount in the Marshall Islands Seamount Group have Ar–Ar plateau ages of 90 Ma.

**Acknowledgments:**Dr. TOKUMARU, A. provided the technical information on Ar–Ar age of Takuyo-Daigo Smt. The manuscript was improved by constructive comments from Dr. KON, Y. The data in this paper have been collected as a part of sponsored projects by Agency for Natural Resources and Energy, Ministry of Economy, Trade and Industry (METI), Japan, and Japan Oil, Gas and Metals National Corporation (JOGMEC). This study was also funded by internal grants from the National Institute of Advanced Industrial Science and Technology (AIST). The authors express their appreciation to everyone involved in this project.

## References

Abrams, L.J., Larson, R.L., Shipley, T.H. and Lancelot, Y. (1993) Cretaceous volcanic sequence and Jurassic oceanic crust in the East Mariana and Pigafetta basins of the western Pacific. *In* Pringle, M.S., Sahger, W.W., Sliter, W.V. and Stein, S. (Eds.), *The Mesozoic Pacific: Geology, Tectonics, and Volcanism, Geophysical Monograph Series*, **77**, 77–101, AGU, Washington, D.C.

Christie, D.M., Dieu, J.J. and Gee, J.S. (1995) Petrologic studies of basement lavas from northwest Pacific guyots. *In* Haggerty, J.A., Premoli Silva, I., Rack, F. and McNutt, M.K. (Eds.), *Proceedings of the ODP, Scientific Results,* **144**, 295–512.

Dalrymple, G.B., Lanphere, M.A. and Clague, D.A. (1980) Conventional and $^{40}Ar/^{39}Ar$ K–Ar ages of volcanic rocks from Ojin (Site 430), Nintoku (Site 432), and Suiko (Site 433) Seamounts and the chronology of volcanic propagation along the Hawaiian-Emperor Chain. *Initial Report of the DSDP*, **55**, 659–676.

Ishizuka, O., Kimura, J.I., Li, Y.-B., Stern, R.J. Reagan, M.K., Taylor, R.N., Ohara, Y., Bloomer, S.H., Ishii, T, Hargrove III, U.S. and Haraguchi, S. (2006) Early stages in the evolution of Izu-Bonin arc volcanism: new age, chemical and isotopic constraints. *Earth and Planetary Science Letters,* **250**, 385–401.

Koppers, A.A.P., Staudigel, H., Pringle, M.S. and Wijbrans, J.R. (2003) Short-lived and discontinuous

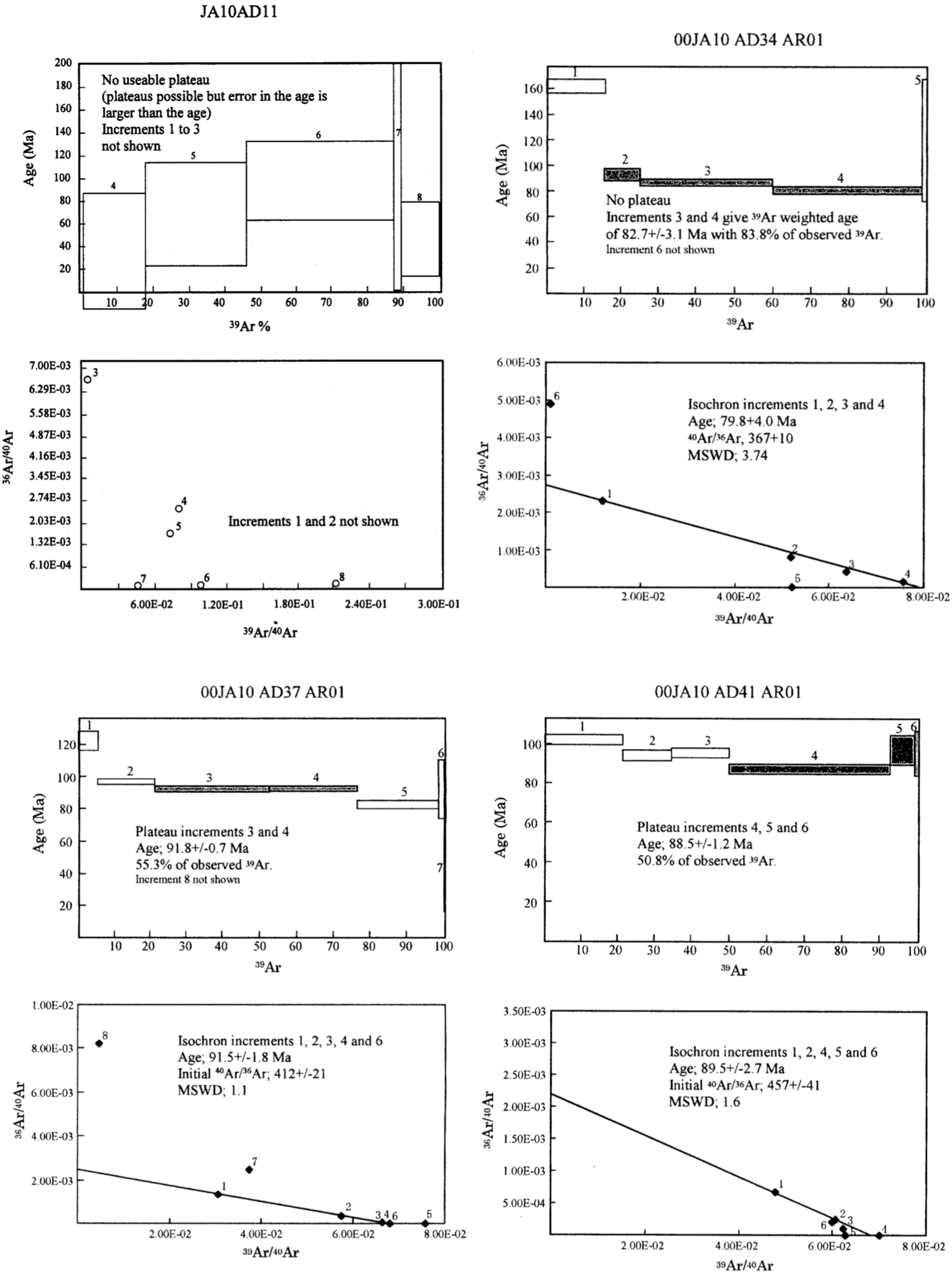


Fig. 16 Step heating age spectra and inverse isochron diagrams for Ar–Ar dating (JA10 Seamount)

intraplate volcanism in the South Pacific: hot spots or extensional volcanism? *Geochemistry, Geophysics, Geosystems*, **4**, 1089. doi:10.1029/2003GC000533

Larson, R.L., Pitman, W.C., III, Golovchenko, X., Cande, S.C., Dewey, J.F., Haxby, W.F. and Labrecque, J.L. (1985) *The Bedrock Geology of the World*. Freeman, New York.

Meschede, M. (1986) A method of discriminating between different types of mid-ocean ridge basalts and continental tholeiites with the Nb–Zr–Y diagram. *Chemical Geology*, **56**, 207–218.

Shervais, J.W. (1982) Ti-V plots and the petrogenesis of modern and ophiolitic lavas. *Earth and Planetary Science Letters*, **59**, 101–118.

Smith, W.H.F., Staudigel, H., Watts, A.B. and Pringle, M.S. (1989) The Magellan Seamountains: Early Cretaceous record of the South Pacific isotopic and thermal anomaly. *Journal of Geophysical Research*, **94**, 10501–10523.

Staudigel, H., Park, K.-H., Pringle, M.S., Rubenstone, J.L., Smith, W.H.F. and Zindler, A. (1991) The longevity of the south Pacific isotope and thermal anomaly. *Earth and Planetary Science Letters*, **102**, 24–44.

Steiger, R.H. and Jager, E. (1977) Subcommission on geochronology: Convention on the use of decay constants in geo- and cosmochronology. *Earth and Planetary Science Letters,* **36**, 359–362.

Sun, S.-s. and McDonough, W.F. (1989) Chemical and isotopic systematics of oceanic basalts: implications for mantle composition and processes. *Magmatism in the Ocean Basins, Geological Society Special Publication*, **42**, 313–345.

Tokumaru, A., Nozaki, T., Suzuki, K., Goto, K.T., Chang, Q., Kimura, J.I., Takaya, Y., Kato, Y., Usui, A. and Urabe, T. (2015) Re-Os isotope geochemistry in the surface layers of ferromanganese crusts from the Takuyo Daigo Seamount, northwestern Pacific Ocean. *Geochemical Journal*, **49**, 233–241.

Usui, A. and Someya, M. (1997) Distribution and composition of marine hydrothermal manganese deposits in the northwest Pacific. *In* Nicholson K., Hein J.R., Buhn B., and Dasgupta S. (Eds.), *Manganese Mineralization: Geochemistry and Mineralogy of Terrestrial and Marine Deposits, Geological Society Special Publication*, **119**, 177–198.

Watkins, D.K., Premoli Silva, I. and Erba, E. (1995) Cretaceous and Paleogene manganese-encrusted hardgrounds from central Pacific guyots. *In* Haggerty, J.A., Premoli-Silva, I., Rack, F. and McNutt, M.K. (Eds.), *Proceedings of the ODP, Scientific Results*, **144**, 97–126.

York, D. (1969) Least squares fitting of a straight line with correlated errors. *Earth and Planetary Science Letters*, **5**, 320–324.

Zindler, A. and Hart, S.R. (1986) Chemical geodynamics. *Annual Review of Earth and Planetary Sciences*, **14**, 493–571.

Recieved October 25, 2021
Accepted June 30, 2022
Published on-line October 4, 2022

## 北西太平洋における海山基盤玄武岩の化学組成及び生成年代

山岡　香子・石塚　治・両角　春寿・日野　ひかり

### 要　旨

北西太平洋海域におけるコバルトリッチクラスト鉱床の探査の一環として，海山基盤玄武岩が採取され，全岩化学組成分析及び K–Ar/Ar–Ar 法年代測定が実施された．海山基盤玄武岩は変質やリン酸塩化の影響を受けて初生的な化学組成の保存が良くないものの，試料が採取された 20 海山は全て典型的な海洋島アルカリ玄武岩の特徴を示した．生成年代については，K–Ar 法年代測定では変質の影響により信頼できる年代値が得られなかったが，Ar–Ar 法年代測定ではいくつかの海山から信頼性の高いプラトー年代が得られた．マーカス・ウェーク海山群に属する海山からは 67 ～ 116 Ma，マゼラン海山群に属する海山からは 87 Ma 及び 105 Ma，マーシャル諸島海山群に属する海山からは 90 Ma の生成年代が得られ，概ね先行研究で報告されている年代と一致した．

地質調査研究報告，第 73 巻，第 3 号，p. 137-142，2022

概報 - Report

# 埼玉県岩殿丘陵西縁部から採取された砂質シルト岩試料の珪藻化石年代

納谷　友規 [1, *]

NAYA Tomonori (2022) Diatom biochronology of the sandy siltstone samples collected from the western margin of the Iwadono Hills, Saitama Prefecture, central Japan. *Bulletin of the Geological Survey of Japan*, vol. 73 (3), p. 137–142, 3 figs, 1 table and 1 plate.

**Abstract:** Diatom analysis was performed to determine the depositional age of previously undated sandy siltstone samples from the western margin of the Iwadono Hills, Saitama Prefecture, central Japan. The age of the samples is assigned to the early Middle Miocene according to the occurrence of diatoms that are correlative to the diatom zone NPD4A (*Denticulopsis lauta* Zone). The occurrence of *Cavitatus lanceolatus* limits the age of these samples to the interval between biohorizon D41.5 (first occurrence of *Cv. lanceolatus*: 15.6 Ma) and D43.2 (last occurrence of *Cv. lanceolatus*: 15.2 Ma). Based on the diatom biostratigraphy and biochronology, these samples can be correlated with the upper part of the Arakawa Formation or the Ichinokawa Formation of the Hiki Group.

**Keywords:** diatom, biostratigraphy, Miocene, Iwadono Hills, Saitama Prefecture, Japan

## 要　旨

岩殿丘陵西縁部の帰属不明の砂質シルト岩試料の堆積年代を明らかにするために，珪藻化石分析を行った．分析した試料からは，珪藻化石帯NPD4A帯（*Denticulopsis lauta*帯）を特徴づける珪藻化石が産出するため，年代は中期中新世前期と判断される．また，*Cavitatus lanceolatus*を産することから，本試料の年代は生層準D41.5（*Cv. lanceolatus*の初産出：15.6 Ma）−D43.2（*Cv. lanceolatus*の終産出：15.2 Ma）の区間に限定される．珪藻化石層序に基づくと，本試料は比企層群荒川層の上部か市ノ川層に対比される．

## 1．はじめに

埼玉県の中央部に位置する比企丘陵と岩殿丘陵（第1図）には海成の中新統が分布している（例えば，小池ほか，1985；間嶋，1989）．高橋・柳沢（2004）は微化石層序に基づく複合年代層序を検討し岩相層序の再検討を行い，この地域の中新統を下位より比企層群と都幾川層群にまとめた（高橋，2008）．比企層群は比企丘陵と岩殿丘陵の北縁を流れる都幾川とその支流沿いに分布し，下位より，小園層，荒川層，市ノ川層に区分される（高橋，2008；栗原・柳沢，2015；荒井・原田，2015）（第2図）．都幾川層群は岩殿丘陵では下位より神戸層，根岸層，将軍沢層，鳩山層，今宿層に区分される（栗原ほか，2003；高橋，2008）（第2図）．比企層群は都幾川層群最下部の神戸層基底によって不整合に覆われ（栗原・柳沢，2015；荒井・原田，2015），この不整合は約15 Maに形成された広域不整合と考えられている庭谷不整合に対比されている（高橋・柳沢，2004）．

従来，岩殿丘陵では北縁部を除き比企層群に相当する地層は分布しないと考えられていたが，近年，岩殿丘陵西縁部において，市ノ川層や荒川層に岩相が類似した地層が報告されるようになった（原田，2009）．筆者が行った5万分の1地質図幅「川越」作成のための地質調査でも，岩殿丘陵の西縁部に市ノ川層と岩相が類似する礫岩層と砂岩層が分布することが確認された．原田（2009）では年代の指標となる化石は報告されておらず，また，筆者による調査でも年代の指標となる化石の産出を確認できなかったため，これらの地層の年代と帰属については不明であった．

北西太平洋地域の珪藻化石層序は前期中新世後期〜中期中新統前期に数多くの生層準を持つため，この年代区間では特に高時間分解能で年代層序を検討することが可能である（Yanagisawa and Akiba，1998）．比企層群と都幾川層群においても，珪藻化石層序が年代層序を構築するために極めて重要な役割を果たしてきた（堀内・柳沢，1994；栗原ほか，2003；高橋・柳沢，2004）．さらに，帰属不明の試料においては，その堆積年代を決定し両層群への帰属を明らかにするためにも有用であり，例えば

[1] 産業技術総合研究所 地質調査総合センター 地質情報研究部門 (AIST, Geological Survey of Japan, Research Institute of Geology and Geoinformation)
[*] Corresponding author: NAYA, T., Central 7, 1-1-1 Higashi, Tsukuba, Ibaraki 305-8567, Japan. Email: t-naya@aist.go.jp

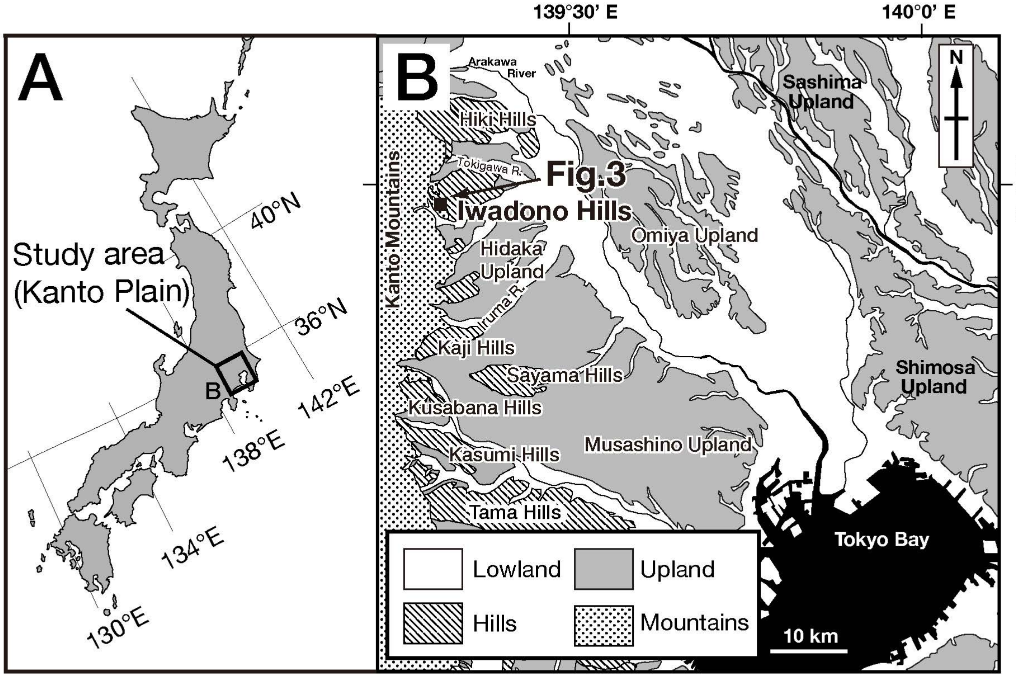


第1図　岩殿丘陵と比企丘陵の位置．地質図は杉山ほか(1997)に基づく．

Fig.1　Locality map of the Iwadono and Hiki Hills in the Kanto Plain. Map after Sugiyama *et al.* (1997).

関東平野地下の温泉ボーリングのカッティングス試料の分析でも利用されている(例えば，納谷ほか，2013)．

原田(2009)が報告した露頭のうち，越生町六地蔵の露頭(第3図)ではシルト岩が観察され，原田(2009)はこの岩相は荒川層に類似すると考えた．シルト岩からは珪藻化石が産出する可能性が高いが，残念ながら現在この露頭は観察不可能である．本研究では，岩殿丘陵における比企層群の有無を検証することを目的として，原田(2009)によってこの露頭から貝化石と一緒に採取された岩片に含まれる珪藻化石を検討した．その結果，この試料の年代を制約する知見が得られたので報告する．

## 2．試料と方法

原田(2009)によって貝化石が報告された越生町六地蔵の露頭(第3図)において，貝化石と一緒に採取された2個の細粒砂を含む砂質シルト岩片(no.1，no.2)を分析試料とした．両試料は露頭から直接採取されたものであり，両試料の採取層準はほぼ同一である．

試料の処理は基本的には納谷ほか(2009)の手法Aに従って行った．ただし，懸濁液は大豆大(0.5 $cm^3$程度)の砂質シルト岩片を瑪瑙乳鉢で軽くつぶした試料を用いて作成した．封入材にはMountmedia(富士フイルム和光純薬株式会社)を用いた．

検鏡は倍率1000倍の生物顕微鏡(ニコンECLIPSE E80i，対物レンズPlan Apo VC 100×：1.40 N.A.)を用いて行い，視野に出現した分類群の殻数を記録し，合計100殻になるまで計数した．100殻計数した後に，さらに広い範囲を検鏡して，化石帯の認定に重要な分類群の有無を確認した．*Chaetoceros*属の休眠胞子については，珪藻殻の計数時に視野のなかに認められた数を別途計数した．珪藻化石帯区分と生層準は，Akiba(1986)とYanagisawa and Akiba(1998)のNPDとDコードを用いた．生層準の年代はWatanabe and Yanagisawa(2005)を用い，Raffi *et al.* (2020)の地磁気極性年代尺度に合わせて調整された柳沢(2021)の年代値を参照した．

## 3．結果

両試料の分析結果を第1表に示す．産出した主な珪藻化石の顕微鏡写真を図版1にまとめた．両試料とも，*Thalasionema* spp.(*T. nitzschioides*, *T.* cf. *nitzschioides*, *T.* cf. *hirosakiensis*を一括してここに含めた)と*Actinocyclus ingens* f. *planus*が多く産出し両分類群が50 %以上を占める．*Denticulopsis lauta*と*D. ichikawae*が共存し，*D. hyalina*を含まないことから，NPD4A帯に属すると判断される．さらに，*Cavitatus lanceolatus*を産することから，D41.5(*Cv. lanceolatus*の初産出：15.6 Ma)−D43.2(*Cv. lanceolatus*の終産出：15.2 Ma)の区間に限定される．

## 4．考察

高橋・柳沢(2004)は岩殿丘陵北側の都幾川沿いの都

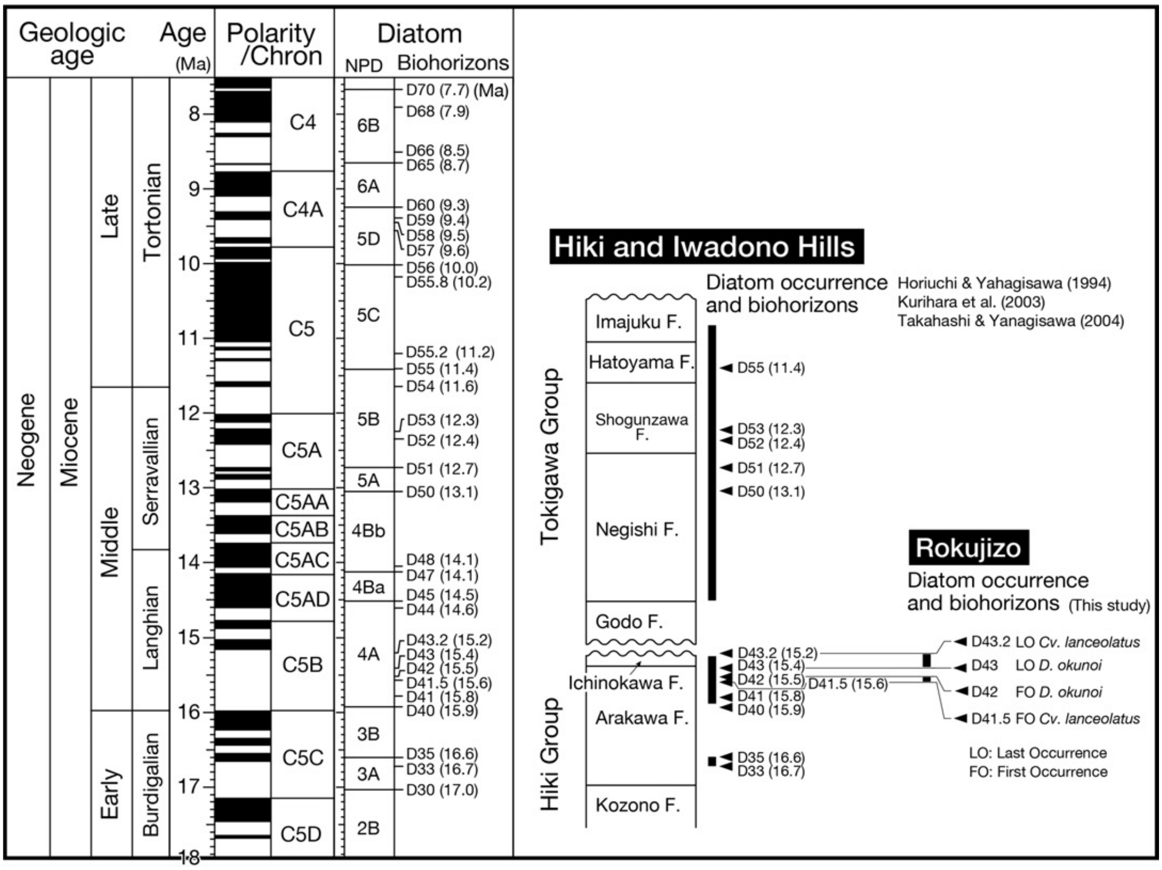


第2図　比企層群と都幾川層群および六地蔵の砂質シルト岩の珪藻化石年代．地磁気極性年代尺度はRaffi *et al.*（2020）に，珪藻化石帯および生層準はAkiba（1986），Yanagisawa and Akiba（1998）に従い，Watanabe and Yanagisawa（2005）で改訂された年代値に基づく．

Fig.2　Diatom biochronology of the Hiki and Tokigawa groups and the sandy siltstone collected from Rokujizo, Ogose Town, Saitama Prefecture. Diatom zonation, biohorizones and ages follow Akiba (1986) and Yanagisawa and Akiba (1998), and are partly revised by Watanabe and Yanagisawa (2005).

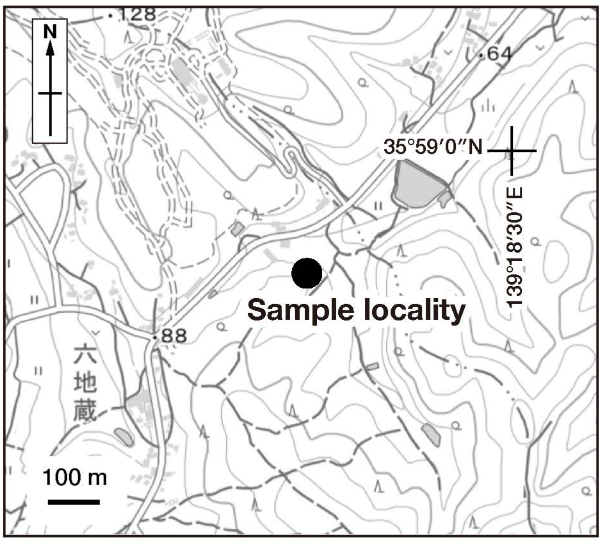


第3図　埼玉県越生町六地蔵付近の珪藻分析試料の採取位置．基図には国土地理院のweb版地理院地図を利用した．

Fig.3　Map showing the locality of diatom samples at Rokujizo, Ogose Town, Saitama Prefecture, Japan. The base map is digital map images published from the website of the Geospatial Information Authority of Japan.

第1表 越生町六地蔵の珪藻化石産出表

Table 1 Occurrence of diatoms in sandy siltstone samples collected from Rokujizo, Ogose Town, Saitama Prefecture, Japan.

| Taxa / Sample number | no.1 | no.2 |
|---|---|---|
| *Actinocyclus ingens* Rattray 1890 | - | 2 |
| *Actinocyclus ingens* f. *planus* Whiting & Schrader 1985 | 24 | 29 |
| *Actinoptychus senarius* (Ehrenberg) Ehrenberg 1843 | 3 | 5 |
| *Cavitatus jouseanus* (Sheshukova) Williams 1989 | + | - |
| *Cavitatus lanceolatus* Akiba & Hiramatsu 1993 | 14 | 9 |
| *Cocconeis* sp. | 1 | - |
| *Coscinodiscus* cf. *lewisianus* Greville 1866 | - | 1 |
| *Denticulopsis ichikawae* Yanagisawa & Akiba 1990 | + | 2 |
| *Denticulopsis lauta* (Bailey) Simonsen 1979 | 15 | 6 |
| *Grammatophora* sp. | 1 | - |
| *Kisseleviella* sp. | + | - |
| *Melorisa* (?) sp. | - | 1 |
| *Paralia sulcata* (Ehrenberg) Cleve 1873 | 9 | 7 |
| *Rhaphidodiscus* sp. | 1 | - |
| *Rhaphoneis gemmifera* Ehrengerg 1844 | - | + |
| *Thalassionema* spp. | 32 | 37 |
| *Thalassiosira* sp. | - | 1 |
| Total nunber of valves counted | 100 | 100 |
| Resting spore of *Chaetoceros* | 9 | 19 |

+: spiceies encountered after the routine count, -: absent

幾川セクションと槻川セクションの珪藻化石年代を検討し、比企層群荒川層と市ノ川層の境界がNPD4A帯中部の生層準D43 (*D. okunoi*の終産出層準：15.4 Ma)付近に，最上部の市ノ川層の上限が，NPD4A帯の生層準D43.2 (15.2 Ma)付近，おそらくはD43.2よりも上位に位置づけられることを示した(第2図)．荒川層の下限の年代は不明だが，少なくとも生層準D33 (16.7 Ma)からD35 (16.4 Ma)の区間を含むことが示された(栗原ほか，2003；高橋・柳沢，2004)(第2図)．一方，岩殿丘陵の都幾川層群下部の根岸層や将軍沢層からは，NPD5B帯に属する珪藻化石が報告されている(栗原ほか，2003)(第3図)．

六地蔵の2試料の珪藻年代はD41.5 (15.6 Ma)～ D43.2 (15.2 Ma)であり，珪藻化石層序に基づけば，比企層群荒川層最上部と市ノ川層に対比される(第2図)．この結果は，岩殿丘陵の西縁部においても比企層群に属する地層が分布することを明確に示している．ただし，両試料には生層準D42 (*D. okunoi*の初産出)とD43 (*D. okunoi*の終産出)を規定する*D. okunoi*が産出しないため，生層準D41.5 (*Cv. lanceolatus*の初産出)～ D42と生層準43 ～ D43.2 (*Cv. lanceolatus*の終産出)のどちらにも対比が可能であり(第2図)，珪藻化石層序から荒川層と市ノ川層への帰属を判断することは困難である．

今回分析した試料はいずれも砂質シルト岩であった．また，原田(2009)によればこの露頭のシルト岩には径15 cm程度の角礫が含まれる．高橋・柳沢(2004)は，荒川層の最上部は塊状の珪藻質シルト岩からなり，市ノ川層はシルト岩と砂岩の互層や不淘汰角礫岩からなるとした．六地蔵の露頭の岩相はどちらかというと市ノ川層に類似することから，周辺に露出する砂岩や礫岩と合わせて市ノ川層に対比される可能性が高い．

**謝辞**：本研究は，産業技術総合研究所地質調査総合センターが発行する5万分の1地質図幅「川越」地域を作成するための調査の一環として行われたものである．東松山市文化財専門調査員の原田吉樹氏には，珪藻化石分析用の試料を提供していただいた．地質情報研究部門の柳沢幸夫博士には草稿に対して貴重なコメントをいただいた．担当編集委員の持丸華子博士および査読者の渡辺真人博士による有意義なコメントは原稿を改善する上で大変有益であった．以上の方々に記して御礼申し上げます．

## 文　献


Akiba, F. (1986) Middle Miocene to Quaternary diatom biostratigraphy in the Nankai Trough and Japan Trench, and modified Lower Miocene through Quaternary diatom zones for middle-to-high latitudes of the North Pacific. *In* Kagami, H., Karig, D. E., Coulbourn, W. T. *et al.*, *Initial Reports of the Deep Sea Drilling Project*, **87**, 393–480. U. S. Government Printing Office, Washington D. C.

荒井　豊・原田吉樹 (2015) 葛袋における都幾川層群の基底礫岩と不整合．埼玉県東松山市葛袋化石調査報告書．東松山市教育委員会，17–32.

原田吉樹 (2009) 埼玉県岩殿丘陵西縁の“N.8期堆積層”と貝類化石．地学研究，**58**，29–33.

堀内誠示・柳沢幸夫 (1994) 埼玉県岩殿丘陵に分布する中新統の珪藻化石層序．地質調査所月報，**45**，655–675.

小池美津子・武井晛朔・下野敏弘・町田二郎・秋元和実・橋屋　功・吉野博厚・平社定夫 (1985) 岩殿丘陵の中新統・都幾川層群．地質学雑誌，**91**，665–677.

栗原行人・堀内誠示・柳沢幸夫 (2003) 埼玉県岩殿丘陵地域に分布する中新統の岩相層序と珪藻・石灰質ナンノ化石層序．地質学雑誌，**109**，215–233.

栗原行人・柳沢幸夫 (2015) 東松山市葛袋地区の地質．埼玉県東松山市葛袋地区化石調査報告書．東松山市教育委員会，8–16.

間嶋隆一 (1989) 埼玉県中央部，荒川から岩殿丘陵にかけて分布する新第三系の層序．静岡大学地球科学研究報告，**15**，1–24.

納谷友規・山口正秋・水野清秀 (2009) 関東平野中央部埼玉県菖蒲町で掘削された350mボーリングコア (GS-SB-1) の珪藻化石産出層準と淡水成層準および海成層準の識別. 地質調査研究報告，**60**，245–256.

納谷友規・平松　力・古澤　明・柳沢幸夫・山口和雄 (2013) 関東平野中央部埼玉県大利根町で掘削された1505m温泉ボーリングの年代層序.　地質学雑誌，**119**，375–395.

Raffi, I., Wade, B. S. and Pälike, H. (2020) Chapter 29, The Neogene Period. *In* Gradstein, F. M. *et al.* eds. *Geologic Time Scale 2020*, 1141–1215. Elsevier, Amsterdam, Oxford, Cambridge.

杉山雄一・須貝俊彦・井村隆介・水野清秀・遠藤秀典・下川浩一・山崎晴雄 (1997) 50万分の1活構造図8「東京」(第2版)．地質調査所.

高橋雅紀 (2008) 岩殿丘陵，関東山地周辺．日本地質学会編，日本地方地質誌3：関東地方，朝倉書店，東京，162–166.

高橋雅紀・柳沢幸夫 (2004) 埼玉県比企丘陵に分布する中新統の層序—複合年代層序に基づく岩相層序の総括—．地質学雑誌，**110**，290–308.

Watanabe, M. and Yanagisawa, Y. (2005) Refined Early to Middle Miocene diatom biochronology for the middle- to high-latitude North Pacific. *Island Arc*, **14**, 91–101.

柳沢幸夫 (2021) 秋田県大仙市下荒川に分布する中新統上部の船川層における暖流系石灰質微化石産出層準の珪藻年代．地質調査研究報告，**72**，459–477.

Yanagisawa, Y. and Akiba, F. (1998) Refined Neogene diatom biostratigraphy for the northwest Pacific around Japan, with an introduction of code numbers for selected diatom biohorizons. *The Journal of the Geological Society of Japan*, **104**, 395–414.


（受 付：2022年6月23日；受 理：2022年10月4日）

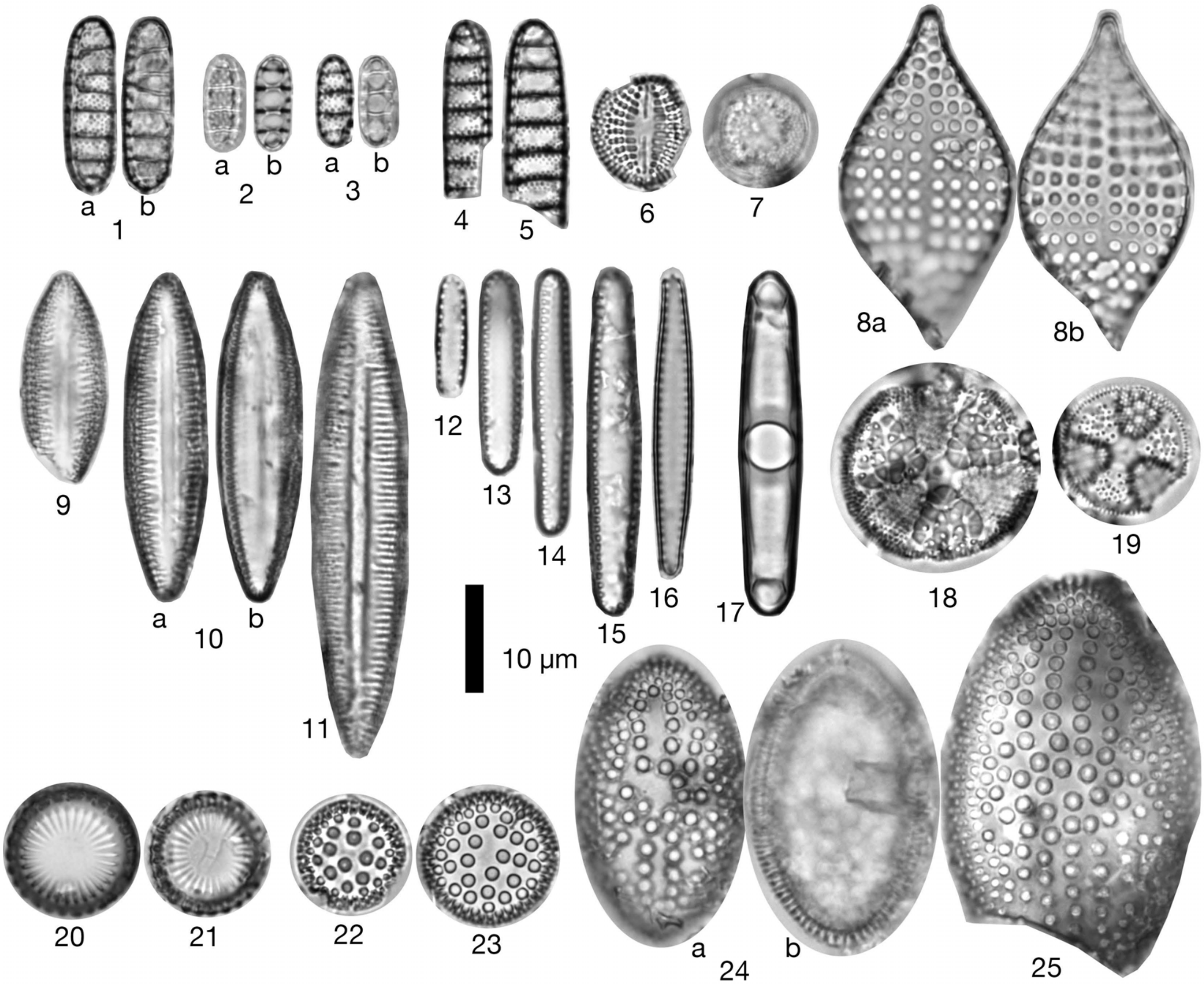


図版 1　越生町六地蔵から産出した珪藻化石

Plate 1　Fossil diatoms in the sandy siltstone samples collected from Rokujizo, Ogose Town, Saitama Prefecture, Japan.

1–3 *Denticulopsis lauta* (Bailey) Simonsen [no.1]

4–5 *Denticulopsis ichikawae* Yanagisawa & Akiba [4: no.1, 5: no.2]

6 *Rhaphidodiscus* sp. [no.1]

7 *Melorisa* (?) sp. [no.2]

8 *Rhaphoneis gemmifera* Ehrenberg [no.2]

9–11 *Cavitatus lanceolatus* Akiba & Hiramatsu [9, 10: no.1, 11: no.2]

12–16 *Thlassionema* spp. [no.1]: 12–14: *T. nitzschioides* (Grunow) Mereschkowsky, 15: *T.* cf. *hirosakiensis* (Kanaya) Schrader, 16: *T.* cf. *nitzschioides* (Grunow) Mereschkowsky.

17 *Grammatophora* sp. [no.1]

18–19 *Actinoptychus senarius* (Ehrenberg) Ehrenberg [no.2]

20–21 *Paralia sulcata* (Ehrenberg) Cleve [20: no.2, 21: no.1]

22–23 *Actinocyclus ingens* f. *planus* Whiting & Schrader [no.1]

24–25 *Coscinodiscus* cf. lewisianus Greville [no.2]

## 地質調査総合センター研究資料集

| | | |
|---|---|---|
| 731 | 磐梯・吾妻・安達太良火山周辺の中期更新世～完新世テフラ層序 | 山元 孝広 |
| 732 | 富士火山の完新世テフラ層序 | 山元 孝広 |
| 733 | 富士火山の火口位置情報 | 石塚 吉浩・山元 孝広・中野　俊・宝田 晋治 |
| 734 | 第 36 回地質調査総合センターシンポジウム「3 次元で解き明かす東京都区部の地下地質」講演要旨集 | 中澤　努・野々垣　進・小松原純子・宮地 良典 (編) |
| 735 | 葛根田花崗岩の石英の岩石学的組織 | 佐々木 宗建・佐脇 貴幸・藤本 光一郎・笹田 政克 |
| 736 | 20 万分の 1 日高変成帯地質図 | 高橋　浩 |
| 737 | 遺跡発掘調査において記載された桜島テフラ　その 1 | 西原　歩・下司 信夫・成尾 英仁 |
| 738 | 日本全国内陸部の地殻内応力マップと微小地震の発震機構解のデジタルデータ | 内出 崇彦・椎名 高裕・今西 和俊 |
| 739 | 熊本，阿蘇およびくじゅう地域の地下水および河川水の化学・同位体組成 | 高橋 正明・稲村 明彦・高橋　浩・森川 徳敏・東郷 洋子・風早 康平・佐藤　努・半田 宙子・仲間 純子・中村 有理・大和田 道子・宮越 昭暢・戸崎 裕貴・冨島 康夫・大丸 純・清水 日奈子・大沢 信二・網田 和宏・堀口 桂香・柴田 智郎・小泉 尚嗣・川端 訓代・安原 正也 |
| 740 | 第 2 白嶺丸重力異常データ | 石原 丈実・小田 啓邦 |

## 地質調査総合センターの最新出版物

| | | |
|---|---|---|
| 5 万分の 1 地質図幅 | 桐生及足利<br>和気<br>豊田 | |
| 20 万分の 1 地質図幅 | 宮津（第 2 版） | |
| 海洋地質図 | No. 91<br>No. 92 | 種子島付近海底地質図<br>久米島周辺海域海洋地質図 |
| 火山地質図 | No. 21<br>No. 22 | 恵山火山地質図<br>日光白根及び三岳火山地質図 |
| 海陸シームレス地質図 | S-7 | 海陸シームレス地質情報集「相模湾沿岸域」 |
| 大規模火砕流分布図 | No. 1 | 姶良カルデラ入戸火砕流堆積物分布図 |
| 特殊地質図 | No. 42 | 多摩川低地の沖積層アトラス |
| その他 | 東・東南アジア磁気異常図 改訂版（第 3 版）<br>中部地方の地球化学図 | |

事務局
国立研究開発法人 産業技術総合研究所
地質調査総合センター
地質情報基盤センター　出版室
https://www.gsj.jp/inquiries.html

Secretariat Office
National Institute of Advanced Industrial Science and Technology
Geological Survey of Japan
Geoinformation Service Center Publication Office
https://www.gsj.jp/en/

地質調査研究報告 第73巻 第3号
令和4年10月26日　発行

国立研究開発法人 産業技術総合研究所
地質調査総合センター

〒305-8567
茨城県つくば市東1-1-1 中央第7

Bulletin of the Geological Survey of Japan
Vol. 73 No. 3 Issue October 26, 2022

**Geological Survey of Japan, AIST**

AIST Tsukuba Central 7, 1-1-1, Higashi,
Tsukuba, Ibaraki 305-8567 Japan

AIST16-G68699-73-3

Online ISSN : 2186-490X
Print ISSN : 1346-4272

# BULLETIN OF THE GEOLOGICAL SURVEY OF JAPAN

Vol. 73 No. 3 2022

## CONTENTS



Geological Survey of Japan, AIST

地 調 研 報
Bull. Geol. Surv. Japan
Vol. 73, No. 3, 2022